

The opposing contributions of type 2 inflammation to
C. difficile and SARS-CoV-2 infections.

Alexandra Donlan
Charlottesville, Virginia

B.S., Biological Sciences, Florida State University, 2017

A Dissertation presented to the Graduate Faculty
of the University of Virginia in Candidacy for the Degree of
Doctor of Philosophy

Department of Microbiology, Immunology, and Cancer Biology

University of Virginia
August, 2021

Thesis Abstract:

Type 2 immunity is characterized by cytokines such as interleukin (IL)-4, IL-5, IL-13, IL-25, IL-33, and cells such as type 2 Innate Lymphoid cells (ILC2s), mast cells, T helper (Th)2 CD4+ T cells, and Immunoglobulin (Ig)E+ B cells. This immune response is most commonly associated with protection against helminth infections, and also for promoting allergy, asthma, and atopic dermatitis. However, the involvement of this branch of immunity has been observed outside these typical conditions, including during viral and bacterial infections. The contribution type 2 immunity plays during these noncanonical responses can be protective or deleterious, depending on the tissue site, pathogen, and other context-dependent factors. In this thesis, we will describe two pathogens, *C. difficile* and SARS-CoV-2, for which type 2 immunity contributes opposing roles in protecting the host from severe disease.

Clostridiodes difficile (*C. difficile*) is the leading cause of hospital-acquired gastrointestinal infections in the U.S. resulting in mild to severe diarrhea, pseudomembranous colitis, toxic megacolon, and even death. *C. difficile* Infection (CDI) is associated with elevated peripheral white blood cell (WBC) counts and intestinal inflammation as indicators of severe disease, suggesting that the host response to infection plays an important role in the outcome of patient morbidity and mortality. Our lab has recently shown that the alarmins IL-25 and IL-33 provide protection from CDI through induction via type 2 innate lymphoid cells (ILC2) that includes

eosinophils and promotes the reduction of inflammatory cells and cytokines. ILC2s and eosinophils produce effector cytokines such as IL-4, IL-5, and IL-13, however the role for these have not been explored in CDI before. Here, we show that these cytokines provide protection from severe disease, further supporting the protective capabilities of type 2 immunity during the hyperinflammatory enteric infection caused by *C. difficile*. IL-5 protected from mortality and resulted in increased eosinophils within the colon, suggesting this cytokine is likely involved downstream of IL-25 in promoting protective eosinophilia. IL-4 and IL-13, however, promoted recovery from disease, highlighting that these two cytokines may be more important for reducing inflammation and tissue damage at later stages during disease. Additionally, the neutralization of IL-13 was associated with increased monocytes and reduced alternatively activated macrophages (AAMs). These data suggested that IL-13 is important for facilitating appropriate monocyte to macrophage transition as well as polarization of AAMs, and that dysregulated responses within these cells impedes effective recovery.

SARS-CoV-2, the causative agent of COVID-19, was first identified in December 2019 in the Wuhan province of China, where it caused severe viral pneumonia. Dysregulated immune responses are strongly associated with severe outcomes from disease, and characterization of these responses could highlight approaches for therapeutic interventions

in patients. We identified IL-13 as being associated with the need for mechanical ventilation in two independent cohorts. The use of Dupilumab, a monoclonal antibody against IL-4Ra, in patients who subsequently acquired COVID-19 was associated with fewer severe outcomes. Neutralization of IL-13 in mice protected against severe disease, further supporting a pathogenic role for this cytokine. Following neutralization of IL-13 during COVID-19, we uncovered that the gene for hyaluronan synthase 1, *Has1*, was the most downregulated gene in the lung, implicating hyaluronan as being regulated by IL-13. Furthermore, deposition of the polysaccharide in lung tissue was reduced following IL-13 neutralization, and blockade of the receptor for hyaluronan, CD44, protected mice from severe disease as well. In patients, elevated hyaluronan was associated with disease in both plasma and lung biopsy samples, further suggesting that hyaluronan is involved in pathogenesis. Finally, hyaluronan was directly induced in the lungs of mice by administration of IL-13, altogether suggesting a novel role for IL-13 to drive hyaluronan deposition.

The results from these studies support the observation that type 2 immunity can be involved in infections other than those caused by helminths, and can contribute protective or pathogenic roles depending on the tissue and microbe. This thesis will discuss the role type 2 immunity plays during these infections, as well as why there are seemingly

opposing consequences for this immune response. Overall, this work increases our understanding of the role for the cytokines IL-4, IL-5, IL-13 in COVID-19 and CDI, and has implications for other infectious diseases.

Acknowledgements

I would first and foremost like to thank my mentor Bill Petri for the exceptional guidance and support during my time as a graduate student. His commitment to, and passion for science are inspiring, and he has continually motivated me to work hard and find joy in what I do. I am grateful for his support in allowing me to pursue projects I found engaging, which has driven my development as an independent scientist. I will also always remember the work we accomplished during the COVID-19 pandemic: the weekly zoom meetings with international collaborators, working on the cutting-edge of scientific discovery, and the ability to begin a clinical trial, all within one year. The opportunities and the experiences I have been exposed to are all due to the wonderful mentorship Bill has provided. I will also always be grateful for his kindness and friendship, which have made working with him that much more enjoyable. Thank you immensely, Bill.

I would also like to thank Judith Allen, from the University of Manchester, who served as a secondary mentor to me since early on during graduate school. After meeting with her for the first time in Oxford for lunch in 2018, I never would have imagined where our collaborations and avenues of scientific discovery would have taken us. I feel very fortunate to have had her guidance and input on all things type-2-immunity related, as well as for personal development and motivation. She, too, has been incredibly kind and supportive, and she is a wonderful role model to look up to.

Thank you also to my committee members, Alison Criss, John Lukens, Hervé Agaisse, and Melanie Rutkowski for their continued support, guidance,

and time. They have been integral for developing my confidence and skill as an independent investigator.

I would also like to thank my lab mates, who are wonderful people and wonderful scientists. Mahmoud and Alyse, who guided me when I first joined Bill's lab, and who were exceptional mentors. Also thank you to Morgan and Jhansi, as members of "Team C. diff" who I have shared an office with. I will always appreciate the scientific discussions which have not only been integral to my own projects and understanding of science, but also for the fun conversations, jokes, and support. Being able to enjoy my days in work because of the interactions I can have with my colleagues is something I am incredibly grateful for, and which has been a source of joy during graduate school.

I also am incredibly grateful to my friends, both those I have made prior to, and during, graduate school. I am happy to have been able to surround myself with supportive, generous, and like-minded people, with whom I made wonderful memories.

Finally, I would like to thank my family. They have always been my biggest cheerleaders and supporters. They have taught me to be resilient, kind, and to know that I am capable of anything I set my mind to. I would not be where I am today without them, and I am so grateful for them celebrating my accomplishments with me along the way.

Abstract.....	ii-iv
Acknowledgments.....	v-vii
Table of Contents.....	viii-ix
1. Chapter 1: Introduction	
1.1 Type 2 Immunity.....	1
1.1.1 IL-25 and IL-33 are type 2 alarmins.....	2-3
1.1.2 IL-4, IL-5, and IL-13 are important effector cytokines	
1.1.2.1 IL-5.....	3
1.1.2.2 IL-4 and IL-13.....	3-7
1.1.2.3 Conclusions.....	7-8
1.2 Type 2 immunity during infectious disease.....	8
1.2.1 Helminth infections.....	8-11
1.2.2 Viral infections.....	11-14
1.2.3 Bacterial infections.....	14-17
1.3 Hyaluronan.....	17
1.3.1 Biology.....	17-20
1.3.2 CD44.....	20-22
1.3.3 Role during inflammation.....	22-24
1.3.3.1 Hyaluronan and CD44 during type 2 immune responses.....	24-25
1.4 <i>Clostridioides difficile</i>	
1.4.1 Background.....	26-27
1.4.2 Pathogenesis.....	27-29
1.4.3 Host immune response to <i>C. difficile</i>	
1.4.3.1 Toxin-mediated inflammation.....	29-30
1.4.3.2 Type 3 inflammation.....	30-32
1.4.3.3 Protective type 2 immune responses.....	32-33
1.5 COVID-19	
1.5.1 Background/biology.....	35
1.5.2 Pathogenesis.....	36-37
1.5.3 Host immune response to SARS-CoV-2	
1.5.3.1 Anti-viral immune responses.....	37-39
1.5.3.2 Dysregulated host immunity	39-40

1.5.3.3	Type 2 immunity during COVID-19.....	41-42
1.5.3.4	Hyaluronan in COVID-19.....	42-45
1.5.3.5	Mouse models of COVID-19.....	45-46
1.6	Conclusions.....	47-49
2.	Chapter 2: Type 2 cytokines IL-4 and IL-5 reduce severe outcomes from <i>Clostridioides difficile</i> infection.....	50-60
3.	Chapter 3: IL-13 promotes recovery from <i>C. difficile</i> infection.....	61-84
4.	Chapter 4: IL-13 is a driver of severe COVID-19.....	85-136
5.	Conclusions and Future directions.....	137-139
5.1	Type 2 immunity is protective during <i>C. difficile</i> infection....	139-143
5.2	Type 2 immunity is pathogenic during COVID-19 pneumonia.....	143-145
5.3	Future Directions	
5.3.1	Alternatively-activated macrophages and recovery from <i>C. difficile</i> infection.....	145-149
5.3.2	Monocyte contributions to <i>C. difficile</i> immune response.....	149-154
5.3.3	Is hyaluronan mediated by IL-13 in the colon and involved in the host response to CDI?	154-159
5.3.4	Other downstream mediators of IL-13-induced pathology during COVID-19.....	159-161
5.3.5	Hyaluronan and CD44 contributions to COVID-19.....	161-164
5.3.6	Mechanisms driving IL-13 production in COVID-19.....	164-165
5.4	Concluding remarks.....	165-168
6.	Materials and Methods	
6.1	Methods for <i>C. difficile</i> studies.....	169-173
6.2	Methods for COVID-19 studies.....	174-186
7.	References.....	187-229

Chapter 1: Introduction

1.1 Type 2 Immunity

Type 2 immunity, often referred to as Th2 immunity, is generally characterized by the production of cytokines such as Interleukin-4 (IL-4), IL-5, IL-9, and IL-13, as well as the recruitment and differentiation of a variety of immune cells including eosinophils, type 2 innate lymphoid cells (ILC2s), alternatively-activated macrophages (AAMs; also referred to as M2), CD4+ T helper 2 (Th2) cells, and Immunoglobulin (Ig)E-producing B cells¹⁻³. Additionally, IgE binding by Fc Epsilon Receptor 1 (Fc ϵ R1) can result in the activation and degranulation of mast cells and basophils, leading to the release of histamines³. Type 2 immunity is important for protection during helminth infections and for maintaining tissue during homeostasis. However, this response can also drive inappropriate, often pathological, responses to non-harmful stimuli, such as with asthma, allergies and atopic dermatitis^{2,4}. Additionally, type 1, type 2, and type 3 immunity can directly negatively regulate one another^{5,6} (discussed in 1.2 and 1.4.3.3), which implicates both the dichotomous nature of these responses, and that there are mechanisms to ensure that an inappropriate immune response to a stimuli is not induced. However, it is also observed that there can be involvement of each branch of immunity during any given response, which, depending on the context, can be of benefit or detriment to the host. This chapter will discuss type 2 immune responses, and how they play a role in non-type 2 mediated infectious disease, both to provide protection or promote severity.

1.1.1 IL-25 and IL-33 are type 2 alarmins that activate ILC2s

Different mechanisms can drive the induction of type 2 immunity, including through pattern recognition receptors (PRRs)³ on dendritic cells (DCs), as well as through epithelial-derived cytokines, often termed alarmins². Alarmins include thymic stromal lymphopoietin (TSLP), tuft-cell-produced IL-25, and IL-33, which are secreted or released from the epithelium following injury, infection, protease activity, or other stimuli⁷. Upon release, these cytokines can induce type 2 immune responses, beginning primarily with the activation of ILC2s, as well as macrophages, DCs, and other myeloid cells. While alarmins can have a wide range of effects on downstream responses, typically they result in the production of IL-4, IL-5, and IL-13⁸.

ILC2s are an integral innate effector cell during type 2 responses that are induced by the release of alarmins^{9,10}. These cells have functions similar to their adaptive counterpart, Th2 CD4⁺ T cells, but lack T cell receptors required for antigen-specificity¹⁰. Additionally, they are often tissue resident, allowing them to respond rapidly; ILC2 numbers can further increase under stimulatory conditions through replication in the tissue or recruitment from the bone marrow¹¹.

Concordantly, during many models of type 2 inflammation including asthma and helminth responses, ILC2s are required for tissue responses that occur prior to, and independently of, T cell expansion and recruitment^{12,13}.

ILC2s produce a wide array of effector cytokines, growth factors, and other mediators for tissue responses, including IL-4, IL-5, and IL-13, as well as

the epidermal growth-factor-like molecule, Amphiregulin^{8,11}. These cells are often a first major source of these interleukins during inflammation, and as such, ILC2s have been shown to be integral in downstream responses in many models^{12,14,15}. The next section will discuss the function of these cytokines downstream of ILC2 production.

1.1.2 IL-4, IL-5, and IL-13 are important effector cytokines

1.1.2.1 IL-5

IL-5 has important effects on both the adaptive and innate immune responses. It was first discovered as a T cell-derived cytokine that was important for differentiation of B cells into IgE antibody-secreting plasma cells¹⁶. However, it is now most commonly associated with the role of driving eosinophil maturation and egress from the bone marrow, as exemplified by the high levels of circulating eosinophils in IL-5 overproducing mice¹⁷.

Using IL-5-reporter mice, it has become appreciated that the primary, innate, producer of IL-5 is ILC2s^{18–20}, expression of which is increased downstream of IL-25 and IL-33^{21,22}. Loss of IL-5 impedes eosinophil recruitment to sites of inflammation, and as such IL-5 blockade has been posed as a treatment for pathology driven by eosinophils during asthma²³. Chapter 2 will discuss the contribution of IL-5 to *C. difficile* infection.

1.1.2.2 IL-4 and IL-13

IL-4 can be produced from most type 2-associated cell populations, including ILC2s and eosinophils. Through its signaling receptor IL-4R α / γ c²⁴, IL-4 is important for the polarization of macrophages towards an alternatively-activated state (discussed below), as well as for promotion of CD4+ Th2 cell differentiation²⁵ and class switching in B cells to produce IgE²⁶. IL-13, the closely related cytokine, has many overlapping, as well as many distinct, functions. During innate responses, IL-13 is produced primarily by ILC2s, but also by eosinophils, macrophages, succeeded by adaptive CD4+ T cells^{10,27}. Primary roles for IL-13 include the recruitment of eosinophils, polarization of AAMs, goblet cell hyperplasia and increased mucus production, as well as driving airway hyperreactivity (AHR) in the lungs, and regulation of the extracellular matrix (ECM), among others²⁷⁻²⁹. Unlike IL-4, however, IL-13 does not have considerable effect on driving adaptive Th2 responses and may have a larger role than IL-4 on innate immunity and non-hematopoietic-derived cells, such as epithelial cells and fibroblasts. Through these and other contributions, IL-13 is considered an integral coordinator of type 2 immunity.

Both IL-4 and IL-13 share the IL-4R α subunit for their receptor and signal through the transcription factor STAT6²⁴. However, IL-4 primarily signals through the type I receptor, a complex between IL-4R α and γ c, with limited signaling through the type II receptor, comprised of IL-4R α /IL-13 R α 1. Engagement of the receptor by IL-4 induces signaling through Janus kinase 3 (Jak3)³⁰ and STAT6²⁴. IL-13, in contrast, primarily utilizes the type II receptor which activates Jak2 or

Tyrosine kinase 2 (Tyk2)³⁰ and STAT6 or STAT3 transcription factors³¹. IL-13 has an additional receptor, IL-13R α 2, that is primarily believed to be a decoy receptor, serving as a negative inhibitor of IL-13 signaling²⁴. However, there is evidence that this receptor can have some signaling capacity, highlighting that more studies on the role of this receptor are needed^{32,33}.

The IL-4R α and IL-13R α 1 chains are present on most cells within the human body, including immune, epithelial, and muscle cells, while the γ c is expressed more specifically on immune cells. Therefore, the capability for IL-4 or IL-13 to signal within different cell populations is regulated by the presence of the appropriate receptor, type I or type II.

Because of the differences in receptor expression and signaling components, IL-13 is considered to be a more integral conductor of type 2 immunity than IL-4. During helminth infections, the presence of IL-13 is required for effective clearance of worms, whereas loss of IL-4 was seen to have little to no effect on this aspect³⁴. Similarly, IL-13, and not IL-4, is a critical component in driving mucus production and AHR in allergic asthma^{35,36} 27, as well as collagen deposition and fibrosis. Further, AHR, which is facilitated by bronchoconstriction, is mediated in part, by airway smooth muscle hypercontractility. IL-13 has been shown to increase smooth muscle contractility, suggesting that this could be one mechanism through which IL-13 promotes AHR in the lung^{37,38}. Although many non-immune functions are driven primarily by IL-13, both IL-13 and IL-4 can have

effects on epithelial tight junctions, by decreasing their expression and resulting in decreased epithelial integrity³⁹.

Macrophages express both type I and II receptors, and signaling by both IL-13 or IL-4 in these cells results in polarization towards an alternatively activated state^{29,30,40}. This is often associated with increased expression of the surface markers CD206 or CD163, as well as intracellular expression of Arginase-1 (Arg1), Relm α , and Ym1³⁰. Metabolism in these macrophages shifts towards a primarily fatty acid oxidative state^{41,42}, which is often associated with decreased phagocytosis and anti-microbial activity and increased anti-inflammatory properties. Furthermore, these macrophage populations produce factors important for tissue repair, such as matrix metalloproteases (MMPs) and collagen, as well as anti-inflammatory mediators such as IL-10 or TGF- β , and chemokines important for the recruitment of other cells^{30,43,44}. Characterization of these cells can be complex, however, as there is significant heterogeneity within their populations, and they provide contributions to immunity that are context specific³⁰. Other contributors to macrophage polarization that contribute to the heterogeneity include IL-10, through utilization of STAT3 and not STAT6. Polarization by IL-10 can promote macrophage phenotypes similar to those induced by IL-4 and IL-13, however, there are significantly different gene expression profiles between these macrophage populations. For example, IL-10 decreases MHC antigen presentation, whereas IL-4 and IL-13 signaling increase

MHCII for activation of CD4+ Th2 cells⁴⁴. Altogether highlighting that these cells are not the same and likely contribute differently to tissue responses⁴³.

Similar to IL-5, monoclonal antibodies blocking IL-4 and IL-13 in patients with type 2-mediated diseases have been approved and shown to be effective in reducing inflammation and pathology. Some examples of these therapeutics include Tralokinumab and Lebrikizumab, which target IL-13 to treat severe atopic dermatitis, ^{45,46}, as well as Dupilumab, a monoclonal antibody against IL-4Ra, which is an exceptionally effective treatment for both asthma and atopic dermatitis^{47,48}.

The protective role of IL-4 during *C. difficile* infection will be discussed in chapter 2, and the contribution of IL-13 to *C. difficile* and COVID-19 will be discussed in chapters 3 and 4 of this thesis.

1.1.2.3 Conclusions

While there are many cytokines, chemokines, and other factors that contribute to type 2 immune induction and effector responses, the cytokines discussed here are considered integral players in facilitating these processes. Driven by alarmins, such as IL-25 or IL-33, ILC2s are induced to serve as first responders to type 2-promoting stimuli, and to begin producing the effector cytokines IL-4, IL-5, and IL-13. Together, these cytokines promote the recruitment and polarization of cells such as eosinophils, macrophages, Th2+ CD4 T cells, and IgE+ B cells. Additionally, primarily through IL-13, there are

impacts to the tissue itself which promote mucus responses, smooth muscle contraction, fibroblast activation, and tissue remodeling. While the primary outcome from these responses is likely coordinated to facilitate the expulsion of parasitic worms, inappropriate induction can result in the pathological inflammation that drives asthma and allergy. Furthermore, type 2 immunity can be induced during disease processes that are not traditionally associated with these responses, such as immunity to viral or extracellular bacterial pathogens. The primary discussion of this thesis will be focused on the contribution of type 2 responses to these non-canonical conditions.

1.2 Type 2 immunity during infectious diseases

As discussed above, type 2 immunity is an important branch of the host immune response to pathogens and can promote expulsion and tissue healing following parasite infection, but can reduce high levels of inflammation driven by bacterial or viral infections as well. The contribution of type 2 immunity is complex and is context dependent. In this next section, I will discuss the contribution of this response to infectious diseases using specific examples.

1.2.1 Helminth Infections

The helminths, or worm parasites, constitute a staggering proportion of the infectious burden around the world, contributing to substantial number of deaths per year and adjusted life years^{49,50}. These infections are associated with the

induction of type 2 immunity for either resistance (expulsion of the worm) or tolerance (wound healing and anti-inflammatory responses)⁸. The use of murine models of helminth infections has given insight into the mechanisms of parasite-mediated pathology and the response from host immune factors to control parasite burden and heal damaged tissue. Additionally, the use of these helminth infection models has resulted in the discovery of novel cell types that are tightly linked to type 2 immunity, including ILC2s and specialized epithelial cells called tuft cells⁸, which are found in the gastrointestinal tract, lungs, and other mucosal sites.

The importance of type 2 immunity during helminth infections is considerable, as worms generate large amounts of tissue damage due to their size and migration through different tissue sites⁸. Additionally, their size and physical location makes them inaccessible by cell-mediated immunity and difficult to phagocytose, necessitating other mechanisms of host defense. As such, worms are primarily killed by the production of anti-microbial compounds from eosinophils, mast cells, and basophils, as well as the production of IgE, which coats the organism and activates mast cells^{51,52}. Type 2 responses following infection also promote a 'weep-and-sweep' response for promoting mechanical removal of worms or their eggs⁸, which is aided by the increase in tissue lubrication following mucus production by goblet cells. Additionally, during helminth infections, AAMs may play context-dependent roles, but often function

to reduce T cell mediated tissue pathology, promote tissue repair, and increase worm killing and clearance⁵³.

Nippostrongylus brasiliensis (*N. brasiliensis*) is a commonly utilized murine helminth model for understanding type 2 mediated, anti-worm immunity. This worm has life cycle stages that occupy both the intestines and lung, making it a useful model for both of these tissue sites⁵⁴. Th2 CD4+ T cells, IgE+ plasma cells, ILC2s and macrophages are all critical cells in mediating anti-worm immunity, and can produce cytokines such as IL-4, IL-5, or IL-13 during infection^{8,9,53}. While initially it was believed that Th2 T cells were sufficient for worm clearance, there is increasing evidence of the important contribution of ILC2s to this response, particularly through the production of effector cytokines, such as those mentioned above⁹. Downstream of ILC2s, IL-4R α is a critical component in mediating immunity against these parasites, as mice lacking this receptor cannot effectively clear worm burden⁵⁵. As discussed above, although IL-4R α is important for both IL-4 and IL-13 signaling, it is hypothesized that there is a larger contribution of IL-13 to worm clearance, which may be, in part, due to the capacity for IL-13 to signal more readily in non-hematopoietic cells²⁷. Additionally, IL-5 promotes the recruitment of eosinophils to the site of infection, where they may be important for reducing larvae in the lungs, as a mechanism of parasite control⁵⁶.

AAMs are another important cell for anti-worm immunity, and are polarized by both IL-4 and IL-13^{40,28,29}. Bouchery et al, 2015 found that IL-13 production by

either Th2 T cells or ILC2s was critical in promoting AAM polarization, and subsequent responses that promoted *N. brasiliensis* larvae killing⁵⁷, which also suggests that IL-13 production is a primary orchestrator for the immune response, regardless of source⁵⁸. Additionally, AAMs can promote tissue repair following high levels of damage accrued by worm migration, limit inflammation, and protect from fatal lung injury^{53,59}.

Together, helminth models of infection have highlighted an important role for type 2 inflammation in facilitating clearance of large extracellular pathogens, reducing pathogenic inflammation, and promoting repair of damaged tissue.

1.2.2.2 Viral

The viruses are obligate intracellular resulting in the requirement for cell-mediated immunity, by which the host response works to contain and clear the virus by killing the infected cells. This is mediated primarily by type 1 immunity, which includes innate cells such as Natural Killer (NK) cells, as well as a strong T cell response composed of CD4+ Th1 cells and cytotoxic CD8+ T cells. Cytokines integral to the type 1 immune response, including IL-12 and IFN γ , can have direct inhibitory effects on type 2 responses^{5,60,61}, suggesting type 2 inflammation could be counteracting anti-viral immunity. In line with this hypothesis, the inappropriate induction or presence of type 2 immunity during viral infections can impede an effective type 1 response, and result in inefficient viral clearance or drive virus-induced type 2 pathology, including AHR^{62,63}.

Because viral infection in the epithelium can result in apoptosis or cell killing as a mechanism for control viral burden^{64,65}, it is possible that cell death following infection results in the release of alarmins, such as IL-25 or IL-33, allowing for the potentiation of these type 2 responses.

Type 2 immunity driven by viral infection not only has negative impacts on antiviral immunity, but may also result in increased incidence of chronic lung diseases such as asthma, particularly in young children^{62,66}. While it is likely that underlying genetics and susceptibility contribute to the formation of these outcomes, increased risk for developing chronic lung disease is also associated with lower respiratory tract infections by Respiratory Syncytial virus (RSV)⁶⁷, likely due to the induction of Th2 responses and subsequent decreased lung function. Correspondingly, in one study asthma was present in 30% of children who had experienced RSV bronchiolitis during infancy, compared to 2% in matched controls⁶⁸.

Influenza is another virus for which induction of type 2 immunity has been observed in many studies. During lethal murine influenza infection, type 2 immune responses including ILC2s and increased levels of IL-4 and IL-13 have been measured^{13,69}. In line with this, during influenza infection IL-13 production by ILC2s results in AHR in humans and mice¹³. Furthermore, patients infected with influenza A, a more deadly strain of influenza, had higher levels of IL-4 during acute disease compared to influenza B⁷⁰. Together, these studies and others suggest that type 2 responses are associated with more severe forms of

viral disease. Additionally, IL-13 can inhibit production of IL-12, a cytokine that is important for the polarization of Th1 CD4+ T cells and promotes IFN γ production, both of which are integral in anti-viral immunity. As a consequence, the reduction of IL-12 by IL-13 can result in impaired anti-viral responses, leading to prolonged persistence of the virus due to ineffective clearance^{27,71}. As such, elevated levels of both IL-4 and IL-13 were associated with poor or delayed viral clearance in the lungs^{62,72}.

While these data suggest an association between disease severity and type 2 responses, there is conflicting evidence as to whether previous presence of allergic asthma in patients increases risk for severity following infection. Asthma patients may be at increased risk for contracting influenza infection⁷³ and increased rates of hospitalization⁷⁴, but some studies have suggested that asthmatics may clear virus more rapidly and have decreased length of hospital stays^{75,76}. However, it would be possible that type 2 inflammation could reduce inflammatory burden in some patients, promoting protective responses, rather than deleterious ones.

Outside of the lung, viral infections in the small and large intestines are also common, including rotavirus and adenovirus in the small intestine, and norovirus both the small and large intestine⁷⁷. While not much is known about the role of type 2 inflammation during enteric viral infections, it was recently discovered that norovirus can infect tuft cells, and that type 2-driven tuft cell expansion could promote infection⁷⁸. Additionally, coinfection in the intestines

with viral and helminth pathogens has been seen to result in impaired antiviral immunity. Coinfection of mouse norovirus with *Trichinella spiralis*, or coinfection of West Nile Virus (WNV) with *Heligmosomoides polygyrus bakeri* (Hpb) were both seen to result in exacerbated disease that was type 2-mediated^{79,80}.

Whether this suggests that other models of type 2 immunity in the gastrointestinal tract, such as allergic inflammation, could result in worse outcomes with enteric viral pathogens is still open for investigation. Studies such as these further support the hypothesis that type 2 inflammation can impede effective antiviral responses, similar to what is observed in pulmonary viral infections.

Due to the importance of effective anti-viral immune responses, future studies to discern a role for type 2 immunity during viral infections could increase our understanding of markers for severe outcomes as well as to give insight into vaccine strategies to minimize non-responders.

1.2.2.3 Bacterial

Similar to viruses, intracellular bacteria will induce a primarily type 1 mediated response, while extracellular bacteria will elicit type 3 (also referred to as type 17) immunity⁸¹. Type 3 immunity is primarily mediated by IL-17, IL-22, neutrophils, ILC3s, and CD4+ Th17 cells, and mainly functions to produce antimicrobial compounds that kill infectious bacteria, such as *Escherichia (E.) coli* and *Klebsiella pneumonia*, and fungi (fungi not discussed here)^{82,83} MyD88 is

also important for type 3 immunity, as it is a critical signal transducer for Toll-like receptors (TLRs) and is important for promoting neutrophil recruitment, including during a murine model for *Clostridioides difficile* infection^{84–86}. The importance of this immune response in host protection from pathogens is exemplified by observation that mice lacking Myd88 or neutrophils⁸⁷ experience more severe disease to many infectious bacteria. However, it is recognized that this induction of a non-specific inflammatory response can result in damage to host tissue and increase disease severity when induced above a threshold that the tissue can tolerate through compensatory mechanisms⁸⁸.

Recently, there has been more evidence to suggest that type 2 immunity can ameliorate some of the damaging effects driven by excessive inflammation associated with type 3 immune responses^{89–91}. For example, IL-13 has many anti-inflammatory effects that include reducing the production of IL-6, IL-8 (CXCL10), MCP1, and TNF α , among others⁹². IL-4 and IL-13 have also been observed to directly attenuate the differentiation and cytokine production of Th17 cells^{83,93}. Additionally, IL-4 can inhibit IL-23 production from antigen presenting cells⁶⁰. Alternatively activated macrophages polarized by IL-4 or IL-13 can have significant anti-inflammatory effects, including promotion of TGF- β and IL-10, inhibiting T cell proliferation⁵³, and promoting tissue repair⁹⁴.

Although the anti-inflammatory effects of type 2 cytokines have been noted over the last few decades, the contribution of this branch of immunity to bacterial infections is still poorly understood. The use of dextran sodium sulfate

(DSS) as a model of Ulcerative Colitis (UC) in mice has shown to be a useful tool in understanding the relationship of type 2 and type 3 immunity in a non-infectious model. The induction of inflammation following DSS exposure mirrors some models of enteric infections, such as *C. difficile* infection, including the increased production of IL-17A, IL-23, IL-6, TNF α , and IFN γ ^{88,95–97}. This allows investigators to build off of the work already established on the role of type 2 responses in mitigating this inflammation. IL-33 has been observed to protect mice from susceptibility to DSS colitis, primarily through the preferential promotion of Th2 CD4+ T cells, ILC2s and alternatively activated macrophages^{98–100}. Alternatively activated macrophages, which can be polarized by IL-4 and IL-13, are associated with alleviated inflammation and promotion of tissue recovery^{97,101,102}. Colonization with the helminth *Taenia crassiceps* or administration of the helminth serine protease *Trichinella spiralis* (TsSp) during DSS colitis protected from the pathogenic outcomes, primarily through alternatively activated macrophages or increased IL-10 expression, respectively^{101,103}. Additionally, it has been reported that the decoy receptor for IL-13, IL-13R α 2, is a biomarker for anti-TNF α non-responder in Crohn's disease patients¹⁰⁴, and that blockade of the decoy receptor promoted recovery from DSS colitis¹⁰⁵, suggesting that active IL-13 can be important for protection against enteric inflammation. Together, these studies demonstrate the ability for type 2 cytokines to reduce inflammation associated with anti-bacterial responses.

Chapters 2 and 3 will discuss the contribution of type 2 immunity to bacterial infections, but future work into understanding these relationships are warranted.

It is important to note that there is also a high degree of evidence to suggest that type 2 responses can drive increased pathology during colitis as well. In patients with UC elevated Th2 responses have been observed, particularly IL-5 and IL-13, suggesting a positive correlation with inflammation^{106,107}. IL-13 expressing NKT cells were capable of driving increased inflammation and disease severity in a study using oxazolone to model UC, and treatment with IL-13 R α 2-Fc ameliorated disease¹⁰⁸.

While many mediators of type 2 and 3 immunity can directly inhibit one another, the relationship between these responses is not strictly in opposition. For example, IL-6, a proinflammatory cytokine known to be important for Th17 differentiation and neutrophil recruitment¹⁰⁹, can also be produced by mast cells¹¹⁰, and drive the polarization of AAMs^{111,112}. Additionally, IL-17 and neutrophils have been associated with type 2 immune-mediated asthma responses and helminth infections in the lung¹¹³, supporting the premise that these immune responses can act in concert and are not mutually exclusive.

1.3 Hyaluronan

Hyaluronan is an abundant structural component of the extracellular matrix (ECM) that also has significant immune regulatory properties. This thesis will discuss the role of hyaluronan and its signaling receptor, CD44, as being

downstream effectors of type 2 immunity, particularly during pulmonary viral infection.

1.3.1 Biology

Hyaluronan (HA) is a large glycosaminoglycan polymer made up of repeating subunits of N-acetyl glucosamine (GlcNac) and glucuronic acid (GlcA)¹¹⁴. As a major component of the ECM with a high affinity for binding water, it serves many functions including lubrication, structural maintenance, space-filling, and filtering^{114,115}. Hyaluronan also contributes to cell migration, inflammation, and proliferation¹¹⁴ through binding to one of its major receptors, CD44. During homeostasis, hyaluronan may be important for the survival and maintenance of alveolar macrophages (AMs), which are integral tissue resident immune cells within the lungs¹¹⁶. The intestines are an important site for water absorption, largely mediated by hyaluronan, which is particularly abundant within the colon and located directly beneath the epithelium¹¹⁴. Additionally, hyaluronan is important for maintaining the epithelial barrier against the microbes found with the lumen of the intestines and may promote anti-inflammatory states within the tissue¹¹⁴.

Hyaluronan is synthesized by three different hyaluronan synthases (Has1-Has3), which are found on the inner plasma membrane of cells such as fibroblasts. Has enzymes link UDP-GlcNac and UPD-GlcA to form a chain which is released into the extracellular space through a pore-like structure¹¹⁷. While the

function of the three Has enzymes is to produce hyaluronan, they may have distinct contributions to this function. Has1 and Has2 may generate hyaluronan fragments of greater molecular size than Has3. Additionally, genetic deletion of Has2 results in embryonic lethality through major abnormalities in heart and blood vessel development, whereas loss of either Has1 or Has3 does not have this effect. Overall, Has2 may contribute more during development than Has1 or Has3¹¹⁷. In addition to hyaluronan synthases that produce hyaluronan, there are also hyaluronidases that are important for regulating its turnover in tissue. These include the intracellular proteins HYAL-1,-2,-3, and -4, PHYAL, and PH-20¹¹⁸. CD44 (discussed below) facilitates uptake of hyaluronan into cells, where it is broken down in a pH-dependent manner by hyaluronidases^{115,118,119}. There are also cell-surface hyaluronidases that breakdown hyaluronan in the extracellular space, including TMEM2¹²⁰. This enzyme may be more responsible for the breakdown of hyaluronan into LMW within a tissue, rather than HYALs, as once believed.

Under homeostatic conditions, hyaluronan is most commonly found as a large (10^6 or 10^7 Da) molecule and is generally considered anti-inflammatory¹²¹. These functions include the reduction of TLR4-mediated inflammation from LPS exposure, preventing macrophage phagocytosis, and inhibiting immune cell recognition of cell surface receptors^{121,122}. During injury or disease, however, enzymatic degradation of hyaluronan by hyaluronidases generates low molecular weight (LMW) fragments which have different impacts

on the tissue environment^{115,123}. Studies have shown that smaller molecular weight fragments of hyaluronan have enhanced capabilities to activate cell signaling pathways through its receptors, and may also increase pro-inflammatory states and activation of macrophages and dendritic cells¹¹⁵. However, it is important to note that the pro-inflammatory nature of LMW-hyaluronan fragments is debated, as studies have found that purified LMW products to be contaminated with lipopolysaccharide (LPS)^{124,125}, as well as the observation that exogenous administration of hyaluronidases did not increase tissue inflammation¹²⁶.

Hyaluronan plays an important role in many tissue sites, both during normal physiological processes as well as during disease and inflammation. However, given the purview of this thesis, the primary focus for the discussion on hyaluronan will be within the context of the lung and the intestine during infectious diseases.

1.3.2 CD44

Different receptors can recognize hyaluronan including CD44, RHAMM, TLR2 and TLR4, and hyaluronan binding protein 2 (HABP2)¹¹⁸. CD44 is the major receptor for hyaluronan, as it is widely expressed, and loss of CD44 results in a large impact on hyaluronan functions within tissue. CD44 expression is found on the surface of many cells including immune cells, fibroblasts, chondrocytes, endo- and epithelial cells¹²¹, highlighting the extensive capacity hyaluronan

signaling can play within a tissue. It plays a significant role in the contribution of hyaluronan to cell migration and cell signaling responses, as well as facilitating HA turnover in the tissue^{119,127}. The CD44 receptor family is comprised of single span transmembrane glycoproteins, that include a standard isoform and likely more than 20 variant isoforms that all arise from different splicing patterns from the same mRNA¹²⁸. While the functions of the variant forms are not fully understood, it is likely that they can play both overlapping and distinct functions in cellular responses¹²⁸. Additionally, although there has been evidence that CD44 can also bind to some heparin-binding growth factors, cytokines and other ECM components, currently, signaling mediated by binding to hyaluronan accounts for the majority the functions ascribed to this receptor¹²³.

During infectious insults, CD44-hyaluronan interactions can also play an important role in the host response. As previously mentioned, LMW hyaluronan is considered more inflammatory than its HMW counterpart, and as such LMW-HA signaling was seen to increase the phagocytic capacity of macrophages for Group A *Streptococcus*¹²⁹. During bacterial pneumonia, the role of CD44 highlights a complex contribution for this receptor during infections that appears to be context dependent. Loss of CD44 during *E. coli* and *Klebsiella pneumoniae*-induced pneumonia resulted in increased inflammation, as well as increased neutrophil accumulation and bacterial outgrowth. In contrast, CD44 knockout mice with *Streptococcus*-induced pneumonia during prolonged lung infection had less bacterial outgrowth and dissemination. Additionally, one study

found that CD44-hyaluronan signaling was involved in upregulating expression of IP-10 during Hepatitis C (HCV) infection, indicating an increase in inflammation¹³⁰. Furthermore, CD44-hyaluronan interactions may play a role in promoting lung fibrosis in a model of interstitial lung disease (ILD) by activation of myofibroblasts and increased collagen production^{131,132}. Therefore, which cells are expressing CD44, the molecular weight of the hyaluronan present, isoform variation, and other considerations are likely important when understanding the contribution of CD44 to any particular insult.

Apart from CD44, it has also been observed that hyaluronan can signal through TLR2 and 4, which is mediated by the presence of structural motifs similar to those found in pathogen associated molecular patterns (PAMPs)¹³³. Signaling by LMW hyaluronan may drive inflammatory processes downstream of these receptors, while HMW hyaluronan interactions with TLR4 may actually protect against LPS-induced shock¹²². Together, these studies highlight the capabilities for HA to be a TLR ligand, while supporting the observation that fragment size is important for regulating the host response to hyaluronan.

1.3.3 Role in inflammation

As previously mentioned, during inflammation, hyaluronidases function to enzymatically break down hyaluronan into LMW fragments. While the contribution of LMW hyaluronan to inflammation is debated, it is widely believed that it promotes inflammatory responses, as well as angiogenesis, cell

recruitment, and cell migration^{117,121,133}. During pulmonary disease, hyaluronan has been associated with the formation of acute respiratory distress syndrome (ARDS), suggesting that hyaluronan can contribute to lung pathology¹³⁴. This function for hyaluronan is likely mediated primarily by one or both of its functions to bind water or regulate inflammation. The ability for hyaluronan to bind high quantities of water in the tissue could indicate that this is responsible for fluid accumulation, resulting in edema during inflammation¹³⁴. Additionally, it has been observed that breakdown of hyaluronan into LMW forms is associated with reduced endothelial and vascular integrity that can contribute to lung injury¹³³. In contrast, the presence of HMW hyaluronan has been shown to be important for tissue protection following inflammation in some models^{135,136}, which implicates a complex interaction of hyaluronan with inflammation and highlights the importance of understanding this polysaccharide within different contexts.

Similar to the lung, the function of hyaluronan in the intestine during inflammation or infectious disease is size and context dependent. During inflammation LMW hyaluronan fragments are predominantly found within the submucosa, compared to HMW hyaluronan, which is found directly beneath the epithelium during homeostatic conditions^{114,137}. This shift in localization and reduction in molecular size may facilitate its inflammatory properties and decrease its contribution to epithelial barrier protection. In a model of DSS colitis in mice, hyaluronan fragmentation preceded tissue damage and inflammation¹³⁷, and knockout of Has3 resulted in decreased leukocyte recruitment and

subsequent tissue damage¹³⁸. However, administration of larger molecular weight hyaluronan was able to decrease tissue inflammation, primarily by engagement with luminal TLR4 to promote epithelial repair. Whether this is size-dependent or the signaling contribution of luminal versus tissue hyaluronan should be further explored, but these data highlight the contributions of hyaluronan to intestinal immunity.

Increased expression of the enzymes responsible for hyaluronan production, hyaluronan synthases, is observed during many inflammatory processes including atherosclerosis, infections, cancer, autoimmune diseases, fibrosis, lung diseases such as asthma and COPD, and many others^{117,118,139,140}. Has1 for example, is upregulated by TGF- β and during renal disease and rheumatoid arthritis¹¹⁷. Both Has1 and Has2 were increased in lung tissue from a model of murine asthma¹¹⁸. Conversely, Has3 was increased in models of COPD¹¹⁸. During many contexts of inflammation, reduction of hyaluronan through hyaluronidase administration or preventing the synthesis of hyaluronan through the use of 4-methylumbelliferone (4-MU) reduced pathology, suggesting a causal role for HA in driving these diseases^{126,140}

1.3.3.1 Hyaluronan and CD44 during type 2 immune responses

In addition to the inflammatory processes described above, there has been an increased recognition for the contribution of hyaluronan and CD44 during asthmatic responses. Increased hyaluronan presence has been observed

in lung tissue and bronchoalveolar lavage (BAL) fluid from patients with asthma^{141,142}. Additionally, fibroblasts from patients with asthma produced higher levels of hyaluronan, primarily LMW, at baseline compared to non-asthmatic controls¹⁴¹. Together, these studies suggest that hyaluronan and CD44 may have some contribution to type 2-mediated disease; however, the drivers of this response during asthma are still largely uncertain¹⁴³. Patients with asthma who were treated with the anti-IL-5 monoclonal antibody mepolizumab had reduced hyaluronan in their sputum 16 weeks after treatment was started¹⁴⁴, suggesting type 2 cytokines could have some direct or indirect effect on hyaluronan deposition. In line with this, treatment with IL-4 or IL-13 resulted in increased hyaluronan production in human fibroblasts¹⁴¹ and keratinocytes¹⁴⁵, however, these studies did not delve further into the contributions of type 2 immunity to hyaluronan deposition in tissue.

While there is some evidence to suggest that hyaluronan is pathogenic during asthmatic responses, including increased TLR and IL-8 expression¹⁴¹, the contribution of hyaluronan during type 2-mediated inflammation is not fully understood. Given the ability for hyaluronan to decrease lung function, increase inflammation, and promote tissue remodeling such as fibrosis, it is likely that HA is involved in promoting pathogenic responses, however, future research into this area will be informative. Chapter 4 of this thesis will discuss the novel finding of the role for IL-13 in promoting hyaluronan deposition and increased disease severity in the lung during COVID-19.

1.4 *Clostridioides difficile*

1.4.1 Background

Clostridioides difficile (*C. difficile*), the Gram-positive, spore-forming, obligate anaerobe, is the leading hospital-acquired infection in the US, resulting in mild to severe diarrhea, pseudomembranous colitis, toxic megacolon, and even death. *C. difficile* infection (CDI) is most often associated with prior disruption to the normal colon microbiota as a result of antibiotic usage which allows for a competitive advantage for *C. difficile* growth. White blood cell (WBC) count above $20 \times 10^9/L$ and high levels of inflammatory cytokines in patients are indicators of severe disease, suggesting that the host response to infection plays a significant role in the outcome of patient morbidity and mortality^{146,147}.

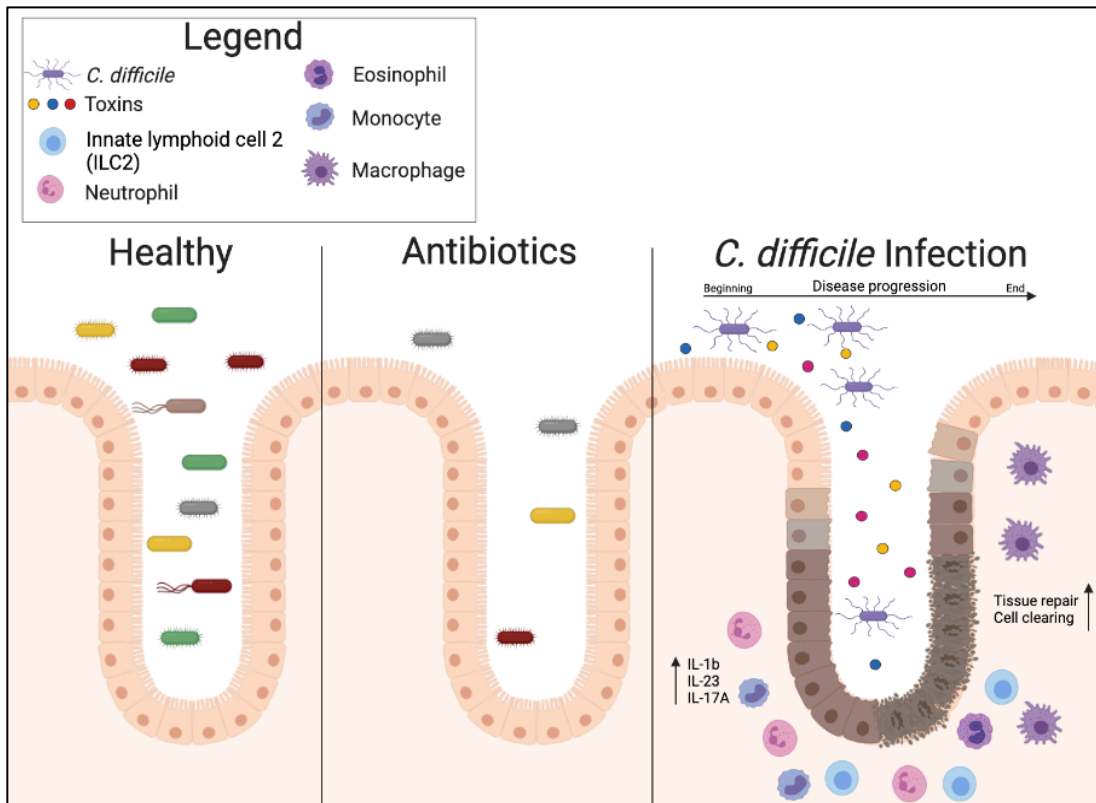
The two main virulence factors of *C. difficile* are Toxins A and B, which can lead to cell death and result in the characteristic epithelial damage associated with *C. difficile* infection¹⁴⁸. These toxins have been observed to activate the inflammasome, leading to a robust inflammatory response that, when in abundance, can be pathogenic and increase host morbidity and mortality¹⁴⁹. A more recently characterized toxin, now found in upwards of 20% of clinical isolates^{149–151}, is the binary toxin *C. difficile* transferase (CDT). CDT-producing *C. difficile* in research settings is often modeled by two Polymerase Chain Reaction (PCR)-Ribotype 027 strains, either M7404 or the epidemic strain R20291. While both express Toxins A and B as well as CDT, R20291 originated from an

outbreak in the UK, and M7404, from Canada^{152–154}. The presence of this toxin is associated with increased severity and mortality in patients^{155,156}, but the mechanism through which this occurs during disease have only recently been elucidated, and appears to involve Toll-like Receptor 2 (TLR2) signaling¹⁵⁷.

1.4.2 Pathogenesis

The most serious and common risk factor for contraction of *C. difficile* infection is the use of antibiotics, which disrupt the normal microbiota of the colon and may allow for competitive advantages for *C. difficile* (**Figure 1.1**)¹⁵⁸. The ability of the normal microbiome to outcompete pathogens for space and nutrients is called colonization resistance, which is thought to be the primary way that humans protect against CDI in the absence of antibiotic usage. Colonization resistance of the normal microbiota may be, in part, attributed to certain byproducts of resident commensal bacteria, including secondary bile acids such as deoxycholate¹⁵⁹. These bile acids may suppress ability of *C. difficile* spores to germinate within the colon, thereby preventing growth. However, with use of antibiotics, secretion of the secondary bile acid decreases, while primary bile acids such as taurocholate, increases. In contrast to secondary bile acids, taurocholate promotes germination of spores and vegetative cell expansion^{160,161}.

Figure 1.1. *C. difficile* Pathogenesis



Created with BioRender.com

Once spores germinate and grow within the large intestine, they can begin to produce their toxins, which results in high levels of epithelial cell death, recruitment of inflammatory cells, and fluid loss resulting in diarrhea (**Figure 1.1**). The contribution of toxins and inflammation to CDI will be discussed below.

1.4.3 Host immune response to *C. difficile*

1.4.3.1 Toxin-mediated inflammation

Infection with *C. difficile* is acute, is characterized by a high inflammatory profile, and the innate immune response is thought of as being highly critical¹⁶². *C. difficile*'s main virulence factors, Toxins A and B, are responsible for glycosylation of the Rho family of GTPases which causes the loss of activity of RhoA, Rac1, and Cdc42, and lead to epithelial cell death¹⁶³ and activation of the pyrin inflammasome^{164,165}. Through this, Toxins A and B can stimulate a potent proinflammatory response through IL-1 β , and IL-8, tumor necrosis factor alpha (TNF α), and IL-6^{166,167}.

The presence of the additional toxin, CDT, increases proinflammatory cytokines such as IL-1 β and IL-6 during infection¹⁵⁷ and has been associated with worsened disease in both humans and animal models. Through intoxicating BMDCs, it was observed that CDT, when administered with TcdA/B, led to a significant increase in IL-1 β production, a hallmark of inflammasome activation. When considered with previous data showing that TcdA/B were able to activate the inflammasome after it had been primed from upstream PAMPs or DAMPs, it

suggested the CDT is an efficient inflammasome primer. Thus, one of the mechanisms through which CDT increases virulence of *C. difficile* strains is by increasing the activation of the inflammasome, leading to abundant downstream pathogenic cytokines and inflammation. Concordantly, Cowardin et. al, observed that the absence of TLR2 abrogated the ability of cells to respond to CDT and loss of TLR2 in vivo abrogated the increased mortality due to CDT. This suggested that CDT was able to prime the inflammasome through recognition by TLR2, and that this was contributing to the increase in pathogenic inflammation caused by abundant inflammasome activation.

Beyond promoting increased inflammasome activation and inflammatory cytokine release, CDT may additionally increase disease severity by causing apoptosis of eosinophils in a TLR2-dependent mechanism.

1.4.3.2 Type 3 immunity

Following IL-1 β and IL-23 release by the activation of the inflammasome, type 3 immunity is induced as the primary immune response against *C. difficile*. IL-23 is important for differentiation of CD4+ T helper cells into Th17 CD4+ cells, which then produce IL-17A¹⁶⁸. This, in turn, is an important cytokine for the recruitment of neutrophils. Additionally, IL-23 itself can be important for the neutrophil recruitment and promotion towards an inflammatory state through STAT3 signaling¹⁶⁹. IL-1 β is another important inflammatory mediator for neutrophil recruitment and polarization of macrophages to pro-inflammatory

states. Additionally, IL-8 and CXCL5, both important for neutrophil recruitment, are recognized as biomarkers in patients for time to resolution from CDI¹⁷⁰.

Through the induction of these different cytokines, neutrophils are typically the primary innate immune cells responding to infection with *C. difficile*¹⁵⁸. High levels of neutrophilic responses have been associated with increased disease severity in patients^{171,172}, and treatments that result in reduced neutrophil responses, such as IL-25 or IL-33 administration, are associated with less severe disease in mice^{90,91}. However, it is recognized that neutrophils are important in protecting against *C. difficile*, likely by producing anti-microbial compounds that are effective in killing the bacteria. Neutropenia in patients has been associated with increased risk for primary and reoccurring CDI¹⁷³. Additionally, murine models lacking Toll-like receptor signaling and MyD88 are more susceptible to worsened disease⁸⁶.

Other cells associated with type 3 responses that are important for the host response include type 3 innate lymphoid cells (ILC3s) and Th17+ CD4+ T cells. IL-23 can induce IL-17A expression in ILCs, likely constituting another source of this pro-inflammatory mediator from the innate immune compartment¹⁷⁴. In a model of *C. difficile* infection following DSS colitis, it was observed that IL-17+ Th17 cells were important for promoting severity, and neutralization of IL-17A additionally provided protection from severe disease⁸⁸. In contrast, ILC3s have been reported to have protective effects during *C. difficile* infection, through the production of IL-22, which is an important type 3 cytokine,

but acts primarily through promoting epithelial repair. The contribution of IL-22 during CDI has been shown to be protective as a murine model lacking IL-22 was more susceptible to disease, highlighting that type 3 immunity impacts the host in multiple ways during *C. difficile* infection¹⁷⁵.

1.4.3.3 Protective type 2 immune responses

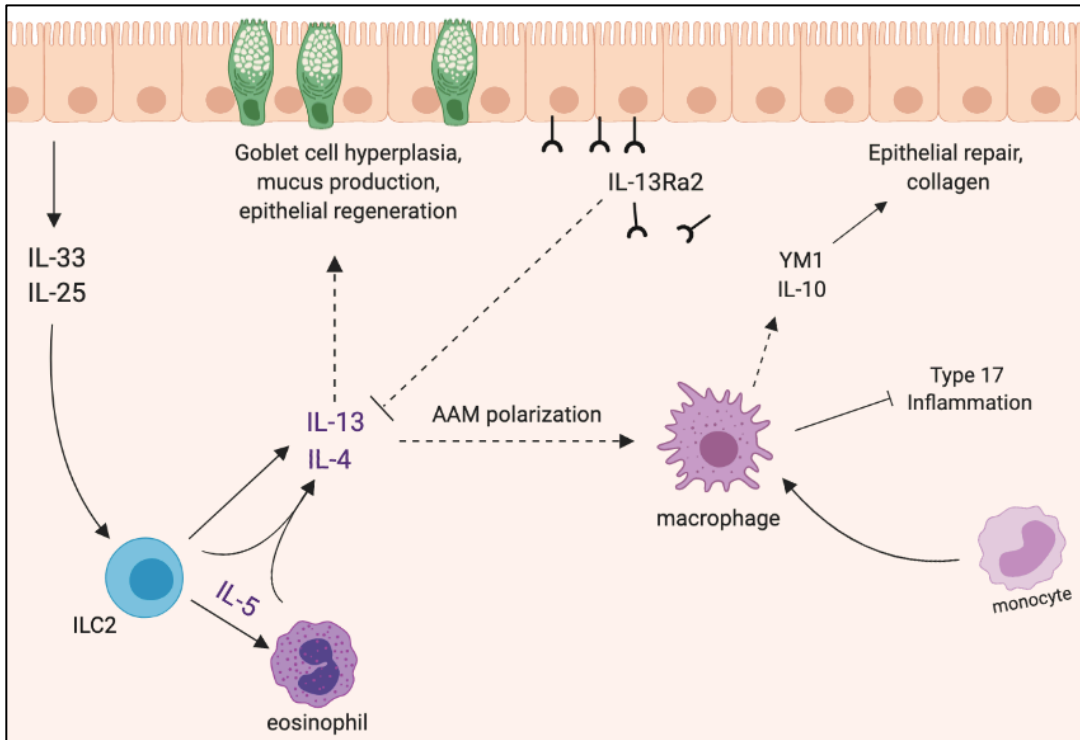
As discussed above, IL-25 is a type 2 alarmin cytokine, released by tuft cells, which can promote the induction of type 2 immunity. Buonomo *et. al*, showed that mice treated with recombinant IL-25 were significantly protected from CDI related mortality and morbidity, and had improved tissue damage when observed by histology⁹⁰. Further, the addition of IL-25 increased colonic eosinophil levels, and this was shown to be the mechanism by which IL-25 provided protection. Eosinophils in this model produced high levels of IL-4, suggesting this is one mechanism of protection by these cells. However, neutralization of IL-4 resulted in no protection from mortality, but rather impeded recovery from infection. The role of IL-4 during CDI will be discussed in chapter 2. The contribution of eosinophils to acute protection, however, is still unknown, but could be mediated by production of anti-microbial compounds or anti-inflammatory factors that reduce immunopathology.

In addition to IL-25, Frisbee *et al*, showed that another type 2 alarmin, IL-33, was important for providing protection from severe CDI⁹¹. In contrast to IL-25, IL-33 required ILC2s for protection, with a limited contribution of eosinophils.

Additionally, whereas IL-13 was reduced following IL-25 treatment, IL-33 increased IL-13 production, suggesting there were different mechanisms of protection downstream of these alarmins.

The importance of eosinophils and ILC2s during protection from *C. difficile* infection is highlighted by the increased disease severity in mice lacking either of these cells^{90,91}. Supporting the hypothesis that type 2 immunity can negatively regulate type 17 inflammation, administration of either of these cytokines resulted in decreased neutrophil recruitment and expression of proinflammatory cytokines such as IL-1 β , IL-6, and IL-23. Additionally, as discussed, infection with *C. difficile* results in large amounts of tissue damage following epithelial intoxication as well as production of inflammatory mediators which results in cell death. Promotion of type 2 responses by IL-25 or IL-33 protected against this damage, likely by decreasing pathologic inflammation or by increasing tissue healing responses.

Overall, the observation that type 2 immunity promotes protection in a model of CDI highlights the ability for this branch of immunity to suppress type 17 inflammation, which may prevent immunopathology. Given the importance of eosinophils and ILC2s during CDI, which produce IL-4, IL-5, and IL-13 (**Figure 1.2**), Chapter 2 and 3 will discuss the contributions of these cytokines to disease.

Figure 1.2. Type 2 immunity during *C. difficile* Infection

Created with BioRender.com

1.5 COVID-19

1.5.1 Background/history

SARS-CoV-2 was first identified in December 2019 in the Wuhan province of China¹⁷⁶, where it caused severe viral pneumonia. By March of 2020, COVID-19 was declared a global pandemic and has since resulted in high death tolls and burdens on the health care systems across the world.

Coronaviruses are a family of ssRNA viruses that primarily infect the upper respiratory tract and cause mild disease, including the common cold¹⁷⁷. However, three novel coronaviruses have emerged within the past 20 years that have highlighted the capacity of viruses in this family to cause severe disease in humans. Severe acute respiratory syndrome (SARS)-CoV, SARS-CoV-2, and Middle east respiratory syndrome (MERS)-CoV are three lower respiratory tract-infecting coronavirus species. SARS-CoV-2 is closely related to SARS-CoV, the cause of the 2002-2004 SARS pandemic. Both originated in Wuhan, Hubei Province, in China resulting from a zoonotic transmission from an animal reservoir, and both utilizing ACE2 as the host receptor for viral entry¹⁷⁷⁻¹⁷⁹. In contrast, MERS, which instead uses dipeptidyl-peptidase 4 (DPP4) as the receptor for viral entry¹⁸⁰, is not highly transmittable between human hosts, and therefore its spread has been contained to the middle east region where outbreaks occur occasionally due to additional spillover events from animal reservoirs¹⁷⁷.

1.5.2 Pathogenesis

SARS-CoV-2 infects cells through binding of the S2 subunit of the spike protein to ACE2, facilitated by TMPRSS2¹⁸¹, primarily on epithelial cells in the lower respiratory tract. Binding and fusion results in release of viral mRNA into the cytosol of the host cells, where it is replicated and transcribed. New virions are assembled by the Golgi and then released from the cell by exocytosis¹⁸², where they can infect additional host cells, or be released into the environment within respiratory droplets.

While SARS-CoV and SARS-CoV-2 are thought to be closely related, SARS-CoV did not become as widespread as SARS-CoV-2. Researchers believe this could be due to a variety of factors, including that SARS-CoV-2 has appeared to have a higher rate of transmission, which may have facilitated the higher incidence of cases across the world¹⁸³. Additionally, due to the higher case fatality rate of SARS-CoV compared to SARS-CoV-2 (9.5-11% vs estimated 1%)^{184,185,183}, public measures to combat the spread may have been more intense, contributing to the shorter duration of its presence in the human population. Furthermore, the peak viral load of SARS-CoV appeared during the second week of illness, after the onset of symptoms, which allowed for earlier detection and a lower degree of transmission¹⁸⁶. In contrast, SARS-CoV-2 titer peaks within the first week post-infection, indicating the hosts are highly contagious prior to symptom onset and potential detection¹⁸⁷⁻¹⁸⁹.

A vast majority of infected patients will effectively clear the infection (discussed below) and experience asymptomatic carriage or mild to moderate illness. However, some patients will progress to developing viral pneumonia, necessitating supplemental oxygen and in severe cases, intubation. A large study of COVID-19 patients from the UK has identified multiple mortality risk factors, including age, ethnicity, chronic illnesses, obesity, and immunosuppression¹⁹⁰. Additionally, the risk for severe disease is higher in males than in females^{191,192}, which may be attributable to increased inflammatory responses in males, although this requires further study. Understanding how these risk factors are associated with severe disease will likely involve complex interactions between genetics, environmental, cultural and economic contributions. The role of the immune response in contributing to severe outcomes will be discussed in this dissertation.

Currently, the anti-viral medication remdesivir is approved for use in patients¹⁹³. While this drug does have a positive outcome for the time to recovery in hospitalized patients, it does not confer a survival benefit¹⁹⁴, highlighting that viral load is not the only driver of disease.

1.5.3 Host Immune response to SARS-CoV-2

1.5.3.1 Antiviral Immune responses

Anti-viral immunity to SARS-CoV-2 is induced when the infected host cells detects viral nucleic acids through pattern recognition receptors (PRRs) including

Toll-like receptors (TLRs) and MDA5¹⁹⁵. This, in turn, results in induction of type 1 interferons, which are integral in anti-viral immunity. It may also result in pyroptosis, an inflammatory programmed cell death response^{196,197}, which is supported by the observation of elevated cytokines associated with pyroptosis, such as IL-1b and IL-18 in patients with COVID-19^{176,198–200}. Production and release of these cytokines promotes the recruitment of immune cells such as monocytes, macrophages and dendritic cells (DCs) which release more inflammatory mediators to combat infection, as well as process antigen for presentation to T cells. Within a few days, CD4+ and CD8+ T cell expansion and recruitment to the local tissue will occur, as well as antibody production from plasma cells. In healthy individuals, the adaptive immune response serves to kill infected cells and neutralize free virions, allowing for the containment and elimination of the virus. The adaptive immune response is then poised to respond rapidly to re-exposure to the SARS-CoV-2 virus and prevent reinfection.

While infection is a natural route through which a host can gain adaptive immunity, vaccine-promoted adaptive immunity is widely utilized to minimize the spread of the virus to prevent severe disease in susceptible populations, as well as to reduce variants from emerging. The first FDA emergency-use authorized vaccines for COVID-19 were approved in December of 2020 from Pfizer and Moderna^{201,202}. These employed a novel approach which delivered mRNA for the SARS-CoV-2 spike protein, packaged within lipid-nanoparticles, to cells. This vaccine platform allows host cells to transcribe the mRNA and express the

foreign protein on their surface, which would then generate an adaptive immune response. Like traditional vaccines, such as those using proteins or inactivated virus, mRNA vaccines promote antibody production by B cells, which recognize the spike protein. Because the spike protein is utilized by the virus to gain entry to host cells, antibody responses which interfere with the binding of spike to ACE2 can prevent cellular infection. In addition to humoral immunity by antibodies, this method is proposed to be advantageous over traditional vaccine strategies because the transcribed protein is also processed by the host cell to be presented on human leukocyte antigen (HLA) molecules to generate T cell responses. The addition of cell-mediated immunity provides another angle for which the immune system can contain viral replication and spread within a host. Following the second dose of either mRNA vaccine (Pfizer or Moderna), there is a decrease in illness of about 94%^{203,204}, highlighting the significant contribution these vaccines may play in limiting severe outcomes from disease.

1.5.3.2 Dysregulated host immunity

Regardless of risk factors, it has become evident that severe forms of disease are linked with host immunity. Characterization of patients' immune responses to the virus has provided insight into how infection results in severe disease as well as identifying potential targets for therapeutic interventions. Multiple cytokines and chemokines, including IL-1, IL-6, IL-8, IL-10, IL-13, TNF α , IP-10, and monocyte chemoattractant protein 1 (MCP-1)^{176,198,200} were

associated with hospitalization and intubation, suggesting that severe disease was accompanied or induced by a strong immune response. High levels of inflammatory mediators, such as these, have been associated with a response termed 'cytokine storm', which is associated with organ failure and potentially acute respiratory distress syndrome (ARDS), common complications of COVID-19. Further studies have indicated that dysregulated or inappropriate immune responses, including activation of immunosuppressive macrophages, exhausted T cells and ineffective anti-viral immunity²⁰⁵, contribute to unregulated cytokine production, tissue damage, and poor viral clearance.

Given the hyperinflammatory response that underlies severe SARS-CoV-2 infection, immunotherapeutics such as dexamethasone, a steroidal drug used to limit inflammation, have been used to treat infected individuals. Use of this treatment resulted in a 12% decrease in mortality in COVID-19 patients compared to usual care (29% vs 41%)²⁰⁶. However, given the variable nature of this disease and the negative side effects of steroid use, further research and additional therapeutics options, including non-steroidal immunomodulatory agents, will be important for providing more targeted and effective approaches.

1.5.3.3 Type 2 immunity in COVID-19

The presence of type 2 immune mediators has been measured in the plasma and tissue of COVID-19 patients, including IL-33, IL-4, IL-13, as well as IL-10. IL-33, which is an integral inducer of type 2 immunity, as an alarmin, has

been observed in COVID-19 positive patients, and is speculated to be an important contributor to pathogenic inflammation in hosts^{207,208}. IL-33 is an important mediator in driving ILC2 and CD4+ Th2 cell populations which can then express high levels of IL-4, IL-5, and IL-13. As such, the presence of ILC2s have been observed in patients with severe COVID-19, as measured within PBMC populations²⁰⁷.

The three effector cytokines IL-4, IL-5, and IL-13 have also been found to be elevated in patients with COVID-19 and severe COVID-19^{176,198}. It is believed that high levels of these cytokines in patients could be responsible for driving pathogenic lung damage and tissue remodeling, such as diffuse alveolar lung damage (DAD), similar to what is seen during other viral pneumonia responses. Furthermore, the presence of AAMs, which are polarized by type 2 cytokines such as IL-4 and IL-13, have been observed in patients with severe disease, suggesting they could be cellular sources of anti-inflammatory mediators such as IL-10, which could limit effective anti-viral immunity²⁰⁹. Additionally, the presence of IL-4 during severe disease is speculated to result in Sphingosine-1 expression in macrophages, which is associated with the formation of DAD²¹⁰. These macrophages may also be sources of collagen deposition, which could be associated with long-term fibrosis responses. However, not much is known about any potential long-term complications post-recovery, and studies into these so-called 'Long-COVID' outcomes will likely be the focus of many studies in the months and years following the pandemic.

Given the ability for type 2 cytokines, especially IL-13, to drive immunopathology during lung diseases such as asthma, it is hypothesized that type 2 cytokines contribute to disease severity in patients. Chapter 4 of this thesis will discuss the role for IL-13 in driving pathology during COVID-19, in part through hyaluronan and CD44 regulation (**Figure 1.3**).

1.5.3.4 Hyaluronan in COVID-19

In addition to typical immune responses mediated by cells and the cytokines they produce, the involvement of the extracellular matrix component, hyaluronan, has also been implicated in pathogenic responses to COVID-19. Elevated levels of hyaluronan have been found in the plasma and tissue of patients who were infected or succumbed to infection^{211–213}. Increased deposition, and especially degradation into lower molecular weight fragments, of this glycosaminoglycan is often driven by inflammation and can result in negative outcomes within tissues. The presence of hyaluronan was observed in respiratory secretions²¹³, lung autopsies²¹², and plasma samples of patients with severe COVID-19, including in patients who had developed ARDS.

Figure 1.3. IL-13 is induced during COVID-19 and increases hyaluronan and CD44 in the lung.

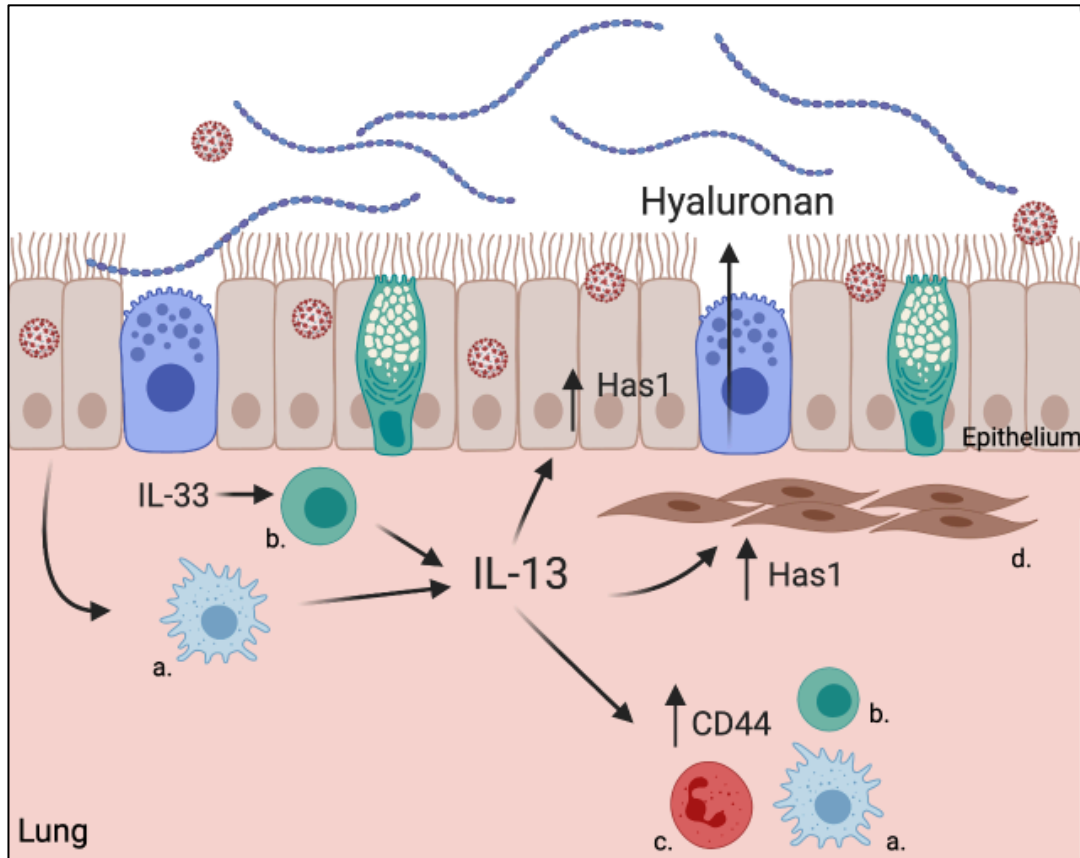


Figure 1.3. IL-13 is induced during COVID-19 and increases hyaluronan and CD44 in the lung. Infection by SARS-CoV-2 in the lung may result in activation of (a.) macrophages or release of IL-33 from the epithelium to promote (b.) type 2 innate lymphoid cells (ILC2s) to produce IL-13. IL-13 in the lung during infection upregulates CD44, likely in immune cells such as macrophages, ILC2s, or (c.) neutrophils. IL-13 also upregulates expression of hyaluronan synthase 1 (Has1) in structural cells such as (d.) fibroblasts or the epithelium. Has1 increases production of hyaluronan and the tissue and airspace of the lung. Created with BioRender.com

Since hyaluronan is associated with ARDS in other disease contexts²¹⁴, it is hypothesized that HA may be contributing to a pathogenic response in patients' lungs during COVID-19. This may be, in part, mediated by the ability for hyaluronan to bind large quantities of water, which can contribute to decreased lung mobility and function²¹⁴. Additionally, as hyaluronan can act as a matrix for immune cells to migrate over via CD44, modulate TLR signaling, or increase immune cell activation through LMW fragments, increased deposition could contribute to the increased inflammation that is observed in patients¹¹⁸. The potential role of hyaluronan and its receptor CD44 to COVID-19 severity will be discussed in Chapter 4.

1.5.3.5 Mouse models of COVID-19

In addition to what we have learned about host immunity in patients, mouse models of disease have been generated to address functional consequences of these responses, as well as to test vaccine and drug development. The most significant barrier to developing mouse models of SARS-CoV-2 infection is the inability of the wildtype virus to bind to the murine ACE2 receptor¹⁷⁹. Following the outbreak of SARS-CoV, which also used ACE2 to infect cells, murine models for disease were developed, providing researchers with an established platform quickly after the start of the 2020 pandemic. One such model was the K18-hACE2 transgenic mouse, which was developed in 2007²¹⁵. In these mice, human ACE2 expression is induced by the cytokeratin-18

(K18) promoter, driving ACE2 expression primarily in epithelial cells. In February of 2020, Jackson Labs began breeding these mice in hopes that they would provide a useful model for SARS-CoV-2. By August of 2020, Winkler et al reported that these mice were permissive to infection with SARS-CoV-2 and developed symptoms of disease²¹⁶. This mouse model will be utilized in Chapter 4 to study the role of IL-13 during COVID-19.

Additional models have been developed in addition to the K18-hACE2 mice and include the transfection by viral vectors^{217,218}, hACE2 expression driven by the mouse ACE2 promoter^{219,220}, or by another epithelial-specific promoter, HFH4²²¹. Additionally, a mouse adapted strain, MA10, was developed by serially passaging SARS-CoV-2 through wildtype mice until inoculation resulted in severe pulmonary disease²²². Each of these models is associated with certain advantages and disadvantages, and so consideration of the research question and objective is important for choosing which model would be most appropriate.

1.6 Conclusions

The host immune response plays a significant and necessary role in defense against pathogenic insults, but proper regulation and balance of an appropriate response is critical in the outcome and consequence for the host. The focus of this dissertation will be to discuss how type 2 immune responses have differential consequences during infection by two pathogens in the context of two different mucosal infection sites.

Considering that the contribution of the immune response to *C. difficile* may have a larger impact on host severity than bacterial burden¹⁴⁷, it is important to understand mechanisms by which the host can reduce pathogenic inflammation. The contribution of IL-25 and IL-33 to this regulation have been shown previously, but the downstream mediators IL-4, IL-5, and IL-13, had not been explored in this infection. We found that both IL-4 and IL-13 appear to have roles in driving host recovery from infection, which may be due to their contribution to anti-inflammatory pathways and tissue healing. We also found that IL-13 was associated with increased alternatively-activated macrophages, and decreased monocytes during the period of recovery from infection, suggesting a dysregulated monocyte-macrophage compartment may be impeding disease resolution. Lastly, IL-5, which is produced by ILC2s to recruit eosinophils - two cell populations important for protection from disease - was found to promote protection from CDI as well. Administration of IL-5 was associated with an increased proportion of eosinophils and decreased neutrophils. The first two chapters of this dissertation will discuss the importance of these type 2 effector cytokines during CDI.

In comparison, infection with SARS-CoV-2 is understood to be inflammatory but mechanisms driving disease severity are only beginning to be understood. Given that type 2 immunity, particularly IL-13, in the lung is an integral orchestrator of pathogenic lung inflammation, we wanted to understand what role it could be playing during this infection. IL-13 was found to be elevated

in patients requiring mechanical ventilation at two independent hospital sites, and patients with the highest levels of IL-13 were more likely to become intubated during their hospitalization. Using a the K18-hACE2 mouse model, we neutralized IL-13 during SARS-CoV-2 infection, and found that mice were significantly protected from disease. RNA-seq of lung tissue implicated *Has1* as being regulated by IL-13, suggesting a novel mechanism for IL-13 to induce hyaluronan deposition in the lung. Intranasal administration of IL-13 to naïve mice resulted in increased hyaluronan deposition, supporting this finding. Hyaluronan was elevated in patients with COVID-19 and neutralization of hyaluronan's receptor, CD44, also significantly reduced severity of disease in mice, highlighting a pathogenic role for this pathway. Our data suggest that targeting IL-13 or hyaluronan signaling during disease may be one mechanism through which to ameliorate severe outcomes in patients. The fourth chapter will focus on the role of IL-13 and hyaluronan in COVID-19.

While this dissertation will discuss the roles of three different cytokines, we were particularly interested in the observation that IL-13 was playing both a protective and deleterious role when comparing these two infections. As discussed above, the roles for IL-13 in the lung can include promoting tissue remodeling, inflammation, and other pathogenic responses, even given that IL-13 acts as an integral mediator of protective anti-helminth immunity. These poor responses may be facilitated to the inability for the lung to tolerate significant amounts of inflammation and tissue remodeling, especially in chronic settings,

which can decrease the ability for the tissue to expand and allow oxygen uptake. In contrast, in the context of hyperinflammatory settings during enteric infections, the anti-inflammatory roles for IL-13 likely serve to dampen pathogenic inflammation. Additionally, given the rapid turnover of the intestinal epithelium and potential higher tolerance for scar tissue formation and fibrotic responses, any deleterious contributions of IL-13 may be outweighed by the protective ones.

Overall, the work highlighted here increases our understanding of the roles type 2 cytokines IL-4, IL-5, and IL-13 can play during noncanonical type 2 immunity, and uncovers a novel role for IL-13 in promoting hyaluronan deposition.

**Chapter 2: Type 2 cytokines IL-4 and IL-5 reduce severe outcomes from
Clostridioides difficile infection**

This chapter was adapted from: Donlan, A. N., Simpson, M. E., & Petri Jr, W. A.
(2020). Type 2 cytokines IL-4 and IL-5 reduce severe outcomes from
Clostridioides difficile infection. *Anaerobe*, 66, 102275.

A.N.D. conceived, designed, and performed the experiments and wrote the
manuscript. M.E.S assisted with tissue and sample processing. W.A.P.
supported all aspects of the work.

2.1 Summary

Clostridioides difficile infection (CDI) is the leading cause of hospital-acquired gastrointestinal infections in the U.S. While the immune response to *C. difficile* is not well understood, it has been shown that severe disease is accompanied by high levels of infiltrating immune cells and pro-inflammatory cytokine production. This study tests the roles of two type 2 cytokines, IL-4 and IL-5, in mediating protection in a murine model of disease. Administration of IL-5 protected from mortality due to CDI, and both IL-4 and IL-5 were protective against severe disease symptoms. Together, the results from this study increase our understanding of how type 2 immune signaling processes are protective from severe *C. difficile* infection.

2.2 Introduction

Clostridioides difficile, a Gram-positive, spore-forming, obligate anaerobe, is the leading hospital-acquired infection in the US, resulting in mild to severe diarrhea, pseudomembranous colitis, toxic megacolon, and even death²²³. *C. difficile* infection (CDI) is most often associated with prior disruption to the normal colon microbiota as a result of antibiotic usage, which allows for a competitive advantage for *C. difficile* growth while also disrupting immune homeostasis facilitated by microbially-induced epithelial cytokines, including IL-25 and IL-33^{90,91}. Type 17 immunity is the predominant immune response against this extracellular pathogen, employing the recruitment of neutrophils to kill the

bacteria⁸⁶. In patients, however, a white blood cell (WBC) count above $20 \times 10^9/L$ and high inflammatory levels are indicators of severe disease, suggesting that the host response to infection may play some role in the outcome of patient morbidity and mortality¹⁴⁷. Accordingly, the use of host inflammatory markers such as TNF α and IL-8 have proven to be strong predictors of mortality in CDI patients¹⁷⁰. On the other hand, it has recently been shown that type 2 immunity is beneficial during infection with *C. difficile*. Type 2 immune responses generally refer to a profile of cytokines including IL-4, IL-5, and IL-13, as well as production of antibodies from plasma cells, particularly members of the IgE subclass¹. Often induced during infection with parasites such as helminths, these responses facilitate pathogen killing and expulsion from the host while attempting to limit excessive tissue damage and promote wound repair^{1,224}. Type 2 responses are also associated with allergies and asthma.

IL-33 was shown to protect from severe CDI by increasing IL-13 and IL-5-producing type 2 Innate Lymphoid Cells (ILC2s)⁹¹, while IL-25 was shown to increase protective IL-4-producing eosinophils in the colon⁹⁰. This protection was validated in humans, where it was observed that eosinophils were associated with survival from CDI²²⁵ while higher levels of the IL-33 decoy receptor sST2, which decreases IL-33 signaling, were associated with death⁹¹. IL-25 signaling in the intestine has previously been shown to increase ILC2 numbers and subsequent production of IL-5 to drive eosinophil recruitment^{20,226}, suggesting the same is true in the colon during CDI. Additionally, IL-4 is important for promoting

Th2 CD4⁺ T cell differentiation, IgE class switching, polarization of alternatively-activated macrophages (AAMs), and may be important for tissue repair²²⁷.

However, the role of IL-4 during *C. difficile* infection is not well understood.

To test our hypothesis that type 2 cytokines are protective during CDI, we infected mice with the epidemic binary toxin-expressing strain of *C. difficile*, R20291, which induces a more severe disease in mice¹⁵⁷. Then we administered IL-4 or IL-5 to mice during infection to observe their effect on survival and disease severity. Administration of either cytokine led to decreased disease severity or mortality, highlighting the beneficial capacity of a type 2 immune response within a highly inflammatory disease state.

2.3 Results

To induce susceptibility to *C. difficile*, we gave mice antibiotics in their drinking water prior to infection with 10^3 - 10^4 spores of the CDT-expressing epidemic PCR-Ribotype 027 strain of *C. difficile*, R20291¹⁵⁷. Because ILC2s, which are considered to be the main producers of the cytokine IL-5¹⁹, have been shown to be protective during CDI⁹¹, we wanted to test whether IL-5 was contributing to this ILC2-mediated protection. To do this, we administered 15 mg of recombinant IL-5 intraperitoneally on the day of infection¹⁹. We observed that the administration of IL-5 resulted in decreased clinical scores and mortality but no change in weight compared to vehicle control (**Fig. 2.1A, B and C**). Given

previous data showing that IL-25 is protective via eosinophils, this suggested that IL-5 may be an important part of this signaling pathway.

Because it has been previously shown that IL-5 is important for eosinophilia²²⁸, we performed flow cytometry on the colon on day 2 of infection to look at infiltrating immune cells. We observed a trend towards an overall decrease in total number of CD45+ immune cells and neutrophils, but no change in eosinophils (**Fig. 2.1D**). While we expected an increase in eosinophil numbers, IL-5 may have secondary roles in reducing total inflammation, meaning that increased proportion of eosinophils is indicative of increased recruitment. To this point, we observed the percentages of myeloid cells in the colon and found that there was a significant increase in the percent of eosinophils following IL-5 administration (**Fig. 2.1E**). Additionally, there was a corresponding decrease in the percentage of neutrophils after IL-5 administration.

Together, these data show that IL-5 reduced severe disease, and that this was likely due to a decrease in inflammatory immune cells such as neutrophils, and an increased proportion of eosinophils in the colon.

IL-25 administration in mice resulted in an increase in IL-4 producing eosinophils, and the concurrent neutralization of IL-4 with IL-25 administration did not negate IL-25-mediated protection, but rather, resulted in delayed recovery⁹⁰. To further investigate the role of IL-4 during CDI, we administered 5 µg of recombinant mouse IL-4 one day prior to infection. Due to the short half-life of IL-4 *in vivo*²²⁹, additional doses of 1 µg were also administered on the day of and

one day post infection. Mice who received IL-4 lost a similar amount of weight as compared to the vehicle control group, but regained weight more rapidly (**Fig. 2.2A**).

Similar to Buonomo et al., IL-4 treated mice also had lower clinical scores after day 3 of infection (**Fig. 2.2B**), indicating that this treatment reduced disease severity, especially during disease recovery. Given IL-4's known roles in tissue repair and inflammation resolution^{227,230}, this observation seems consistent with these functions. IL-4 did not have any impact on mortality from disease compared to control (**Fig. 2.2C**), suggesting that processes important for this may be upstream of IL-4.

2.4 Discussion

Here, we have shown that the type 2 cytokines IL-5 and IL-4 reduced severe disease during *C. difficile* infection, highlighting the general capacity of type 2 immunity to facilitate protection. This work builds on our understanding of the protection provided by IL-33 and IL-25, which were found to protect by limiting proinflammatory cytokines and cells, and protecting barrier function^{90,91}.

While ILC2s and eosinophils are protective during disease, the role of IL-5 had not been previously explored. Here, we have shown that IL-5 does provide protection from severe disease and mortality, and this corresponds with an increase in the proportion of eosinophils in the colon. We also observed a trend towards decreased immune infiltration, suggesting that IL-5 may contribute to

decreasing inflammation. It is important to note that administration of IL-5 did not fully phenocopy IL-25 administration⁹⁰, suggesting that there is signaling upstream of IL-5 that is important for IL-25-mediated protection.

IL-4 is also a type 2 cytokine that has been observed downstream of IL-33 and IL-25. Following IL-25 administration, the primary cell producing IL-4 in the colon was eosinophils⁹⁰, suggesting that eosinophils might protect by producing IL-4 during CDI. Here, we demonstrated that IL-4 protects against severe disease, as shown by a decrease in weight loss and clinical scores following infection. Interestingly, the most significant difference between the IL-4 administered group and vehicle control was during the later stages of infection, suggesting that the main contribution of IL-4 is during the period of recovery. Given that three days post infection is likely too early for the induction of adaptive immunity, this suggests that IL-4 is acting upon innate immune cells. These cells may be important for the clearance of inflammation or promotion of tissue repair, which would be critical to the resolution of disease.

Future experiments to determine the downstream mechanisms of IL-4 and IL-5 will be important to increase our understanding of the processes that contribute to beneficial immunity. Overall, this study shows that the type 2 immune cytokines IL-4 and IL-5 are protective during severe infection with *C. difficile*, supporting the observation that type 2 immunity defends the host against this disease. Utilization of this knowledge may lead to future immunotherapeutics for the treatment of this disease.

Figure 2.1

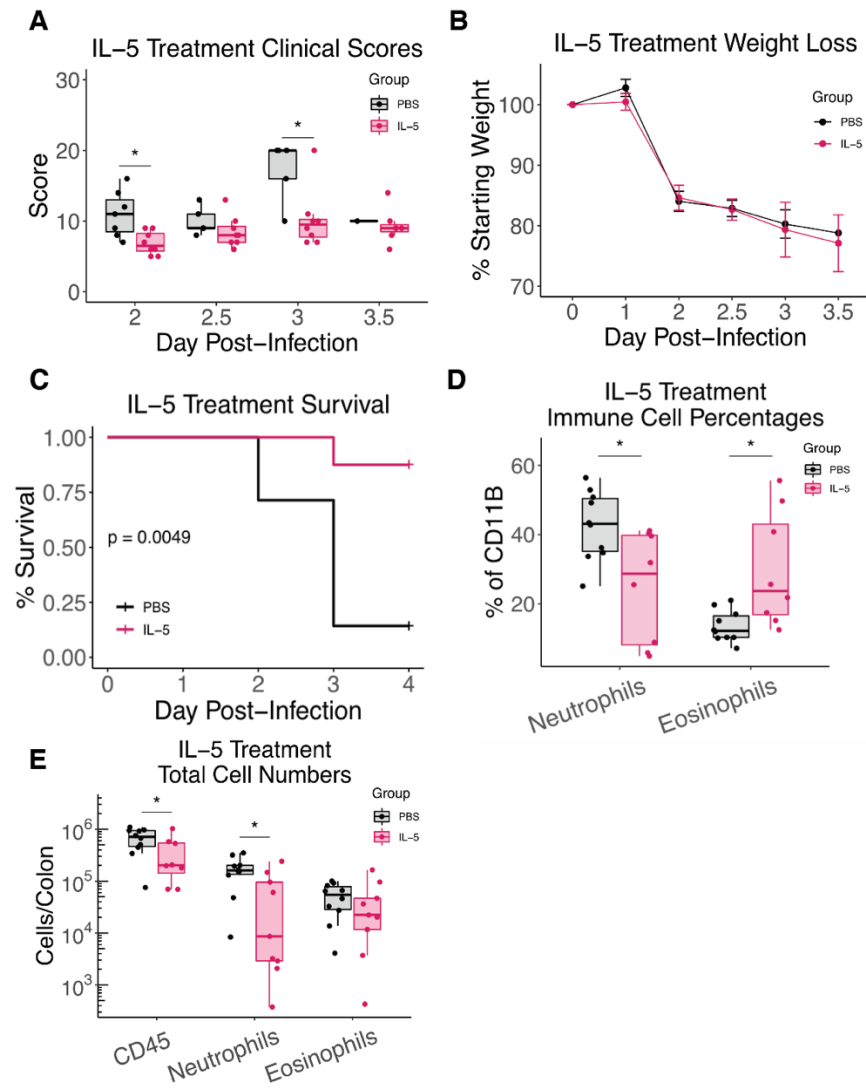


Figure 2.1. IL-5 protects from severe *C. difficile* infection and alters the immune compartment. (A) Mice were administered antibiotics in their drinking water for three days, followed by two days of clean water and one i.p. injection of Clindamycin before challenge with 10⁴ spores of *C. difficile* strain R20291 and i.p. injection of 5 mg rIL-5 or PBS control. Compared to control, mice treated with rIL-5 had (B) lower clinical scores, which are indicative of disease severity, and (C) reduced mortality by three days post-infection (DPI). (D) Mice treated with IL-5 did not have any change in weight loss compared for control. (E) Flow cytometry on colonic lamina propria cells was run on day 2 of infection. IL-5 treatment resulted in slightly lowered total CD45⁺ cells ($p = .06$), and significant reductions in neutrophils (CD11B⁺ Ly6G⁺ Ly6C⁻) ($p = .02$). (F) IL-5 treatment resulted in decreased proportion of neutrophils ($p = .018$) and an increased proportion of eosinophils (CD11B⁺ Siglec-F⁺) ($p = .027$) as a percentage of CD11B⁺ myeloid cells. N = 10 mice/group. Values shown with (*) are statistically ($p < .05$) different using a Student's t-test.

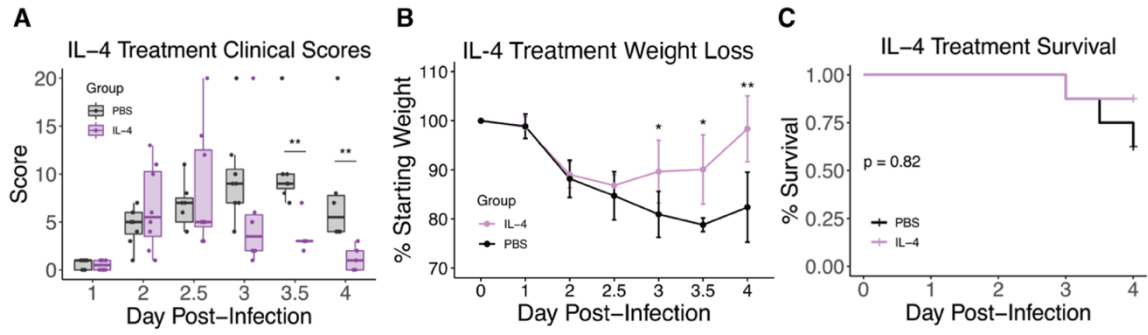
Figure 2.2

Figure 2.2. IL-4 protects from disease by enhancing recovery. Administration of rIL-4 on days -1, 0, and 1 (A), resulted in more rapidly recovered weight loss starting on day 3 of infection, compared to the PBS control group which began recovery on day 4 (B). (C) IL-4 treatment also resulted in decreased clinical scores on day 3.5 and 4. (D) Mortality between the two groups was not changed by IL-4 treatment. N = 10 mice/group. Values shown with (*) are statistically ($p < .05$) different using a Student's t-test.

Chapter 3: IL-13 promotes recovery from *C. difficile* infection

Donlan, A.N., Leslie, J.L., Simpson, M.E., Petri, W.A., Vasquez, T., Petri, W.A.

Jr, MD. PhD

A.N.D. conceived, designed, and performed all experiments and wrote the manuscript. J.L.L and M.E.S assisted in tissue processing and invaluable discussion. W.A.P. assisted with technical support and running of many experiments. T.V. performed IL-10, IL-6, and CCL2 ELISAs. W.A.P. Jr supported all aspects of the work

3.1 Summary

Clostridioides difficile infection (CDI) is the leading hospital-acquired infection in North America. We have previously discovered that antibiotic disruption of the gut microbiota decreases intestinal IL-33 and IL-25 and increases susceptibility to CDI. We further found that IL-33 promotes protection through type 2 Innate Lymphoid Cells (ILC2s), which produce IL-13. However, the contribution of IL-13 to disease has never been explored. We found that administration of IL-13 protected, and anti-IL-13 exacerbated CDI as measured by weight loss and clinical score, particularly during disease resolution. Additionally, concordant with IL-13 being important for M2 macrophage polarization, we saw a decrease in M2 macrophages (CD11B+CD64+CD206+) following neutralization of IL-13 ($7.3 \times 10^4 \pm 1.2 \times 10^4$ vs $3.1 \times 10^4 \pm 1.2 \times 10^4$; $p = .008$). We also observed monocyte accumulation as early as day three post-infection following IL-13 neutralization, suggesting IL-13 may be directly or indirectly important for their recruitment or transition into macrophages. Neutralization of the decoy receptor IL-13Ra2 resulted in protection from disease, likely through increased available endogenous IL-13. Our data highlight the protective role of IL-13 in promoting recovery from CDI, and the association of poor responses with a dysregulated monocyte-macrophage compartment. These results increase our understanding of type 2 immunity in CDI and may have implications for treating disease in patients.

3.2 Introduction

We have previously shown that administration of recombinant IL-33 during murine CDI provides protection from severe disease, and this was facilitated by type 2 innate lymphoid cells (ILC2s)⁹¹. During disease, ILC2s from IL-33-treated mice expressed increased levels of IL-13, implicating this cytokine in mediating protection from IL-33, but the role of IL-13 during CDI has not been explored.

IL-13 is an important effector cytokine for type 2 immune responses and has roles in driving polarization of alternatively-activated macrophages^{28,29}, decreasing Th17-associated inflammation^{61,93}, and promoting eosinophil recruitment as well as goblet cell hyperplasia²⁷.

As discussed in chapter 2, the closely related cytokine, IL-4, was increased following administration of IL-25, and neutralization of IL-4 resulted in delayed, while administration promoted, recovery in mice⁹⁰. Because of the similarity in functions to IL-4, we hypothesized that IL-13 would be important for during resolution from infection with *C. difficile*. Through neutralization and administration of IL-13, we observed that this cytokine was associated with promoting recovery from disease. We also observed that IL-13 neutralization was associated with increased Ly6C-high monocytes and reduced CD206+ macrophages, suggesting that these cells may impede or promote recovery responses, respectively. Together, our data shed light on another important contribution of type 2 immunity to protection from infection with *C. difficile*.

3.3 Results

To test the role of endogenous IL-13 during CDI, we infected mice with the R20291 spores of *C. difficile*, and administered i.p. injections of anti-IL-13 neutralizing antibodies or IgG control on days 0 and 2 post infection. Mice who received anti-IL-13 antibodies developed disease similar to control, but had delayed recovery by clinical scores and weight (**Figure 3.1A**). In contrast, administration of recombinant IL-13 promoted recovery in mice (**Figure 3.1B**). Neither neutralization or administration had significant impact on mortality due to disease (**Figure 3.1, C and D**). Together, however, this implicated the importance of IL-13 in promoting recovery in a murine model of CDI. Additionally, *C. difficile* burden was not different between IL-13 neutralized mice and controls on either day three or four post infection (**Figure 3.1E**), suggesting that changes to bacterial burden was not driving differences in recovery outcomes.

Because overabundant immune responses during CDI have been shown to be deleterious for host outcomes, we tested whether the neutralization of IL-13 was impeding the resolution of inflammation, resulting in delayed recovery. By day four post-infection, when mice typically would begin recovering, neutralization of IL-13 resulted in increased inflammation within the lamina propria. There were elevated levels of total immune cells (**Figure 3.2A**), as well as inflammatory myeloid cells such as neutrophils and monocytes (**Figure 3.2, B and C**). Because IL-13 can have an important role in promoting the polarization of alternatively-activated CD206+ macrophages^{29,30}, which can be important for

anti-inflammatory processes and tissue repair, we wanted to test whether changes to these cells due to neutralization may precede the increased inflammation seen on day 4. On day three post-infection, there were no differences in total number or proportion of CD64+ (FcGR1) macrophages²³¹ in the lamina propria, but there were significantly reduced CD206+ macrophages (**Figure 3.2E**). When gating on CD64+ cells, notably, we observed that there was a significant increase in a population of cells expressing low levels of this marker (**Figure 3.2F**). Using a waterfall plot, which shows the transition from Ly6C high monocyte, to MHCII+ tissue macrophage²³¹, we observed that these CD64-low cells were mainly LyC6-high MHCII low/-, suggesting that these cells represent monocytes that are beginning to differentiate into tissue macrophages. In contrast, CD64-high cells appeared to be comprised of cells further along that transition pathway from LY6C+ MHCII- monocytes to Ly6C-MHCII+ macrophages. Accumulation of these CD64-low, transitional cells, then, could be impeding recovery by contributing to increased inflammation. Additionally, this could suggest the reduced capacity of monocytes to transition into tissue macrophages due to potentially increased inflammatory environment. In support of this, although there was no change in CD64+ cells on day three post-infection, we observed a trend towards decreased CD64+MHCII+ macrophages (**Figure 3.3**) by day 4 post-infection. Together, these data support the hypothesis that there is dysregulated monocyte and macrophage responses following IL-13 neutralization.

IL-13 can promote the expression of IL-10 in AAMs⁴⁴, and as such, treatment with IL-13 also resulted in increased IL-10 expression by day 5 post-infection (**Figure 3.4**). IL-10 is a potent anti-inflammatory cytokine, which suggested that IL-10 could be important for IL-13-mediated recovery responses. Because alternatively activated, CD206+, macrophages have been implicated in the recovery and resolution of other inflammatory insults, we wanted to observe whether they corresponded to the recovery process of CDI. Using flow cytometry, we observed the myeloid compartment in the lamina propria of mice on days two, four, and five post infection, compared to uninfected mice with or without antibiotics (**Figure 3.5, A and B**). As expected, we saw an increase in inflammatory cells such as neutrophils and monocytes following infection. CD206+ macrophages were predominant in the uninfected colon, but expanded further by day 5 post-infection, suggesting they are associated with the recovery phase of disease (**Figure 3.5C**).

Next, we measured IL-13 levels during the disease course, but did not observe any increase in expression by ELISA (**Figure 3.5D**). The lack of increased protein could be compensated through potentially increased receptor expression facilitating increased signaling. IL-10, however, increased during disease recovery and was significantly correlated with IL-13 levels (**Figure 3.5, D and E**). YM1, a type 2 marker, was also increased following infection, supporting data from Frisbee et al. Additionally, as an indicator that a pro-inflammatory mediator was associated with acute disease as opposed to recovery, we

measured IL-6, which was most highly abundant on day two post-infection (**Figure 3.5D**).

Because CD206+ macrophages are typically monocyte-derived²³², to test whether CCR2+ monocyte-derived macrophages are important for infection, we depleted these cells using anti-CCR2 antibodies²³³, on day two post infection. Loss of monocytes at this time point resulted in worsened disease, suggesting an important contribution during host immunity (**Figure 3.6A**). However, this approach would additionally deplete monocytic lineages not dependent on IL-13, which may account for the large impact on survival outcomes. In contrast, monocyte depletion at earlier time points resulted in no change to disease (**Figure 3.6B**) which may suggest that early monocytes give rise to inflammatory cells that are balanced by anti-inflammatory cells generated at subsequent time points.

The decoy receptor for IL-13, IL-13R α 2, has been shown to be important for recovery in a DSS colitis animal model¹⁰⁵, and as such, we wanted to test whether this negative regulator of IL-13 could be involved in CDI as well. We measured levels of this receptor during infection by ELISA, and observed that it increased during the recovery phase of disease (**Figure 3.7A**). Since the expression of IL-13R α 2 is positively regulated by increased IL-13 signaling, as a method for negative feedback, this supports the hypothesis that IL-13 could be contributing during the recovery process. Additionally, IL-13R α 2 can be positively regulated by other proinflammatory factors such as TNF α and IL-17²³⁴. Since

both of these cytokines are increased during CDI in the animal model, this may indicate that the inflammatory response initiated by *C. difficile* infection is poised to dampen a type 2 immune response mediated by IL-13. IL-13R α 2 was also negatively correlated with weight (**Figure 3.7B**), further suggesting that high levels may not be beneficial to the host. To test the contribution of IL-13R α 2 to CDI, we administered neutralizing antibodies on days 1 and 3 post-infection. IL-13R α 2 neutralization resulted in improved weight and clinical scores, indicating that this decoy receptor negatively regulates protective type 2 immunity through IL-13 (**Figure 3.7C and D**).

3.4 Discussion

The importance of type 2 immune responses in protecting against pathogenic type 17 inflammation following *C. difficile* infection is further supported here, by the evidence that IL-13 contributes to recovery from infection.

IL-33 was previously shown to be protective during CDI through the induction of ILC2s, which in turn, produced higher levels of IL-13 following IL-33 treatment. However, the contribution of IL-13 during CDI had not been explored. Here, we report that neutralization or administration of IL-13 during a murine model of CDI had an impact on the recovery phase of disease, suggesting that IL-13 may contribute during this response.

IL-13 can be an important regulator of inflammation, and is often considered an anti-inflammatory cytokine outside the context of pathogenic type

2 inflammation such as asthma. Importantly, IL-13 is understood to contribute to the polarization of CD206+ alternatively-activated macrophages, which are generally associated with anti-inflammatory functions and tissue repair^{27,30,93}.

In our model, when IL-13 was neutralized, we did observe a decrease in CD206+ macrophages by day four post infection, implicating them as potential downstream mediators of IL-13 functions. We observed the highest levels of these CD206+ macrophages during the recovery phase of disease, highlighting that they may be involved in the process. Furthermore, we observed that neutralization of IL-13 resulted in increased Ly6C-high monocytes that accumulated in a transitional phase prior to becoming tissue macrophages. Whether this is due to increased chemokine expression, or if increased inflammation reduces the capacity for monocytes to transition into macrophages, is unknown. IL-13 has been observed to have roles in reducing CCL2 expression, resulting in decreased monocyte recruitment from the bone marrow. However, increased inflammation in the colon during DSS colitis was also associated with an accumulation of Ly6C-high monocytes²³⁵, suggesting that inflammation may have an impact on monocyte-derived macrophage development or accumulation of monocytes within the tissue.

Although IL-13 was induced downstream of IL-33, which protected mice from mortality and severity during acute disease, our data suggested that IL-13 was not the primary facilitator of acute protection awarded by IL-33. However, it is likely that IL-13 mediates many of the responses important for reducing

inflammatory cells within the tissue. The potential for this is highlighted by the increase in immune cells by day four post infection following IL-13 neutralization, suggesting the environment is more inflammatory.

We have previously shown that IL-4 is involved in the recovery from *C. difficile* infection⁹⁰. Given that IL-4 and IL-13 share a high degree of similarity in sequence, signaling, and influence on immune responses, it would be reasonable to hypothesize that these cytokines have overlapping functions during CDI. If one can compensate for the other when absent, it is possible that dual neutralization or administration may uncover a larger contribution for this signaling pathway during infection.

Overall, this work increases our understanding of the protective capabilities for type 2 immunity during *C. difficile* infection, and may represent broader implications for other enteric inflammatory responses.

Figure 3.1

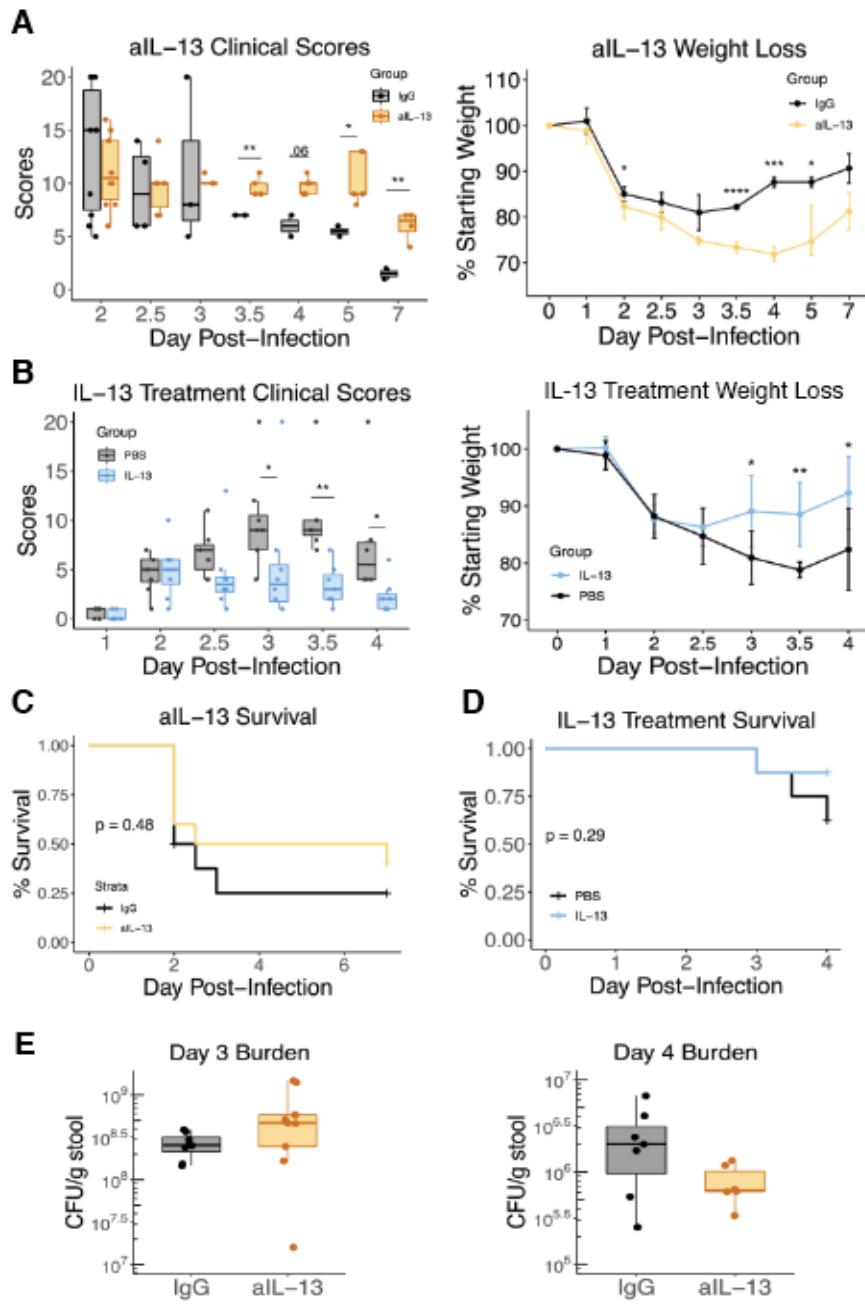


Figure 3.1. IL-13 provides protection from *C. difficile* infection. A) Weight loss and clinical scores for mice i.p. injected with 150 μ g of anti-IL-13 antibodies or IgG control on days 0 and 2 post-infection with 100-1000 spores of *C. difficile*. B) Weight loss and clinical scores of mice i.p. injected with 100 μ L of 5 μ g of recombinant IL-13 or PBS control. C,D) Kaplan-Meier curves for treatments in A) and B). E) *C. difficile* burden on days 3 and 4 post-infection. * = $p < 0.05$; ** = $p < 0.01$; *** = $p < 0.001$. Student t-test.

Figure 3.2

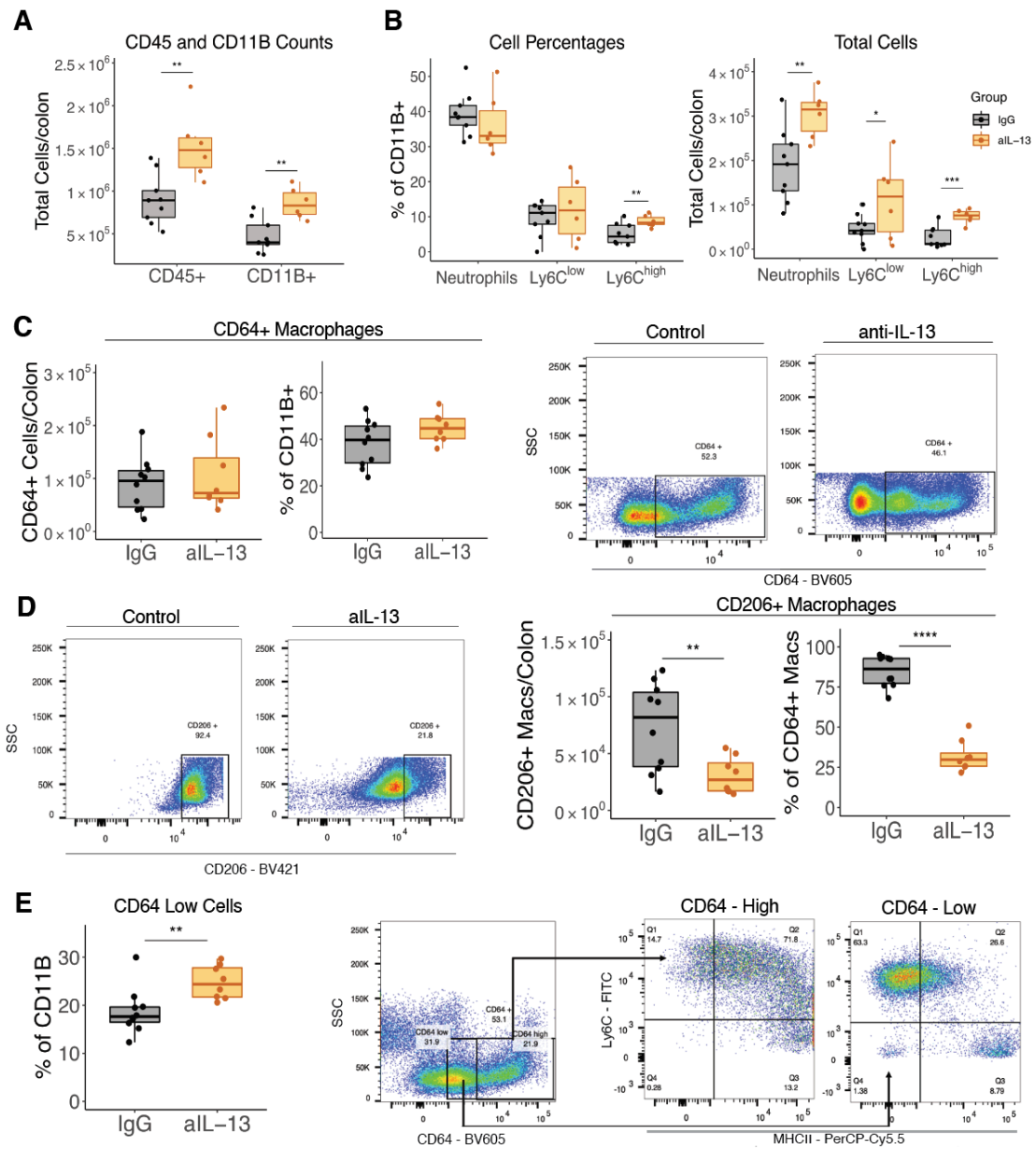


Figure 3.2. Neutralization of IL-13 increases inflammation and monocyte accumulation while decreasing abundance of CD206+ macrophages in the colon. Mice were treated anti-IL-13 antibodies on days 0 and 2 post-infection with *C. difficile*. A) Total number per colon of CD45+ and CD11B+ cells on day four post-infection. B) Total number per colon and percent of CD11B+ myeloid cells for CD11B+Ly6G+Ly6Clow neutrophils, CD11B+Ly6G-Ly6C -high and -low monocytes on day four post-infection. C) Percent of CD11B+ cell and total cells per colon of CD11B+CD64+ macrophages on day three post-infection. D) Representative flow plots of (C). E) Percent of CD64+ macrophages and total cells per colon of CD11B+CD64+CD206+ macrophages on day three post-infection. Representative images below. F) Percent of CD11B+ cells of CD11B+CD64-low cells on day 3 post-infection. G) Representative flow plot and waterfall plot (Ly6C vs MHCII) of CD64-low and CD64-high gated cells. . * = $p < 0.05$; ** = $p < 0.01$; *** = $p < 0.001$. Student t-test.

Figure 3.3

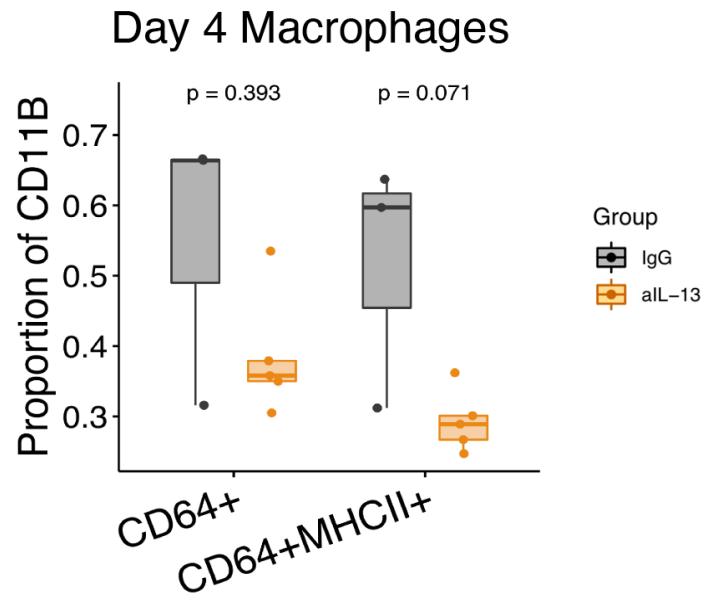


Figure 3.3. IL-13 neutralization results in trend towards decreased macrophages by day 4 post infection. Mice were treated anti-IL-13 antibodies on days 0 and 2 following infection with *C. difficile* and colonic tissue was taken on day four post-infection. Percent of CD11B for CD64+ and CD64+MHCII+ cells between IgG and anti-IL-13 treated mice. T-test; p values shown. N = 7.

Figure 3.4

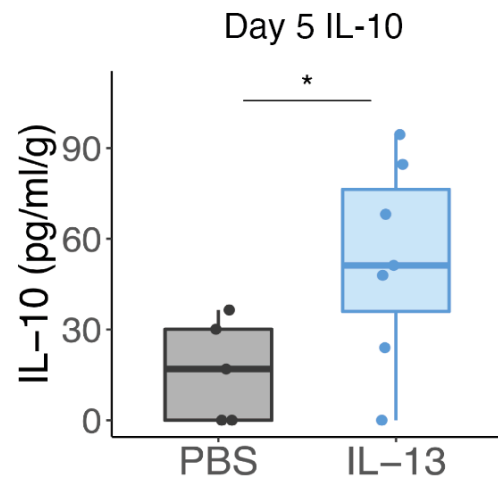


Figure 3.4. IL-13 treatment alters IL-10 on day 5 post-infection. Mice were i.p. injected with 100 μ L 5 μ g of recombinant IL-13 or PBS control on days 0, 1, and 2 post-infection with *C. difficile*. Cecal tissue was taken on day 5 post-infection and IL-10 levels were measured by ELISA and normalized to tissue weight. T-test; * = $p < 0.05$. N = 12.

Figure 3.5

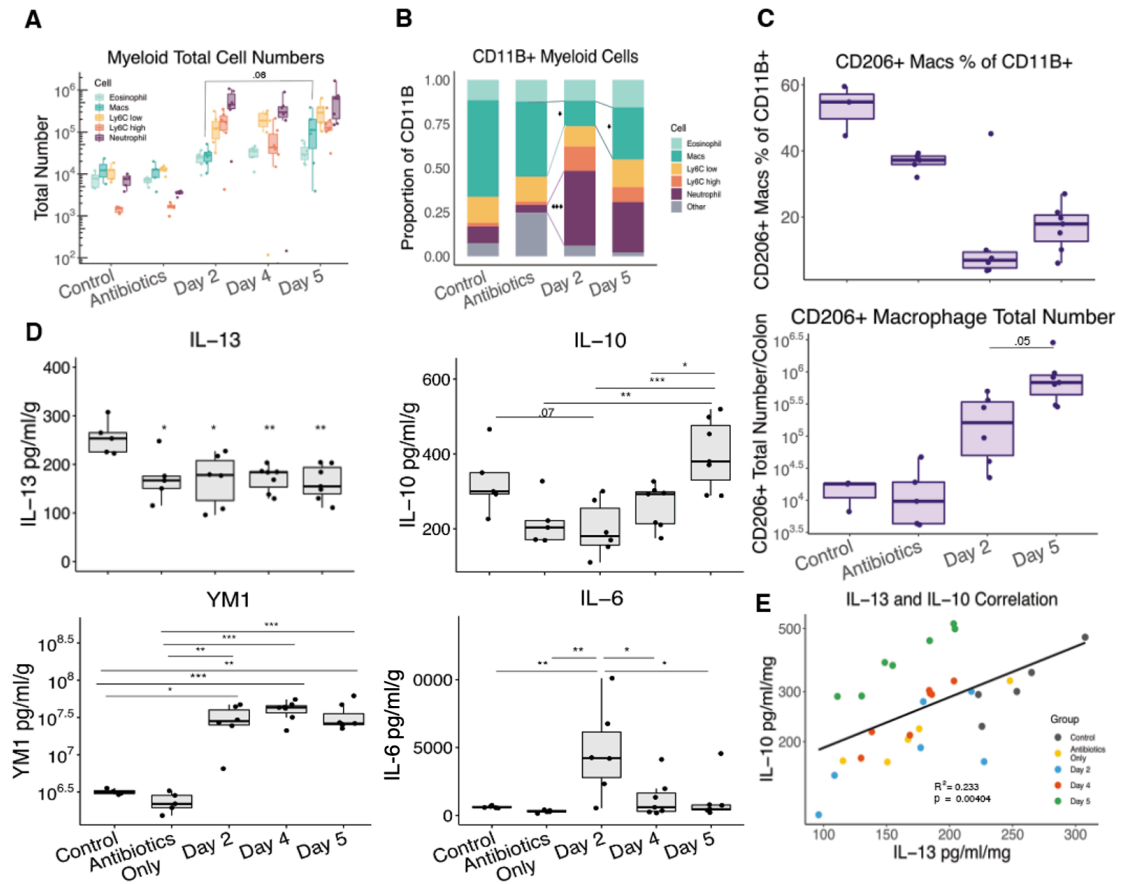


Figure 3.5. Recovery from *C. difficile* is associated with macrophages and anti-inflammatory cytokines. Mice were left as uninfected controls, or given normal antibiotic regimen with or without subsequent infection with 500 spores of R20291 *C. difficile*. Mice were euthanized on day 2, 4 and 5 post-infection. A, B) Total number per colon and percent of CD11B+ cells of neutrophils, monocytes, eosinophils, and CD64+ macrophages. C) Total number and percent CD11B+ cells of CD64+CD206+ macrophages. D) Cecal tissue was lysed and IL-13, IL-10, YM1, and IL-6 ELISAs were performed. E) Scatter plot showing correlation between IL-13 and IL-10. Colors indicate which group samples belong to. Linear regression and p-value shown. Tukey's HSD; * = $p < 0.05$; ** = $p < 0.01$; *** = $p < 0.001$. Student t-test.

Figure 3.6

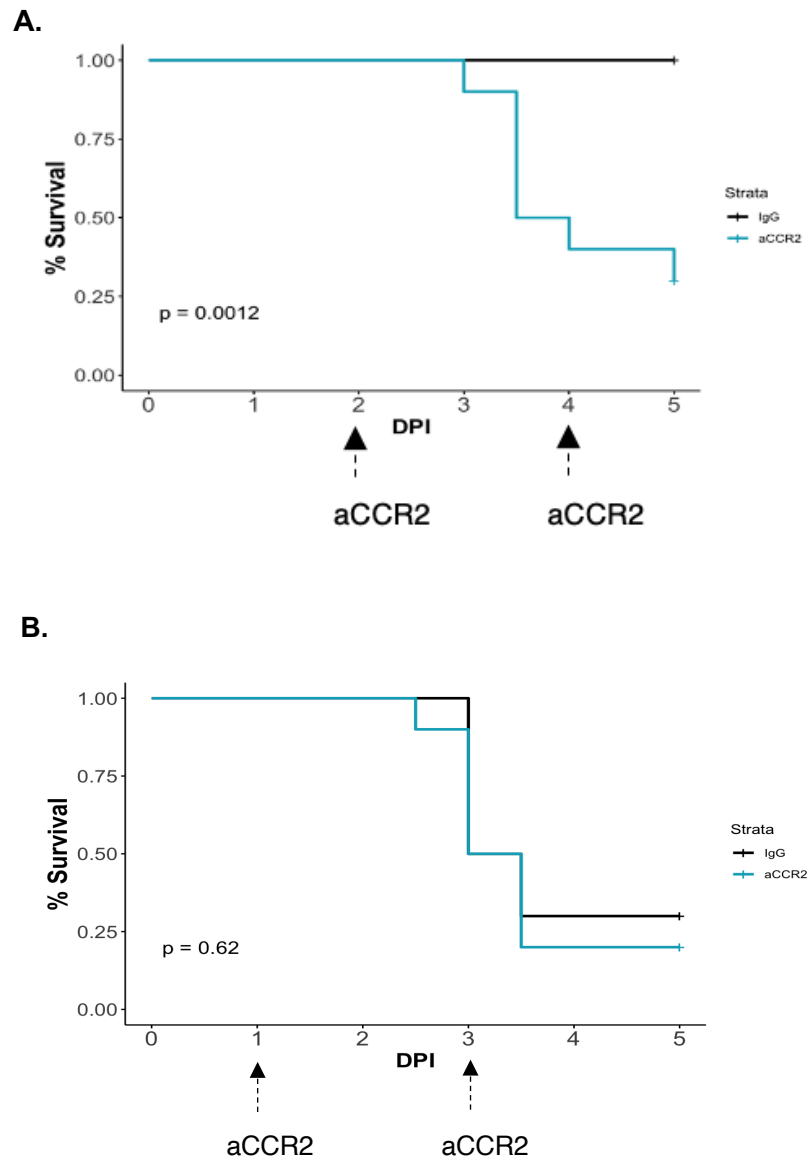


Figure 3.6. Depletion of monocytes at later timepoints worsens disease.

Mice were administered 500 μ g of anti-CCR2 depleting antibodies on days A) 2 and 4, or B) 1 and 3 post-infection. Kaplan-Meier curves shown (log rank test).

Figure 3.7

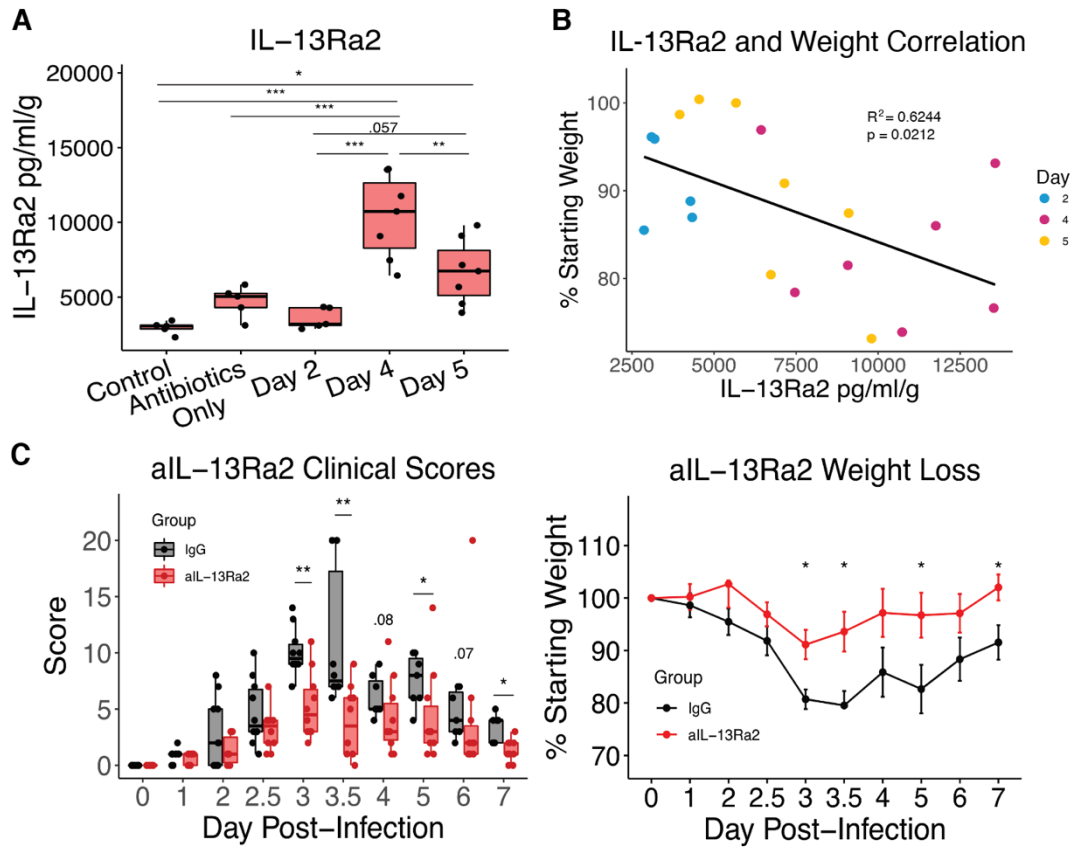


Figure 3.7. IL-13Ra2 neutralization protects during CDI. A) IL-13Ra2 protein levels in cecal lysates from days 2, 4, and 5 post infection and uninfected mice with or without antibiotic administration were tested by ELISA and normalized to tissue weight (Tukey's HSD). B) Linear regression of IL-13Ra2 levels with weight loss (Spearman). C,D) Mice were injected with 250 μ g of anti-IL-13Ra2 or IgG1 control on days 2 and 4 post infection. C) Clinical scores and D) weight loss (T-test). * = $p < 0.05$; ** = $p < 0.01$; *** = $p < 0.005$.

Chapter 4: IL-13 is a driver of COVID-19 severity

Authors: Alexandra N. Donlan, *Tara E. Sutherland, Chelsea Marie, Saskia Preissner, Benjamin T. Bradley, Rebecca M. Carpenter, Jeffrey M. Sturek, Jennie Z. Ma, G. Brett Moreau, Jeffrey R. Donowitz, Gregory A. Buck, Myrna G. Serrano, Stacey L. Burgess, Mayuresh M. Abhyankar, Cameron Mura, Philip E. Bourne, Robert Preissner, Mary K. Young, Genevieve R. Lyons, Johanna J. Loomba, Sarah J Ratcliffe, Melinda D. Poulter, Amy J. Mathers, Anthony J. Day, *Barbara J. Mann, *Judith E. Allen, *William A. Petri, Jr.

JCI Insight. In Press.

*Co-senior authors

The following authors contributed in Conceptualization (AND, TS, BM, AJD, WP); Methodology (SB, MA, GM, BM); Validation (JD, GB, MS); Formal analysis (TS, CM, SP, RP, BB, JS, JM, GL), Resources (AND, MP, AM, BB); Data Curation (MY, RC); Writing - Original Draft Writing (AND); Review & Editing (all authors); Visualization (AND); Supervision (WP, JA); Funding acquisition (WP, JA, RP, SP, JS, BB); Project administration (WP).

4.1 Summary

Immune dysregulation is characteristic of the more severe stages of SARS-CoV-2 infection. Understanding the mechanisms by which the immune system contributes to COVID-19 severity may open new avenues to treatment. Here we report that elevated interleukin-13 (IL-13) was associated with the need for mechanical ventilation in two independent patient cohorts. In addition, patients who acquired COVID-19 while prescribed Dupilumab, a mAb that blocks IL-13 and IL-4 signaling, had less severe disease. In SARS-CoV-2 infected mice, IL-13 neutralization reduced death and disease severity without affecting viral load, demonstrating an immunopathogenic role for this cytokine. Following anti-IL-13 treatment in infected mice, hyaluronan synthase 1 (*Has1*) was the most downregulated gene and accumulation of the hyaluronan polysaccharide was decreased in the lung. In patients with COVID-19, hyaluronan was increased in the lungs and plasma. Blockade of the hyaluronan receptor, CD44, reduced mortality in infected mice, supporting the importance of hyaluronan as a pathogenic mediator. Finally, hyaluronan was directly induced in the lungs of mice by administration of IL-13, indicating a new role for IL-13 in lung disease. Understanding the role of IL-13 and hyaluronan has important implications for therapy of COVID-19 and potentially other pulmonary diseases.

4.2 Introduction

SARS-CoV-2, the infectious agent causing the ongoing global COVID-19 pandemic, is a virus that primarily infects the lower respiratory tract of hosts by gaining entry to cells via the receptor angiotensin converting enzyme 2 (ACE2) facilitated by the transmembrane receptor neuropilin-1^{181,236}. The clinical course following infection varies widely from asymptomatic carriage to life-threatening respiratory failure and death.

Since early in the pandemic, it was recognized that patients with severe forms of disease, e.g. requiring hospitalization or ventilation, exhibited elevated levels of inflammatory cytokines²³⁷. This inflammatory state was associated with end-organ damage and in some cases death^{199,238}. While it remains unclear how the individual cytokines associated with this response may be involved in severe outcomes in patients, inflammation is thought to be a primary driver of later stages of this disease. In support of this hypothesis, the use of the anti-inflammatory steroid, dexamethasone, decreased mortality by 29% in COVID-19 patients who required mechanical ventilation²⁰⁶.

Aligned with these clinical observations, efforts to characterize the host response to infection and identify contributors to severe clinical outcomes have been ongoing since the pandemic began. Proinflammatory mediators such as the cytokines IL-6 and TNF α have been associated with severe disease. Cytokine-targeted therapies have been proposed and in some cases are in clinical trials. For example, the recently completed Adaptive COVID-19 Treatment Trial 2 (ACTT-2) showed a faster time to recovery with remdesivir plus the Janus kinase

inhibitor baricitinib compared to remdesivir alone²³⁹, as well as ACTT-4 which is comparing baricitinib plus remdesivir vs dexamethasone plus remdesivir (ClinicalTrials.gov Identifier: NCT04640168).

Descriptive studies of the immune response to SARS-CoV-2 have shown it to be highly heterogeneous^{240–242}, including the observations that CD4⁺ T cells from COVID-19 patients secreted the Th1 cytokine IFN- γ , the Th17 cytokines IL-17A and IL-17F, and the Th2 cytokine IL-4^{243,244}. This level of diversity and variability make it especially challenging to find specific drivers of disease and options for therapies. Consequently, understanding the mechanisms by which distinct immune responses contribute to COVID-19 severity will be crucial to designing personalized or targeted interventions, and ultimately to improve upon the current steroid-based treatments.

In this study, we characterized the immune response of patients with COVID-19 and identified the type 2 cytokine, IL-13 as associated with severe outcomes. Using a mouse model of COVID-19, we discovered that IL-13 promotes severe disease, and that this response is likely to be at least partially mediated by the deposition of hyaluronan in the lungs.

4.3 Results

IL-13 is associated with severe COVID-19 in two patient cohorts

We analyzed plasma cytokines in 178 patients with COVID-19 at the University of Virginia Hospital, 26 of whom received their care as outpatients and

152 as inpatients (**Table 4.1A**). Cytokines were measured in the plasma sample taken closest to the first positive COVID-19 RT-qPCR test (**Figure 4.1**). To understand the potential interrelationships between the different cytokines measured in our cohort, we generated a heatmap for patients, grouped by hospitalization and ventilation status (**Figure 4.2A**). While ventilated patients appeared to have elevated levels (dark purple) of many of the measured cytokines, there was a high degree of heterogeneity among the patients. Cytokines were arranged by principal component 1 (PC1) from **Figure 4.2B**.

The scatterplot of PC1 and PC2 from a principal coordinate analysis (PCA) (**Figure 4.2B**) showed separation, albeit with overlap, of outpatients, with less severe disease, (blue dots) from inpatients (yellow dots). IL-13 was in the top 6 of the 47 cytokines/growth factors in PC1 of the PCA (**Table 4.2**). This is of importance because the components estimated via PCA are able to retain information, separating patients by disease severity (inpatient vs outpatient). IL-13's position as a high-ranking contributor to PC1 suggested its overall importance in the disease process. Additionally, network analysis of all of the cytokines measured showed the close relationship between IL-13 and other type 2 cytokines identified in PC1, including IL-9 and IL-25 (**Figure 4.3A**).

IL-13 is implicated in numerous processes, including (i) recruitment of eosinophils and M2 macrophages to the lung, (ii) induction of mucus secretion into the airways and goblet cell metaplasia, (iii) proliferation of smooth muscle cells, and (iv) fibrosis via fibroblast activation and subsequent collagen

deposition^{245,246}. Therefore, IL-13, as an integral orchestrator of pathogenic responses in the lung, was of particular interest to us. Plasma levels of IL-13 were significantly higher in COVID-19 positive patients compared to uninfected patients (**Figure 4.2C**), consistent with previous reports^{176,200,247}. Moreover, we found plasma IL-13 levels were also significantly elevated in patients who required mechanical ventilation (**Figure 4.2D**). Additionally, when stratified into three IL-13-expression level groups, patients in the higher-expressing tiers were more likely to be ventilated and the risk of ventilation was 2.7 times for those in the top tier compared to those in lowest tier (HR 2.71; 95% CI, 1.11-6.58) (**Figure 4.2, E and F**). To determine whether this association with IL-13 and disease severity was not because patients who required ventilation had elevated cytokines due to a longer duration of illness by the time their sample was taken, we performed a linear regression between IL-13 and days from symptom onset to blood draw (**Figure 4.3B**) and saw no significant correlation. However, we did observe that IL-13 plasma levels increased from patients' initial to secondary blood draw, on average (**Figure 4.4**), suggesting levels of IL-13 could be increasing within an individual patient's disease course. To assess the ability of IL-13, alone or in combination with other cytokines, to be able to predict ventilation outcomes in patients, we performed a receiver operating characteristic (ROC) analysis. We found that IL-13 alone performed modestly (area under the ROC curve [AUC] = 0.659). Inclusion of the cytokine IL-6 increased the predictive capability (AUC = 0.775), and additional inclusion of IL-8 and MIP- β further

improved the model (AUC = 0.822) (**Figure 4.2G**). To validate results from the University of Virginia Hospital, cytokines from an additional 48 inpatients with COVID-19 from Virginia Commonwealth University Medical Center were analyzed (**Figure 4.1B and Table 4.3**). IL-13 levels measured in plasma were found to be elevated in the hospitalized patients who received oxygen via high flow nasal canula or mechanical ventilation compared to inpatients who did not (**Figure 4.2H**).

Consistent with our study, Lucas *et al.* 2020 found that IL-13 increased from day 5 to 20 of illness in severe COVID-19 patients requiring ICU and/or mechanical ventilation. Together, these data highlight that IL-13 may be an important component of host responses to SARS-CoV-2 infection and could be driving severe disease.

Type 2 immunity is induced in k18-hACE2 mice

To test the contribution of IL-13 to respiratory failure in COVID-19, we utilized a K18-hACE2 transgenic mouse model of COVID-19^{216,248,249}. In this model mice progress to severe disease starting at day five post-infection (pi) with SARS-CoV-2, with most mice succumbing to infection by day seven or eight.

We characterized the impact of SARS-CoV-2 infection in the mouse lung. We performed an analysis of differentially regulated genes from whole tissue RNAseq using Reactome, an open-sourced tool for pathway analyses. This revealed a significant enrichment of genes involved in IL-4 and IL-13 signaling in

infected lung (FDR adjusted p-value = 0.03) on day five post infection (**Table 4.4**). Importantly, *Il4ra* and *Il13ra1* were upregulated, indicating the potential for increased signaling even in the absence of detectable increases in cytokine expression. Additional type 2 immune effectors known to be regulated by IL-4 and IL-13 including *Chitinase-like 3 (Chil3)*, *Resistin-like alpha precursor (Retnla)*, *Ccl11* and *Arginase 1 (Arg1)* were impacted by SARS-CoV-2 infection (**Figure 4.5A**).

In support of enhanced type 2 associated genes, protein expression of Ym1 (*Chil3*) and RELM α (*Retnla*) was increased in the lungs following infection (**Figure 4.5, B and C**), as measured by immunohistochemistry (IHC). Together, this highlighted that many components of type 2 immunity were induced in the lungs due to infection. It is important to note that IL-4 and IL-13 share a receptor subunit and induce common pathways, so it is difficult to delineate their respective contributions to the upregulation of type 2 effector genes²⁴. However, because we observed an association of IL-13 but not IL-4 (**Figure 4.1**) with severe disease in patients, we hypothesized that IL-13 signaling in the lung following infection was contributing to worse outcomes.

IL-13 neutralization in mice reduces disease severity

To directly test whether IL-13 was deleterious following SARS-CoV-2 infection, we administered intraperitoneal (i.p.) injections of anti-IL-13 or an isotype matched control IgG on days 0, 2 and 4 post infection. Infected mice

receiving anti-IL-13 had significantly reduced symptoms as measured by clinical scores²⁴⁸ (**Figure 4.6A**), weight loss (**Figure 4.6B**) and mortality (**Figure 4.6C**), demonstrating a pathogenic role for this cytokine during disease. Importantly, anti-IL-13 did not alter viral load in the lungs on day five (**Figure 4.7A**), suggesting disease amelioration was not due to reduced infectious burden but likely due to events downstream of IL-13 signaling.

Dupilumab is a monoclonal antibody that blocks IL-13 and IL-4 signaling. It is directed against the IL-4R α subunit that is shared with the IL-13 receptor²⁵⁰. Based on our findings, we considered the possibility that patients prescribed Dupilumab for asthma, atopic dermatitis or allergic sinusitis may be protected from severe COVID-19. To test this hypothesis, we conducted a retrospective analysis of a large international COVID-19 cohort comprised of 350,004 cases; 81 of which had been prescribed Dupilumab prior to, and independently of their COVID-19 diagnosis (**Table 4.5**). We generated a sub cohort using 1:1 propensity score matching as well as an additional sub cohort for patients with diagnosed asthma, atopic dermatitis or rhinosinusitis, for which Dupilumab is prescribed. Importantly, Dupilumab use was associated with a lower risk of ventilation and death in COVID-19 (**Figure 4.6D** and **Table 4.6**). To assess whether Dupilumab was associated with clinical proxies of inflammation, we also examined levels of C-reactive protein (CRP), an acute phase protein that increases during inflammation and correlates with poor outcomes in COVID-19²⁵¹. CRP levels were reduced in Dupilumab-prescribed patients with COVID-19

(**Table 4.7**), suggesting that blocking type 2 immunity may lower over-all disease pathology and increase survival rates. As a validation cohort we also examined Dupilumab and COVID-19 in the National COVID Cohort Collaborative (N3C). The 31 patients who contracted COVID-19 while on Dupilumab also had a lower rate of hospitalization, ventilation, and death compared to matched controls (**Table 4.8**).

To further understand the potential mechanism by which IL-13 exacerbated disease we used the mouse model to ask whether the reduction in disease severity following IL-13 neutralization corresponded with changes in the lung tissue. We therefore assessed histological parameters of pathology by H&E staining. We have previously reported that infection with SARS-CoV-2 in this model results in lung damage²⁴⁸, however, IL-13 blockade resulted in little change in lung injury (**Figure 4.7, B and C**). In contrast, goblet cell metaplasia was subtly, albeit significantly, induced following infection, and this increase was reduced by neutralization of IL-13 (**Figure 4.7D**). During type 2 inflammation in the lung IL-13 is a significant driver of goblet cell responses²⁴⁶ (14), and our data provide evidence that IL-13 signaling is active in COVID-19 but less dramatic, histologically, than in other models of type 2 immunity^{252,253}.

To further investigate how IL-13 neutralization protected from COVID-19, we assessed expression of the type 2 associated proteins Ym1 and RELM α . Fluorescence microscopy of the lung revealed a significant decrease in RELM α following neutralization of IL-13, which was evident in both the parenchyma and

within the epithelial cells (**Figure 4.6, E and F**). However, no change in Ym1 following IL-13 neutralization was detected (**Figure 4.7E**). In addition, no overt changes in cytokine levels or cell composition in the bronchoalveolar lavage fluid (BALF) were observed (**Figure 4.7, F and G**). We concluded that the mechanism by which IL-13 was promoting more severe COVID-19 was not necessarily through the type 2 pathways typically observed in the lung.

Hyaluronan is associated with severe COVID-19

Given the above, we took an unbiased approach to evaluate the impact of IL-13 during COVID-19. RNA-seq analysis was performed on whole lung tissue from IL-13-neutralized and control-treated mice at day five pi to evaluate transcriptional responses downstream of IL-13. Intriguingly, this analysis identified the enzyme hyaluronan synthase 1, *Has1*, which was upregulated during infection, as the most downregulated gene following IL-13 neutralization (**Table 4.9 and Figure 4.8A**). In addition to *Has1*, other genes associated with the signaling or synthesis of the hyaluronan (HA) polysaccharide, *Cd44*, (**Figure 4.8A**) and *Has2* (**Figure 4.9A**), respectively, were also downregulated following IL-13 neutralization. Additionally, hyaluronidases, which break down hyaluronan that has been endocytosed, were upregulated during infection (**Figure 4.8A and Figure 4.9A**) altogether supporting a potentially role for hyaluronan during COVID-19. Deposition of this polysaccharide was found to be significantly increased in SARS-CoV-2 infected compared to uninfected mice, specifically in

the parenchyma of the lungs (**Figure 4.8, B and C**). Following IL-13 neutralization in infected mice, hyaluronan deposition was significantly reduced in the parenchyma (**Figure 4.8, B and C and 4.9B**).

Our finding in the mouse model that IL-13 regulates the HA pathway in COVID-19 was noteworthy as there is evidence to support a pathological role for HA in humans with lung disease¹²⁶ including COVID-19^{140,211,212,254,255}. We observed that patients infected with SARS-CoV-2 had higher plasma levels of hyaluronan (**Figure 4.8D**). Additionally, hyaluronan was elevated in the postmortem lung tissue from patients who died of severe COVID-19 (**Figure 4.8, E and F, and Figure 4.9H**), supporting prior observations²¹². It is important to note, however, that hyaluronan can be elevated due to an array of factors, including occupation, respiratory diseases, or other infections unrelated to SARS-CoV-2²⁵⁶, which likely accounts for the variation in COVID-19 negative patients. One uninfected patient, in particular, with high levels of hyaluronan had died due to cardiac arrest while experiencing a post-operative wound infection, both which could have resulted in the increased hyaluronan that we observed.

In a murine influenza model, administering hyaluronidase to break down pathogenic HA resulted in ameliorated disease¹²⁶. We followed a similar approach to test the impact of hyaluronan during COVID-19, by administering hyaluronidase i.n. on day five pi. This resulted in modest, albeit not statistically significant, protection from weight loss and clinical scores (**Figure 4.9, D-F**). This could suggest that IL-13-dependent accumulation of hyaluronan may not act

alone to drive severe disease, or that timing of hyaluronidase administration is for the effect this treatment may have. Importantly, however, bovine hyaluronidase used here also reduces chondroitin sulfate²⁵⁷, which may have unpredictable effects. We therefore pursued this observation by testing if blockade of the hyaluronan receptor CD44, which was also downregulated by IL-13 neutralization (**Figure 4.8A**), would be protective. This receptor is present on multiple cell types, including inflammatory cells, that may utilize CD44-HA interactions for migration, activation, proliferation, or other functions that could contribute to pathogenic responses^{258,259}. Blockade of CD44 from days one through four post-infection resulted in improved clinical scores and survival (**Figure 4.8, G and H** and **Figure 4.10G**).

Because the finding that neutralization of IL-13 during COVID-19 led to reduced hyaluronan deposition was novel, we investigated whether IL-13 administration could directly result in increased hyaluronan deposition in the lungs of mice. To uninfected mice, we administered IL-13Fc intranasally (i.n.) on days zero and two, before collecting lung tissue and sera on day three. This resulted in significantly increased deposition of hyaluronan in the tissue by IHC (**Figure 4.11, A-D**), as well as increased levels of hyaluronan in the serum (**Figure 4.11E**) supporting the discovery that IL-13 can regulate hyaluronan deposition and accumulation in the lungs. Together, these data indicated that hyaluronan production and signaling are downstream of IL-13 and contribute to disease outcome in mice and patients.

4.4 Discussion

Here, we have shown that the type 2 cytokine, IL-13, is associated with severe COVID-19. The IL-13 blocking drug, Dupilumab, in turn is associated with better outcomes in COVID-19 patients and additionally, neutralization of IL-13 in mice infected with SARS-CoV-2 protects from death, in part by blocking excessive hyaluronan synthesis and excessive deposition. Overall, this work opens a new avenue in the study of COVID-19 by demonstrating a causal role for type 2 immune responses and downstream hyaluronan accumulation in respiratory failure, and offers potential avenues for immunotherapy of this disease. Considering the extreme heterogeneity in immune responses to COVID-19 it is unlikely that IL-13 blockade will work in all patients. Nonetheless, understanding the underlying mechanism and identifying those most likely to benefit from such a treatment would be a major advance.

The mechanism through which IL-13 promoted severe disease was challenging to identify, as there was only a modest impact on the downstream effectors of IL-13 that are commonly seen during allergic or asthmatic inflammation. Although there were decreases in type 2 associated responses, e.g., goblet cells and RELM α , following IL-13 blockade, the biological significance of their contribution was likely minimal given the low magnitude of their induction compared to other models of type 2 immunity in the lung. Additionally, periostin, a marker for asthma responses in the lung²⁶⁰ was also decreased following IL-13 neutralization (data not shown), suggesting the

neutralization of IL-13 was affecting typical downstream pathways. However, it was not increased following infection, indicating that asthmatic-like responses such as eosinophilia or tissue remodeling were not occurring by day five post-infection.

Notably, in our RNAseq dataset Stat6 and Gata3 were not upregulated during COVID-19 in mice, which may reflect an inability to detect changes in these mRNAs at that timepoint. However, it is also possible that some type 2 associated genes are driven by other type 2 mediators such as STAT3, which is upregulated following infection (**Figure 2A**)^{261,262}. Since STAT3 is involved downstream of other cytokines, such as IL-6 and IL-10 this could implicate a complex interplay of these responses, and would be consistent with our finding that responses downstream of IL-13 did not follow canonical type 2-mediated pathology.

The identification of *Has1* as the most downregulated gene following IL-13 neutralization in infected mouse lungs, along with downregulation of *Has2* and *Cd44*, two other genes involved in the HA pathway, enabled the discovery of a novel route by which IL-13 impacts pathology via upregulation of hyaluronan synthesis during infection. We showed that IL-13 neutralization not only decreased *Has1* gene expression and lowered hyaluronan levels/deposition, but IL-13 administration also directly increased hyaluronan accumulation in the lung.

Downstream of hyaluronan production, neutralization of the hyaluronan receptor, CD44, improved survival in infected mice. Previous work has shown

that IL-13 can result in the induction of CD44^{263,264}, and elevated CD44 has been found in patients with asthma²⁶⁵. While the relationship between CD44 and IL-13 is still not fully characterized, these observations highlight the ability for CD44 to be regulated by IL-13 and other components of type 2 inflammation. While our work stops short of a full mechanistic understanding of the function of hyaluronan in COVID-19, it is interesting to speculate that this polysaccharide may contribute to inflammation in the lung by providing a matrix for inflammatory cells to migrate over and adhere to, as well as via signaling through its receptor CD44.

Additionally, excessive build-up of hyaluronan, which binds a large amount of water, could contribute to severely impaired oxygen uptake or result in edema, which are significant components of disease in hospitalized patients.

Because increases in hyaluronan have been observed in patients with COVID-19, this study provides a potential link between the association of IL-13 with severe disease¹⁹⁸ and increased hyaluronan seen in other studies^{211,212}. Understanding the relationship between IL-13 and HA may be widely relevant to respiratory diseases beyond COVID-19.

Neutralization of IL-13 also resulted in changes to other genes that may be of interest in future studies on the contributions of IL-13 to lung inflammation during COVID-19. *Arg1*, the gene that encodes for Arginase-1 (Arg1), was significantly downregulated following anti-IL-13 treatment. Arg1 expression is often utilized as a marker for AAMs, which IL-13 is known to promote^{28,29}. Additionally, RELM α can be a marker of AAMs, and in combination with the

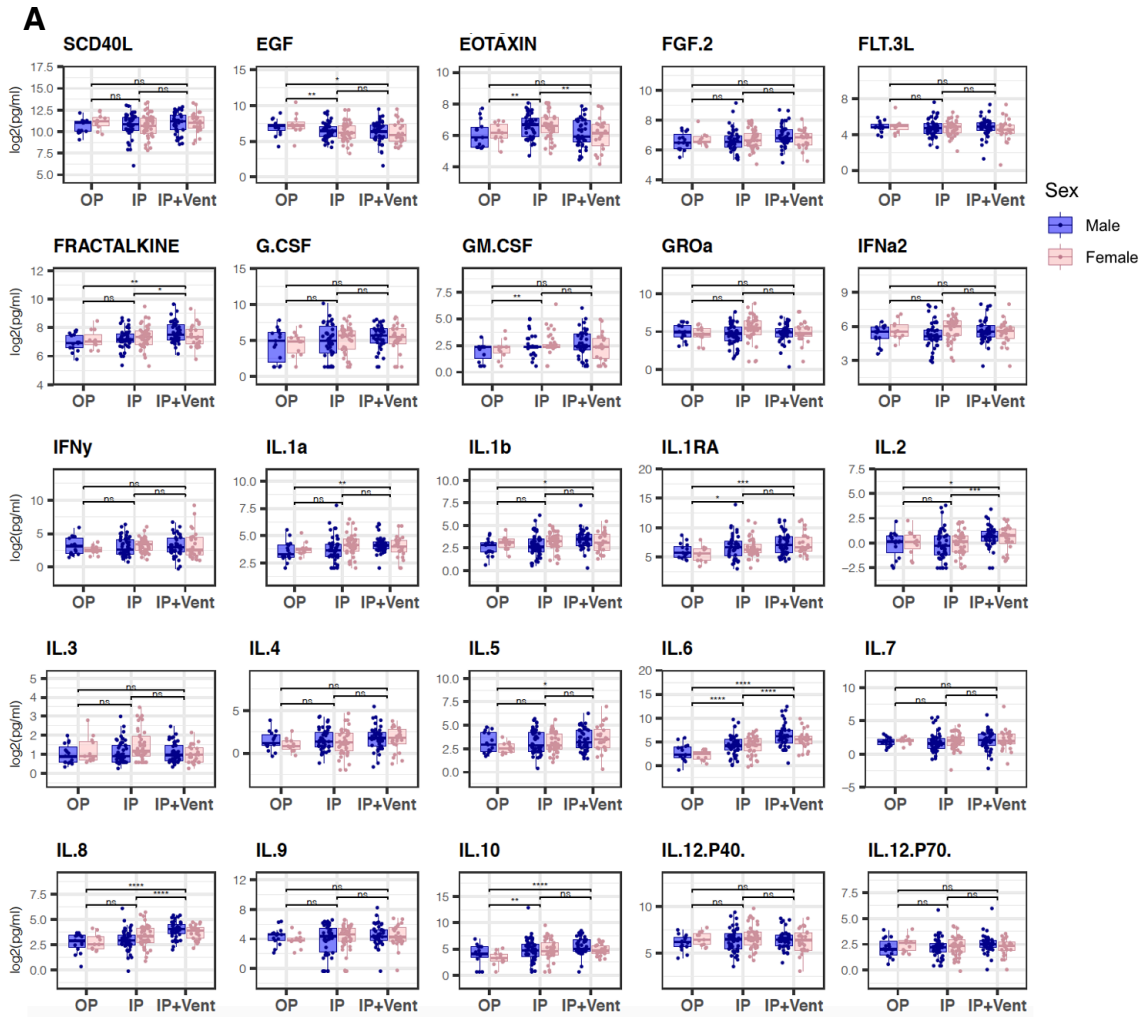
observation of decreased Arg1 may suggest that these macrophages could be downstream of IL-13 signaling during COVID-19. The presence of AAMs, or similarly characterized macrophages, has been observed in patients with severe disease²⁶⁶, together suggesting that IL-13 may promote these cells as a pathogenic mediator for disease and potentially longer-term pathology associated with long-COVID-19. While the role for these cells during COVID-19 has not been fully explored, they may contribute to dysregulated immunity, IL-10 production, or other deleterious tissue responses.

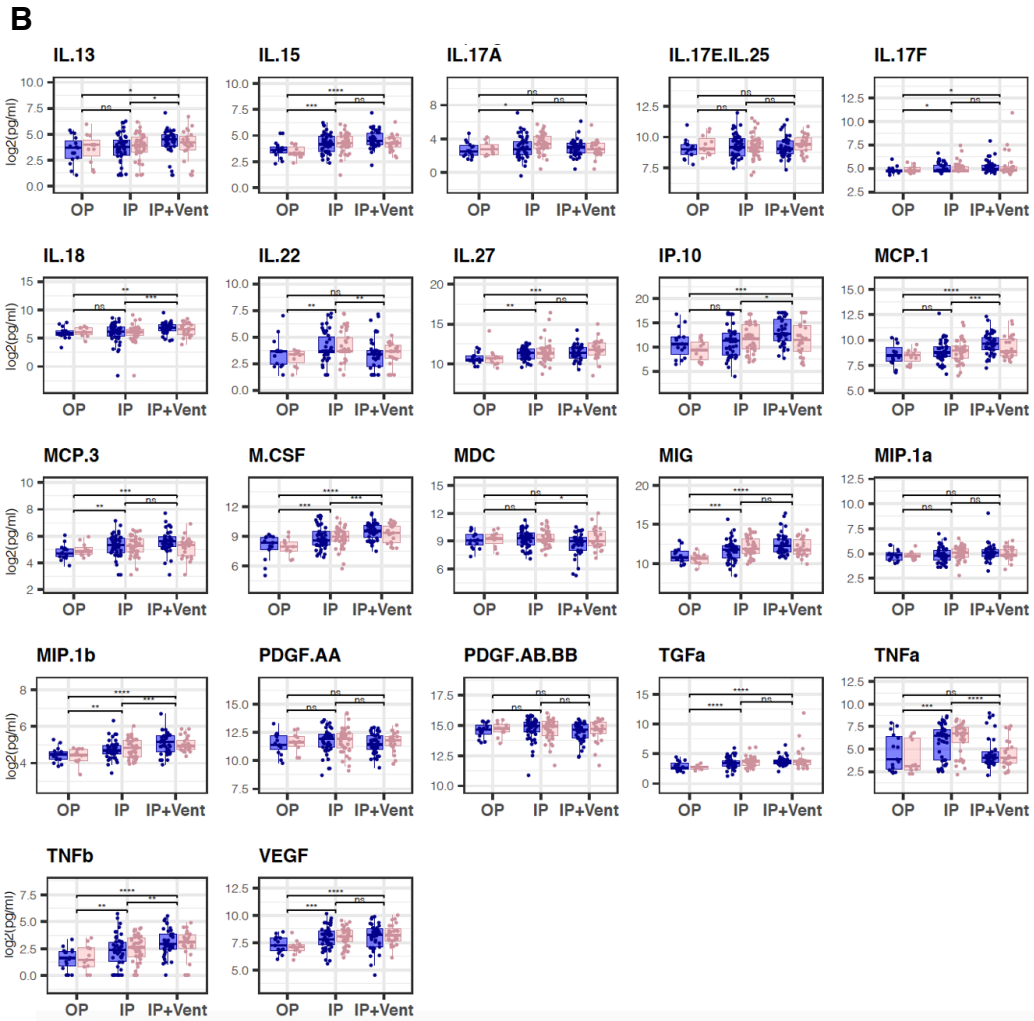
Overall, this work in humans and mice implicates IL-13 as an important driver of severe outcomes during COVID-19, in part through hyaluronan-CD44 engagement in the lungs. Understanding the pathogenic role of IL-13 in the murine model, combined with the results correlating Dupilumab use with better patient outcomes, emphasizes the potential impact this work may have on improving patients' lives.

Table 4.1. Age, sex and clinical status of UVA patients.

	Outpatient (n = 26)	Inpatient (n = 152)
Age	42.4 (15.1)	59.2 (16.7)
Sex		
• Male	11 (42.3%)	66 (43.3%)
• Female	15 (57.7%)	86 (56.6%)
Race		
• Caucasian	5 (19.2%)	60 (39.5%)
• African-American	7 (26.9%)	34 (22.4%)
• Asian	2 (7.7%)	3 (2.0%)
• Other	12 (46.1%)	55 (36.2%)
Ethnicity		
• Hispanic	13 (50.0%)	61 (40.1%)
• Non-Hispanic	12 (50.0%)	91 (59.9%)
Timing of blood draw from day of symptom onset (mean, SD)	4.40 (2.95)	11.3 (11.2)
Missing/unknown	6 (23.1%)	40 (26.3%)
Respiratory Status at time of blood draw		
• No oxygen requirement	25 (96.2%)	45 (29.6%)
• Supplemental oxygen only	1 (3.8%)	57 (37.5%)
• Mechanical ventilation	0	50 (32.9%)
At any time during illness	25 (96.2%)	28 (18.4%)
• No oxygen requirement	1 (3.8%)	59 (38.8%)
• Supplemental oxygen only	0	65 (42.8%)
• Mechanical ventilation		
Ct Value (mean, SD)	28.2 (9.22)	27.1 (6.15)
Missing/Unknown	11 (42.3%)	113 (74.3%)
Comorbidity*	7 (26.9%)	101 (66.4%)
• Diabetes	5 (19.2%)	66 (43.4%)
• Cancer	1 (3.8%)	14 (9.2%)
• Immunosuppression	0	11 (7.2%)
• Kidney Disease	0	30 (19.7%)
• Heart Disease	1 (3.8%)	28 (18.4%)
• Lung Disease	1 (3.8%)	22 (14.5%)
• Liver Disease	0	2 (1.3%)
• Stroke	1 (3.8%)	13 (8.6%)
<p>*Presence of any one of these pre-existing illnesses; diabetes, cancer, kidney, heart, lung, or liver disease, stroke, organ transplant, other immunosuppression. (William, E.J. et al, OpenSAFELY: factors associated with COVID-19 death in 17 million patients. Nature https://doi.org/10.1038/s41586-020-2521-4)</p>		

Figure 4.1





C

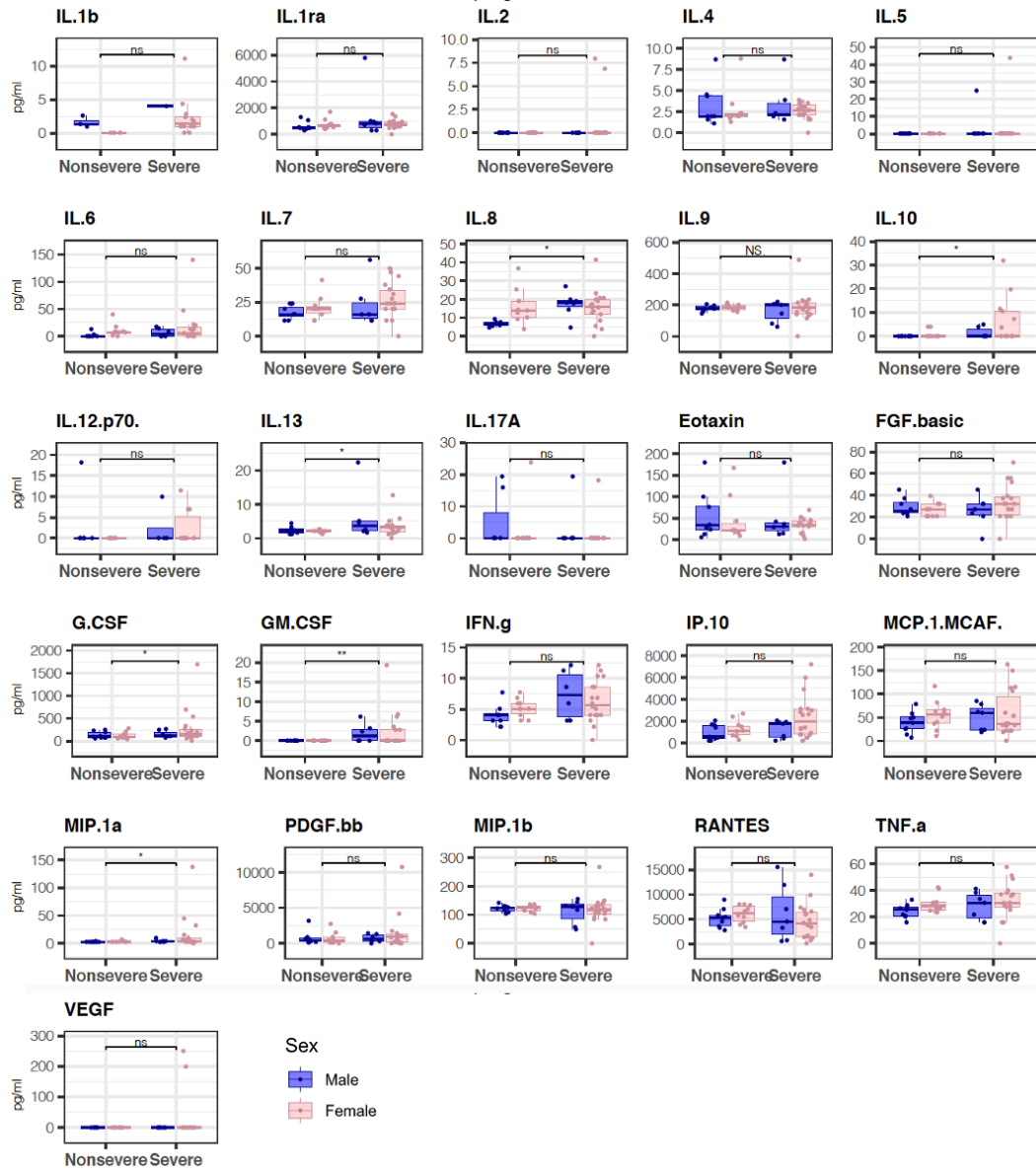


Figure 4.1. Visualization of cytokines in outpatients and inpatients with COVID-19 and in uninfected controls. A) A total of 47 cytokines, chemokines and growth factors were measured from plasma of COVID-19 positive patients, and cytokines of interest were plotted by sex (blue, Male; pink, Female) and compared between patients with differing severity of illness using a Mann-Whitney U test. (OP, outpatient; IP, inpatient; IP+Vent, ventilated inpatient). B) 26 cytokines and growth factors were measured in plasma from 19 non-severe and 26 severe (requiring supplemental oxygen) COVID patients from VCU. Nonsevere and severe groups for each cytokine were compared using a Mann-Whitney U test.

Figure 4.2

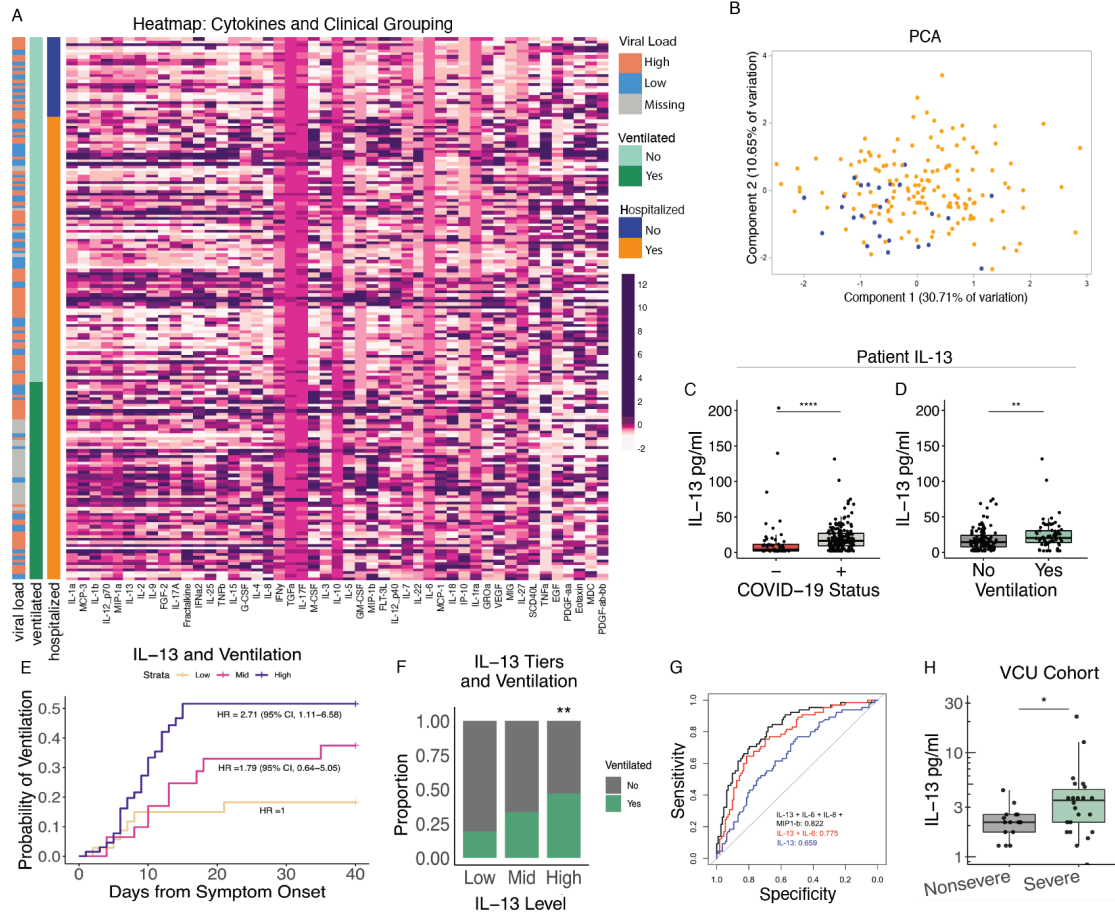


Figure 4.2. Type 2 immune response in patients with severe COVID-19

disease. (A-E) Cytokines were measured in plasma from 26 outpatients and 152 inpatients with COVID-19 infection at the University of Virginia Hospital using a 48-plex cytokine array. A) Heatmap of plasma cytokines, supplemental oxygen requirement and nasopharyngeal viral load, with rows ordered by patient status (outpatient (OP) vs inpatient (IP)) and columns by cytokine principal component 1 which included IL-13 (Table S2). B) Scatterplot comparing principal component 1 and 2 from Principal Component Analysis (PCA) of the plasma cytokines (orange inpatients and blue outpatients). C) Plasma IL-13 levels in COVID-19 patients who were or were not diagnosed with COVID-19 or D) did or did not require mechanical ventilation (Wilcox test). E) Kaplan-Meier survival analysis of the relationship between IL-13 level and mechanical ventilation. Comparison made to lowest IL-13 quantile (Cox proportional hazards test adjusted for age, sex, and comorbidities; CI = confidence interval). F) Proportion of COVID-19 patients requiring mechanical ventilation stratified by IL-13 plasma cytokine levels (Chi-square analysis). G) ROC curve with AUC plotted from: IL-13 alone (blue), IL-13 and IL-6 (red), or IL-13, IL-6, IL-8, and MIP-1b (black). H) IL-13 levels in 19 non-severe and 26 severe (requiring supplemental oxygen) COVID-19 patients from Virginia Commonwealth University Hospital (Wilcox test). * = $p < 0.05$; ** = $p < 0.005$.

Table 4.2. Contributors to Component 1 in PCA plot.

Principal Component 1		
Order	Cytokine	PC.1.Loading
1	IL-1a	0.86636
2	MCP-3	0.82474
3	IL-1b	0.79245
4	Il-12p70	0.79093
5	MIP-1a	0.78886
6	IL-13	0.77694
7	IL-2	0.76816
8	IL-9	0.75838
9	FGF2	0.75743
10	IL-17a	0.73832
11	Fractalkine	0.72882
12	IFNa2	0.71946
13	IL-25	0.71022
14	TNF-b	0.70035
15	IL-15	0.67703

Table 4.2. Contributors to Component 1 in PCA plot. Principal component analysis was performed using the Proc Factor in SAS. For principal component one, those cytokines with a loading score of 0.5 or above were retained.

Figure 4.3

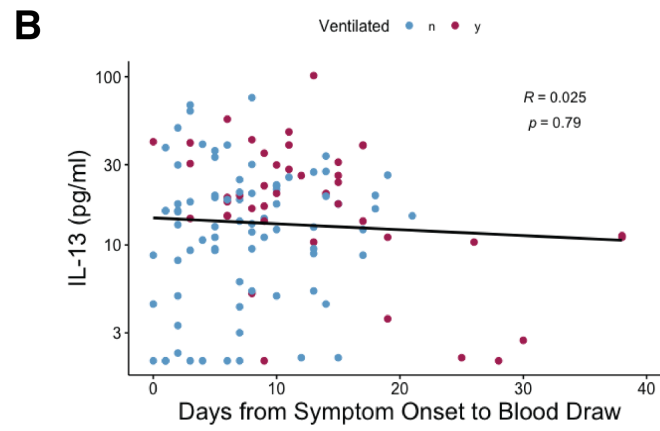
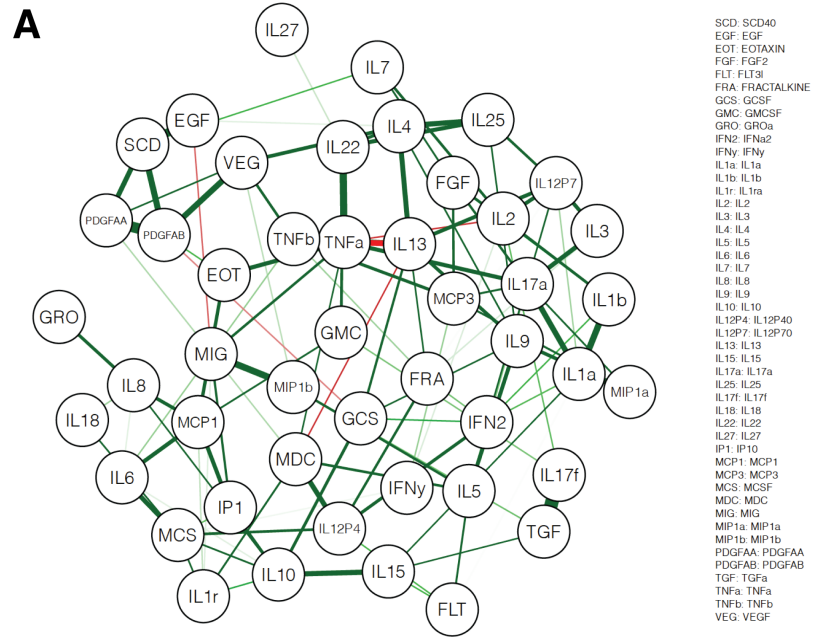


Figure 4.3. Network analysis of cytokine genes in patients with COVID-19.

The network analysis captured the structural relationships among cytokine measurements with graphical LASSO. The nodes represented individual cytokines and edges represented their correlations in that highly correlated cytokines were connected closer with thick edges. Green line = positive correlation; red line = negative correlation.

Figure 4.4

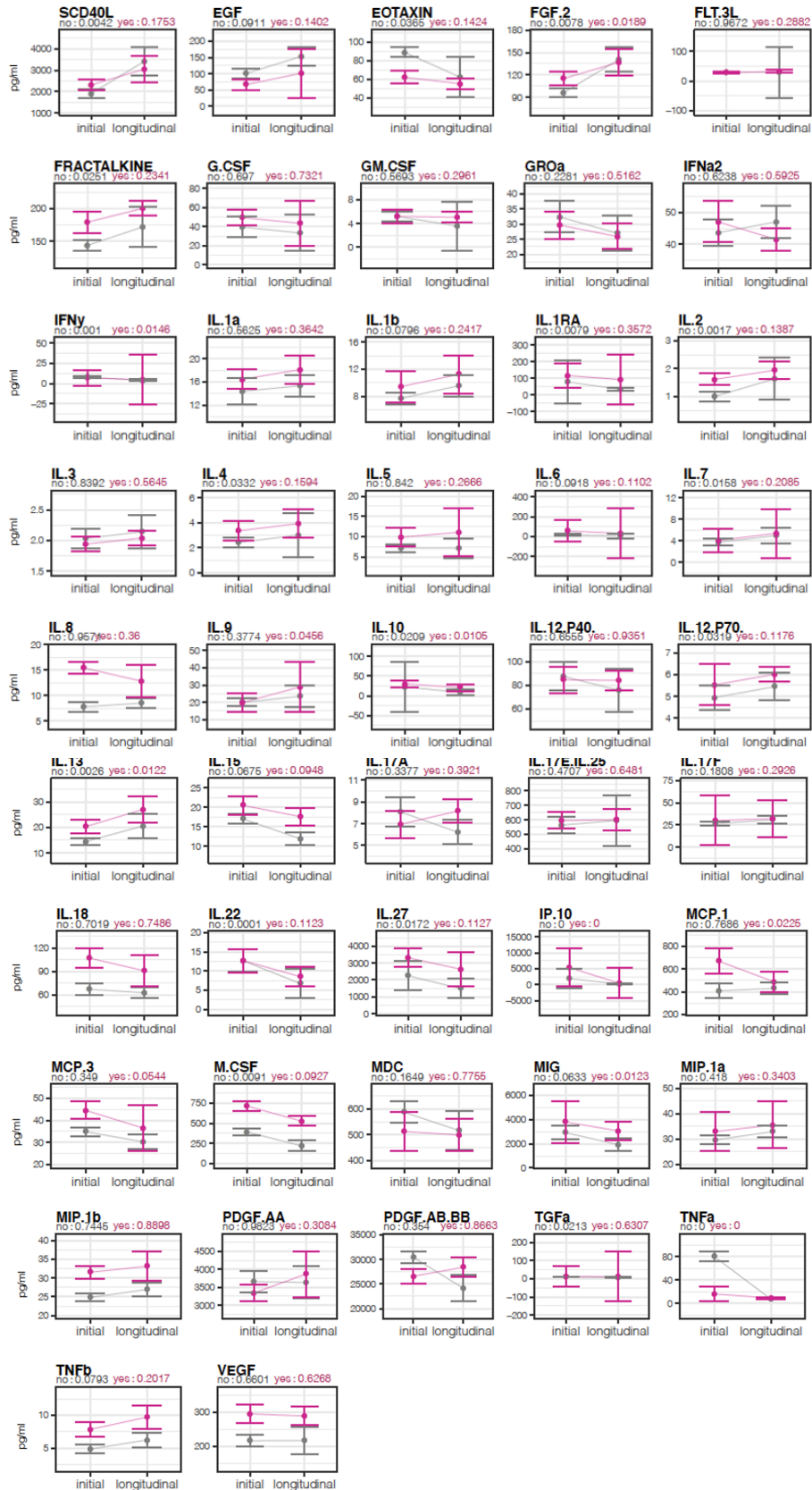


Figure 4.4. Initial vs longitudinal comparison for cytokines in COVID-19 positive patients. 47 cytokines, chemokines and growth factors measured in plasma samples from COVID-19 positive patients at the UVA Medical center. Mean and SE plotted for patients who were (pink) or were not (grey) ventilated at initial and longitudinal sample collection. Due to incomplete overlap in available samples between initial (N = 183) and longitudinal (N = 70) blood draws, Mann-Whitney U test was performed comparing initial to longitudinal groupings.

Table 4.3. Age, sex and clinical status of VCU patients.

	Non-severe (n = 22)	Severe (n = 25)
Age	48.3 (17.0)	30.2 (9.3)
Sex		
• Male	10 (45.5%)	18 (72.0%)
• Female	12 (54.5%)	7 (28.0%)
Race		
• Caucasian	1 (4.5%)	5 (20.0%)
• African-American	17 (77.3%)	19 (76.0%)
• Asian	1 (4.5%)	0 (0.0%)
• Other	3 (13.6%)	1 (4.0%)
Ethnicity		
• Hispanic	3 (13.6%)	1 (4.0%)
• Non-Hispanic	19 (86.4%)	24 (96.0%)
Timing of blood draw from day of symptom onset (if known) (mean, SD)	6.95 (3.43)	10.1 (12.3)
Respiratory Status at time of blood draw		
• No oxygen requirement	15 (68.2%)	2 (8.0%)
• Supplemental oxygen only	7 (31.8%)	20 (80.0%)
• Mechanical ventilation	0 (0.0%)	3 (12.0%)
At any time during illness		
• No oxygen requirement	15 (68.2%)	2 (8.0%)
• Supplemental oxygen only	7 (31.8%)	15 (60.0%)
• Mechanical ventilation	0 (0.0%)	8 (32.0%)
Comorbidity*	15 (68.2%)	21 (84%)
• Diabetes	9 (40.9%)	10 (40.0%)
• Cancer	3 (13.6%)	6 (24.0%)
• Immunosuppression	4 (18.2%)	2 (8.0%)
• Kidney Disease	4 (18.2%)	5 (20.0%)
• Heart Disease	6 (27.3%)	6 (24.0%)
• Lung Disease	6 (27.3%)	6 (24.0%)
• Liver Disease	2 (9.1%)	4 (16.0%)
• Stroke	1 (4.5%)	2 (8.0%)
*Presence of any one of these pre-existing illnesses; diabetes, cancer, kidney, heart, lung, or liver disease, stroke, organ transplant, other immunosuppression. (William, E.J. et al, OpenSAFELY: factors associated with COVID-19 death in 17 million patients. Nature https://doi.org/10.1038/s41586-020-2521-4)		

Table 4.4. Enriched pathways in differentially regulated genes in murine COVID-19 infection.

Reactome Analysis of Differentially Regulated Genes in Covid-19 Infection

Pathway Name	Entities Found	Entities Total	Entities Ratio	Entities Pval	Entities FDR	Rxns Found	Rxns Total	Rxns Ratio	RNA seq
Signaling by Interleukins	581	647	0.044	0.00154	0.0291	489	493	0.038	▲
Deubiquitination	259	288	0.020	0.00125	0.0243	77	77	0.006	▲
Interleukin-4 and Interleukin-13 signaling	187	216	0.015	0.00168	0.0312	46	47	0.004	▲
Antiviral mechanism by IFN-stimulated genes	81	94	0.006	0.00129	0.0250	27	31	0.002	▲
FCGR3A-mediated IL10 synthesis	45	141	0.010	0.00138	0.0266	20	20	0.002	▼
Aquaporin-mediated transport	44	68	0.005	0.00172	0.0318	24	25	0.002	▼
Antimicrobial peptides	40	123	0.008	0.00161	0.0302	39	58	0.004	▲
Glucagon signaling in metabolic regulation	32	40	0.003	0.00181	0.0329	6	6	0.000	▼
Interaction between L1 and Ankyrins	28	33	0.002	0.00114	0.0225	4	4	0.000	▼
Dissolution of Fibrin Clot	12	14	0.001	0.00179	0.0327	19	19	0.001	▲
Defective HLCS causes multiple carboxylase deficiency	6	10	0.001	0.00148	0.0281	4	4	0.000	▼

Table 4.4. Enriched pathways in differentially regulated genes in murine COVID-19 infection. Enrichment analysis was applied to the total gene counts using the CAMERA algorithm. Pathways are arranged by descending number of entities found.

Figure 4.5

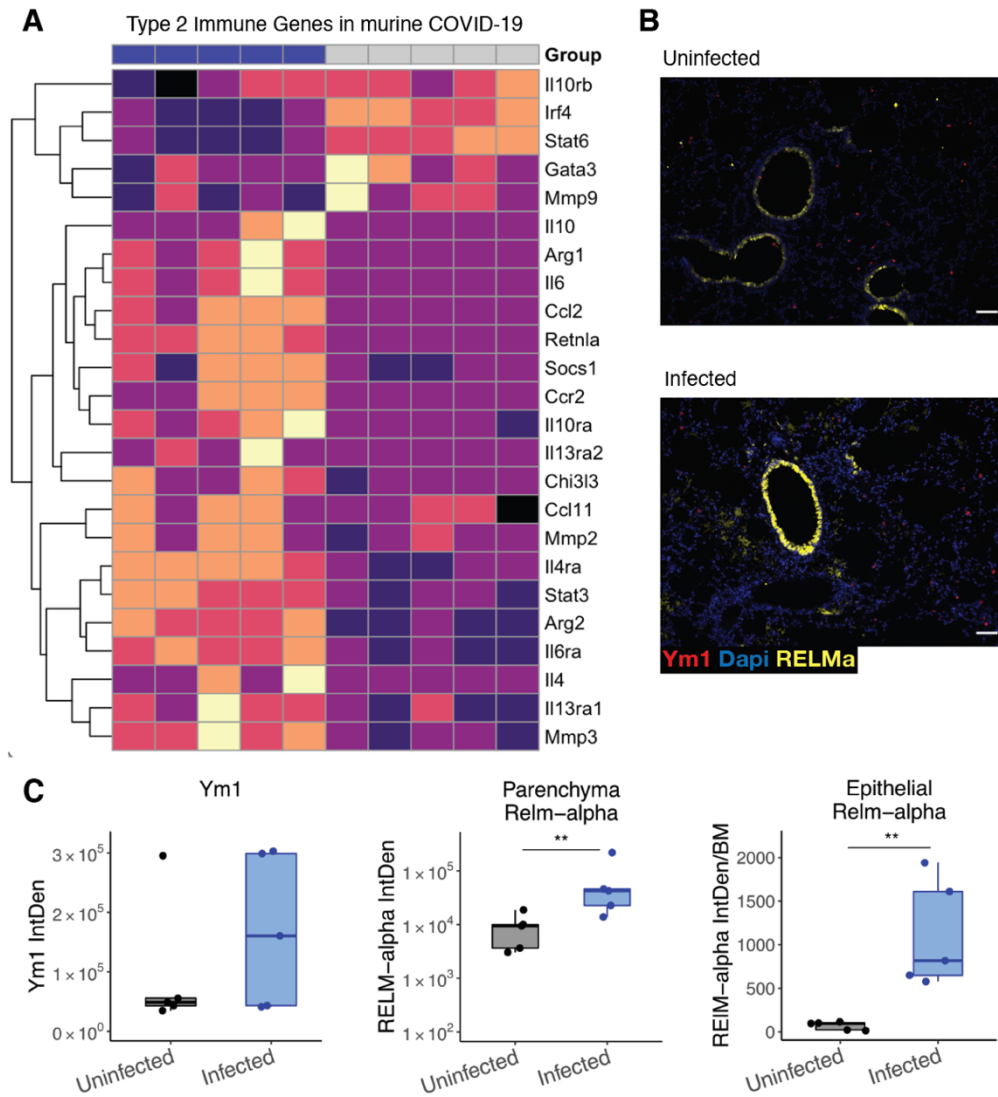


Figure 4.5. Type 2 immune response in lungs of mice following infection with SARS-CoV-2. 10-week-old male mice (Tg K18-hACE2 2PrImn) were infected with 5×10^3 PFU of SARS-CoV-2 and lung tissue examined on day five post-infection by RNA-seq and immunohistochemistry (IHC). A) Type 2 gene expression in the lungs of infected vs uninfected mice (heat map of normalized values of manually curated list of type 2 immune pathway genes). B) Immunohistochemistry of the type 2 immunity proteins RELM α (RELM α) and Ym1 in the lungs of infected and uninfected mice (AW, airway). C) Quantification of IHC scoring for RELM α and Ym1 (mixed effect model). IntDen = Integrated Density; BM = Basement membrane. Scale bar = $70 \mu\text{m}$. *= $p < 0.05$; **= $p < 0.005$

Figure 4.6

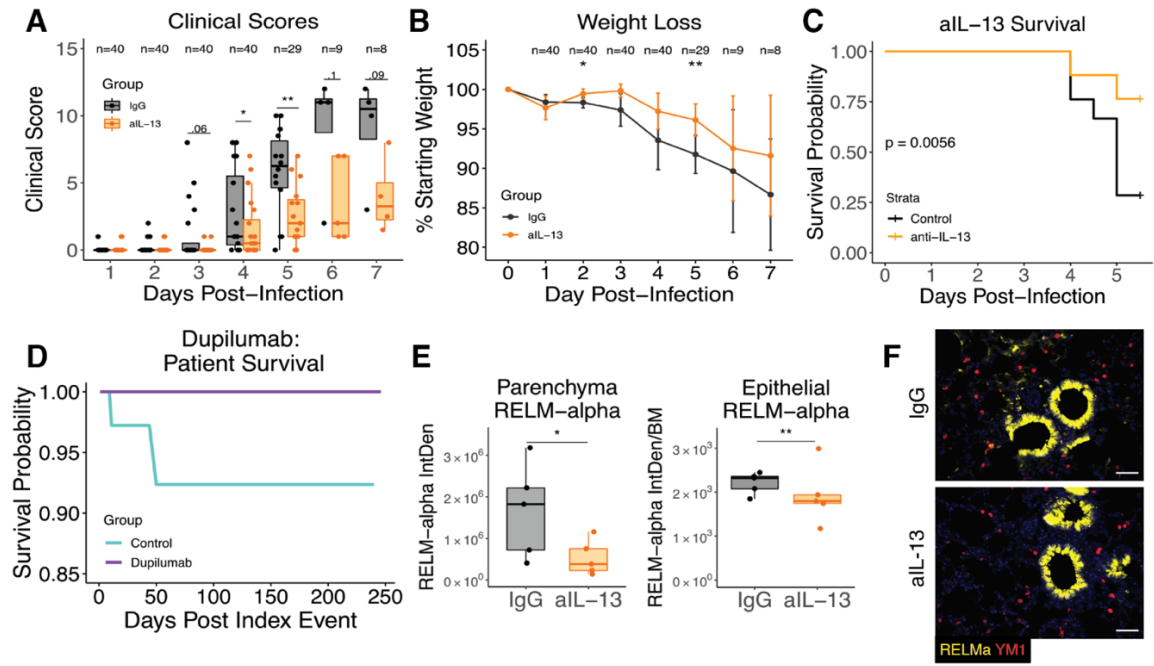


Figure 4.6. IL-13 neutralization protects from severe COVID-19 in K18-hACE2 mice. Mice were infected on day 0 with 5×10^3 PFU of SARS-CoV-2 and administered 150 μ g of anti-IL-13 or an IgG isotype control antibody intraperitoneally on days 0, 2, and 4. A) Clinical scores of illness severity on days 1-7 pi. Clinical scoring was measured by weight loss (0-5), posture and appearance of fur (piloerection) (0-2), activity (0-3) and eye closure (0-2). B) Weight loss on days 1-7 pi. C) Kaplan-Meier survival analysis in mice. D) Kaplan-Meier curve generated from data obtained from TriNetX: 1:1 matching based on 81 patients who had been prescribed Dupilumab independently of their COVID-19 diagnosis. E) Quantification of intensity of staining for parenchyma and epithelial RELM α following IL-13 neutralization (log transformed, mixed effect model). F) Immunohistochemistry of lung tissue stained for RELM α (yellow) in parenchyma or airway, and DAPI (blue). (N = 5 mice/group; A & B combined from three independently conducted experiments). *= $p < 0.05$; **= $p < 0.005$.

Figure 4.7

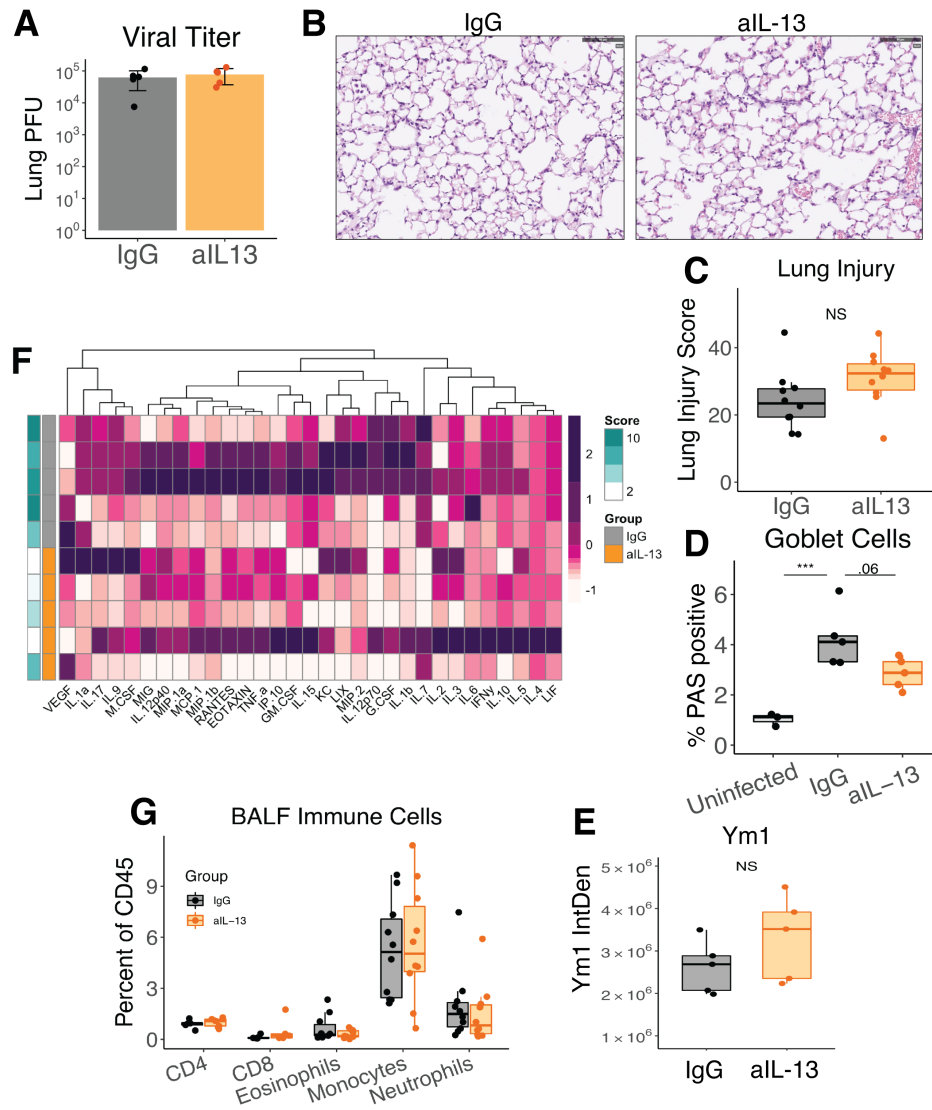


Figure 4.7. Impact of anti-IL-13 on lung injury and inflammation in a mouse model of COVID-19. Mice were infected with 5×10^3 PFU of SARS-CoV-2 on day 0 and given 150 μg of anti-IL-13 or IgG isotype control on days 0, 2, and 4. On day five, mice were euthanized and BALF collected. For histology, lungs were inflated with formalin before removing and fixing prior to H&E staining. A) Viral burden in lungs on day five pi was measured by plaque forming units (PFU). B) Hematoxylin and eosin stain of infected mouse lung with or without anti-IL-13 and C) Quantified lung injury score. D) Goblet cells quantified from PAS staining of lung tissue from day five p.i. E) Ym1 with or without anti-IL-13. F) Cytokines in BALF were measured by Luminex (plotted with group identity and clinical score) and G) immune cells in BALF quantified by flow cytometry. NS= not significant; *** = $p < 0.01$

Table 4.5. Patient characteristics for the full cohort with and without usage of Dupilumab.

Characteristics	With Dupilumab	Without Dupilumab
Age		
Age at index event (yrs \pm 1 σ std dev)	44.3 \pm 17.7	43.3 \pm 20.9
Sex		
Female	68%	55%
Male	32%	45%
Ethnicity		
Race: White	59%	53%
Race: Black	24%	15%
ICD 10 R00-R99 ("Symptoms, signs and abnormal clinical and laboratory findings, not elsewhere classified")	91%	59%
Vitals		
Respiratory rate [breaths/min]	16.6 \pm 6.5	17.0 \pm 29.8
Heart rate [beats/min]	81.3 \pm 12.1	81.6 \pm 17.8
Oxygen saturation [%]	88.4 \pm 21.1	85.6 \pm 23.1
BMI [kg/m ²]	33 \pm 8.4	29.5 \pm 8.4
Blood pressure [mm Hg]	128 / 77	127 / 76
Procedures performed		
Medicine Services and Procedures	70%	41%
Evaluation and Management Services	75%	51%
Medical and Surgical Procedures	21%	17%
Anesthesia	19%	8%
Medications (co-medications taken)		
Dermatological agents	96%	50%
Musculoskeletal medications	65%	39%
Otics agents (infections of the ear)	23%	13%
Hormones	95%	44%
Respiratory agents	89%	44%
CNS-acting agents	86%	53%
Antimicrobials	86%	47%
Ophthalmic agents	84%	47%
Gastrointestinal medications	81%	42%
Cardiovascular medications	75%	39%
Genitourinary medications	70%	34%

Lab-measured properties		
Metabolic panel		
Sodium [mmol/L]	139 ± 2.44	139 ± 3.16
Potassium [mmol/L]	4.07 ± 0.38	4.13 ± 0.54
Chloride [mmol/L]	103 ± 3.66	103 ± 4.14
Bicarbonate [mmol/L]	24.6 ± 2.58	25.4 ± 3.18
Urea nitrogen [mg/dL]	13.5 ± 6.65	15.6 ± 10.2
Creatinine [mg/dL]	0.834 ± 0.226	1.01 ± 2.07
Glucose [mg/dL]	124 ± 63.5	114 ± 54.9
Calcium [mmol/L]	9.3 ± 0.527	9.26 ± 0.582
Magnesium [mmol/L]	1.98 ± 0.3	2 ± 0.426
Phosphate [mmol/L]	3.3 ± 0.604	3.49 ± 1.08
Complete Blood count		
Erythrocytes [Mill/ μ L]	4.6 ± 0.521	4.5 ± 0.669
Leukocytes [1000/ μ L]	8.64 ± 2.66	8.33 ± 4.36
Hemoglobin [g/dL]	13.3 ± 1.8	13.2 ± 2.01
Hematocrit [%]	39.3 ± 8.39	39.4 ± 6.80
Liver function		
ALT [U/l]	25.6 ± 17.9	29 ± 48.8
AST [U/l]	25.2 ± 16.0	28.1 ± 71.8
Coagulation		
INR	1.02 ± 0.38	1.17 ± 0.74
Lipid panel		
Cholesterol in LDL [mg/dL]	102 ± 30.6	101 ± 35.8
Cholesterol in HDL [mg/dL]	54.1 ± 14.0	51 ± 16.2
Triglycerides [mg/dL]	127 ± 71.3	131 ± 109

Table 4.6. Outcomes with and without Dupilumab in TriNetX cohort.

	With Dupilumab	Without Dupilumab	Risk difference (95% CI)
Full Cohort			
Patients	81	350004	
Ventilated	0	1307	0.37% (0.35-0.39)
Deceased	0	6942	1.98% (1.94-2.03)
1:1 Propensity Score Matching			
Patients	81	81	
Deceased	0	10	12.3% (5.2-19.5)
Diagnoses Matching			
Patients	65	35564	
Ventilated	0	238	0.67% (0.58-0.75)
Deceased	0	652	1.83% (1.69-1.97)

Table 4.7. Lab values and standard deviations (SD) for serum levels of C-reactive protein (CRP) for COVID-19 patients in this study.

Group	CRP (mg/l)	SD	Sub-cohort difference
Survived	34.3	58.0	65.7
Deceased	100.0	107.0	
Not Ventilated	39.6	65.6	35.3
Ventilated	74.9	98.5	
With Dupilumab	25.3	68.3	12.3
Without Dupilumab	37.6	63.8	

Table 4.8. N3C Dupilumab COVID severity outcomes.

	w/ Concurrent Dupilumab	Matched controls w/o Dupilumab	Odds Ratio	P-value
Patients	31	155		
Hospitalized	<20	<20	0.64	.57
w/ Ventilation	0	<20	n/a	>.99
Deceased	0	<20	n/a	>.99

Table 4.8. N3C Dupilumab COVID severity outcomes. A total of 785 patients with a record of dupilumab prescription were in the N3C Data Enclave on November 16, 2020. Of these, 31 Dupilumab patients had a COVID+ test within 61 days after a dupilumab dose, resulting in a test positivity rate of 3.9% (95% CI: 2.8, 5.6). A total of 247,391 COVID+ patients with no record of Dupilumab were available for selection of matched controls. Five matches could be found for each patient. In the matched analytic dataset of COVID+ patients, no differences were seen in the hospitalization (OR=0.64, p=0.57) or death rates (p>0.99); though <20 deaths were seen in the entire dataset. In hospitalized patients, no differences were observed in the rates of ECMO (p>0.99) or IMV (p>0.99).

Table 4.9. Candidate IL-13-regulated pathogenic effectors: top 15 protein coding genes downregulated by anti-IL-13 treatment relative to IgG isotype on day five of murine Covid-19 infection.

IgG vs aIL-13

Gene Symbol	Gene Name	FC (log2)	P value	P adj	Ensembl ID	Entrez ID
Has1	hyaluronan synthase 1	-2.26	0.0012	0.05	ENSMUSG00000003665	15116
Arg1	arginase, liver	-1.60	0.0015	0.06	ENSMUSG00000019987	11846
Areg	amphiregulin	-1.27	0.0000	0.01	ENSMUSG00000029378	11839
Kcne4	potassium voltage-gated channel, Isk-related subfamily, gene 4	-1.24	0.0001	0.01	ENSMUSG00000047330	57814
Ackr3	atypical chemokine receptor 3 (Cxcr3)	-1.08	0.0001	0.01	ENSMUSG00000044337	12778
Chek1	checkpoint kinase 1	-1.07	0.0027	0.08	ENSMUSG00000032113	12649
Pkhd1	polycystic kidney and hepatic disease 1	-0.96	0.0001	0.01	ENSMUSG00000043760	241035
Gm13889	predicted gene 13889	-0.94	0.0006	0.04	ENSMUSG00000087006	620695
Eef1e1	eukaryotic translation elongation factor 1 epsilon 1	-0.94	0.0005	0.03	ENSMUSG00000001707	66143
Npr3	natriuretic peptide receptor 3	-0.92	0.0007	0.04	ENSMUSG00000022206	18162
Hdx	highly divergent homeobox	-0.90	0.0004	0.03	ENSMUSG00000034551	245596
Cxcl14	chemokine (C-X-C motif) ligand 14	-0.89	0.0000	0.00	ENSMUSG00000021508	57266
Lif	leukemia inhibitory factor	-0.88	0.0026	0.08	ENSMUSG00000034394	16878
Zfp711	zinc finger protein 711	-0.87	0.0024	0.07	ENSMUSG00000025529	245595
Rgs4	regulator of G-protein signaling 4	-0.87	0.0000	0.00	ENSMUSG00000038530	19736

Figure 4.8

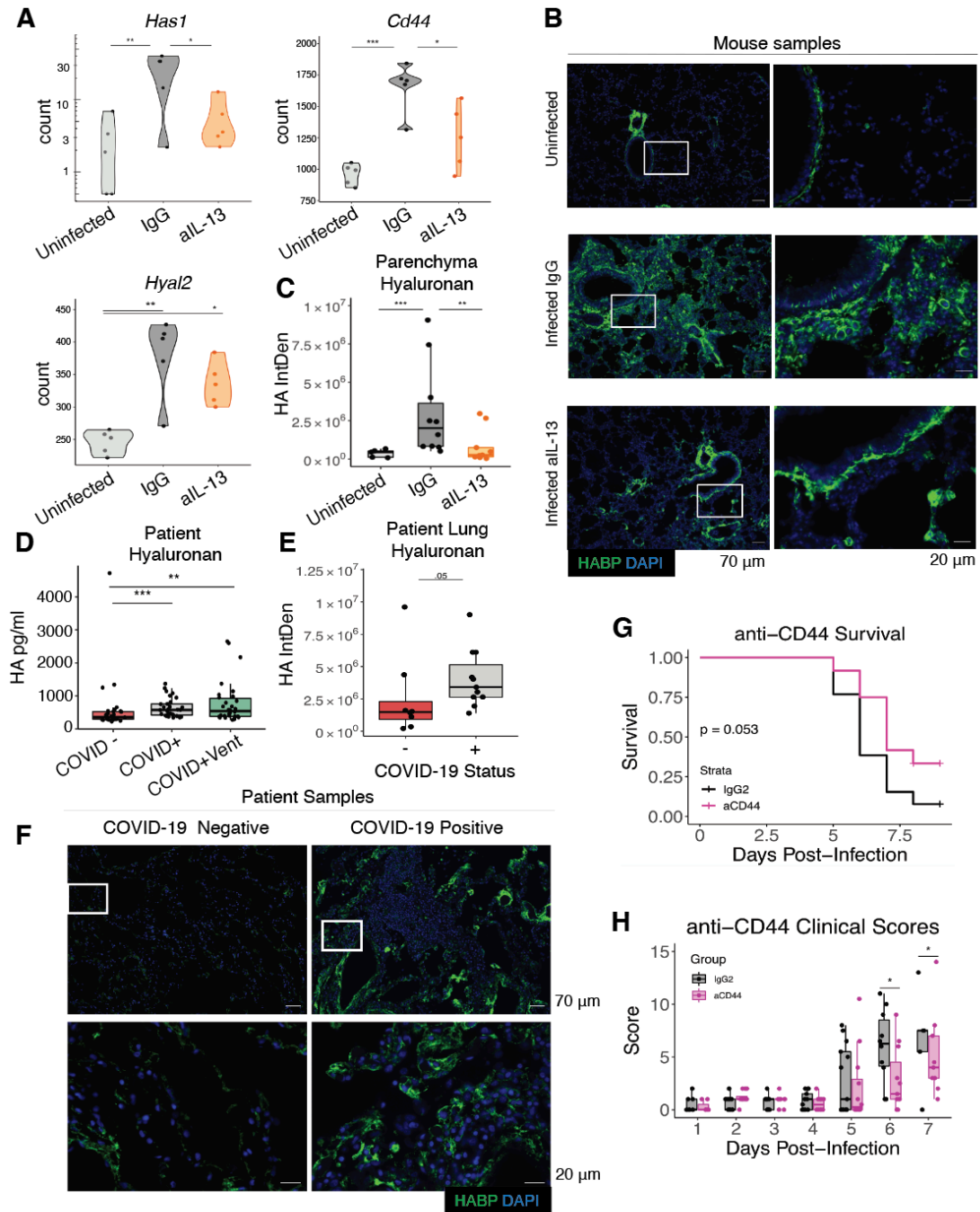


Figure 4.8. Hyaluronan and COVID-19 disease. Mice received i.p. injections of anti-IL-13 on days 0 and 2 pi, were euthanized on day 5 and lung tissue was split and placed either into trizol tissue reagent for RNA analysis or formaldehyde for paraffin embedding and immunohistochemistry. A) Gene expression in mouse lung of hyaluronan synthase (*Has1*), the hyaluronan receptor *Cd44* and Hyaluronidase 2 (*Has2*) of infected mice with anti-IL-13, isotype control antibody and uninfected controls. B) Staining of hyaluronan in mouse lung (with HABP) Scale bar = 70 μ m. Rectangles indicate area magnified in image to left; Scale bar = 20 μ m. C) Quantification of hyaluronan deposition in tissue following infection and neutralization of IL-13 (mixed effect model; combined 2 experiments). D) Hyaluronan was measured in the plasma of COVID-19-negative controls and in patients with COVID-19 that did or did not require supplemental oxygen. Postmortem lung samples were obtained from fatal COVID-19 cases and control tissue from COVID-19 negative deaths. E) Quantification of hyaluronan deposition in fatal COVID-19 disease (N=11) and controls (N=8) (log transformed, mixed effect model) using hyaluronan-binding protein (HABP). F) Representative images of staining for hyaluronan (with HABP) from human lung samples, Scale bar = 70 μ m. Rectangle indicates area magnified in image below; Scale bar = 20 μ m. Mice were administered anti-CD44 or IgG2 isotype control on days 1, 2, 3 and 4 pi. G) Kaplan-Meier survival curve and H) Clinical scores for mice; combined two, independent experiments.*=p<0.05; **=p<0.005; ***=p<0.0005.

Figure 4.9

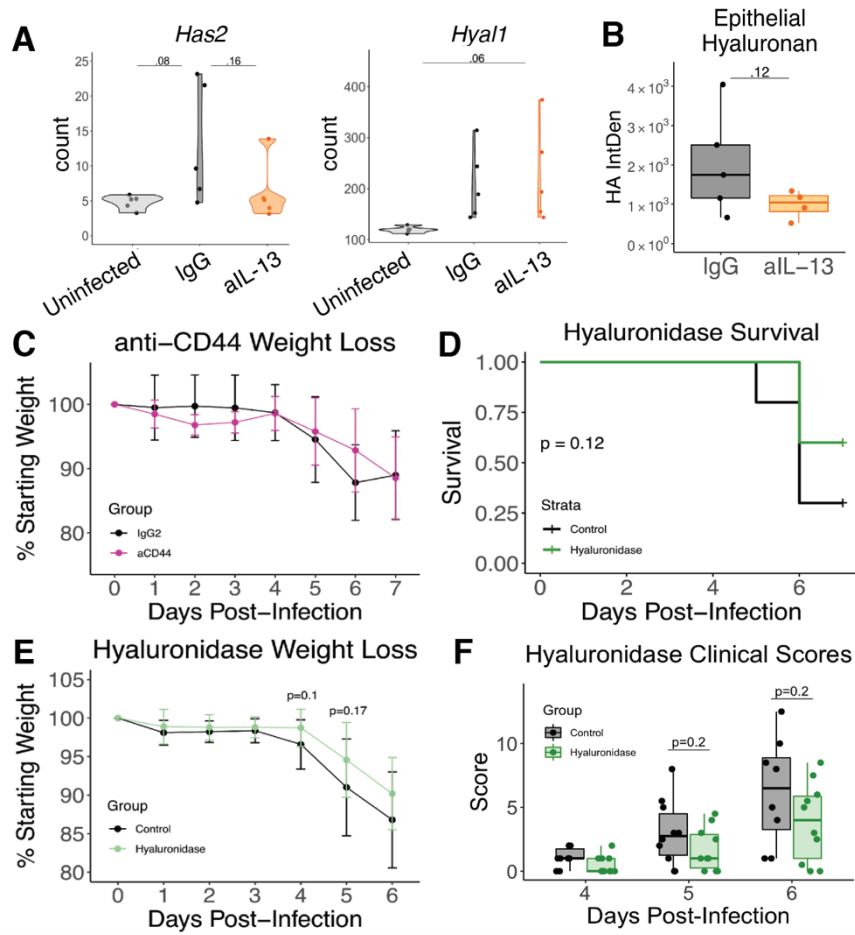


Figure 4.9. Hyaluronan and its receptor contribute driving severe COVID-19 in mice. Mice were infected with 5×10^3 PFU of SARS-CoV-2 on day 0 and given $150 \mu\text{g}$ of anti-IL-13 or IgG isotype control on days 0, 2, and 4. On day five, mice were euthanized and sections of lung were stored in trizol. RNAseq was done on lung tissue. Read counts of A0 hyaluronan synthase 2 (*Has2*) and B) hyaluronidases 1 (*Hyal1*) were analyzed between anti-IL-13 treated mice and isotype controls. C) Quantification of intensity of epithelial hyaluronan from fluorescent staining (log-transformed, mixed-model). D) Kaplan-Meier survival curve, E) clinical scores and F) weight loss from mice infected with 5×10^3 PFU of SARS-CoV-2 who were administered hyaluronidase on day five pi; combined, two independent experiments. Infected mice were administered anti-CD44 antibodies or isotype IgG2 control on days 1,2,3 and 4 pi G) weight loss were quantified; combined two, independent experiments. H) Lung sections stained with hyaluronan binding protein (HABP, green) and DAPI nuclei stain (blue) for SARS-CoV-2 infected mice treated with IgG or anti-IL-13. Each image is representative of an individual; scale bar = $70\mu\text{m}$. *= $p < 0.05$; **= $p < 0.005$

Figure 4.10

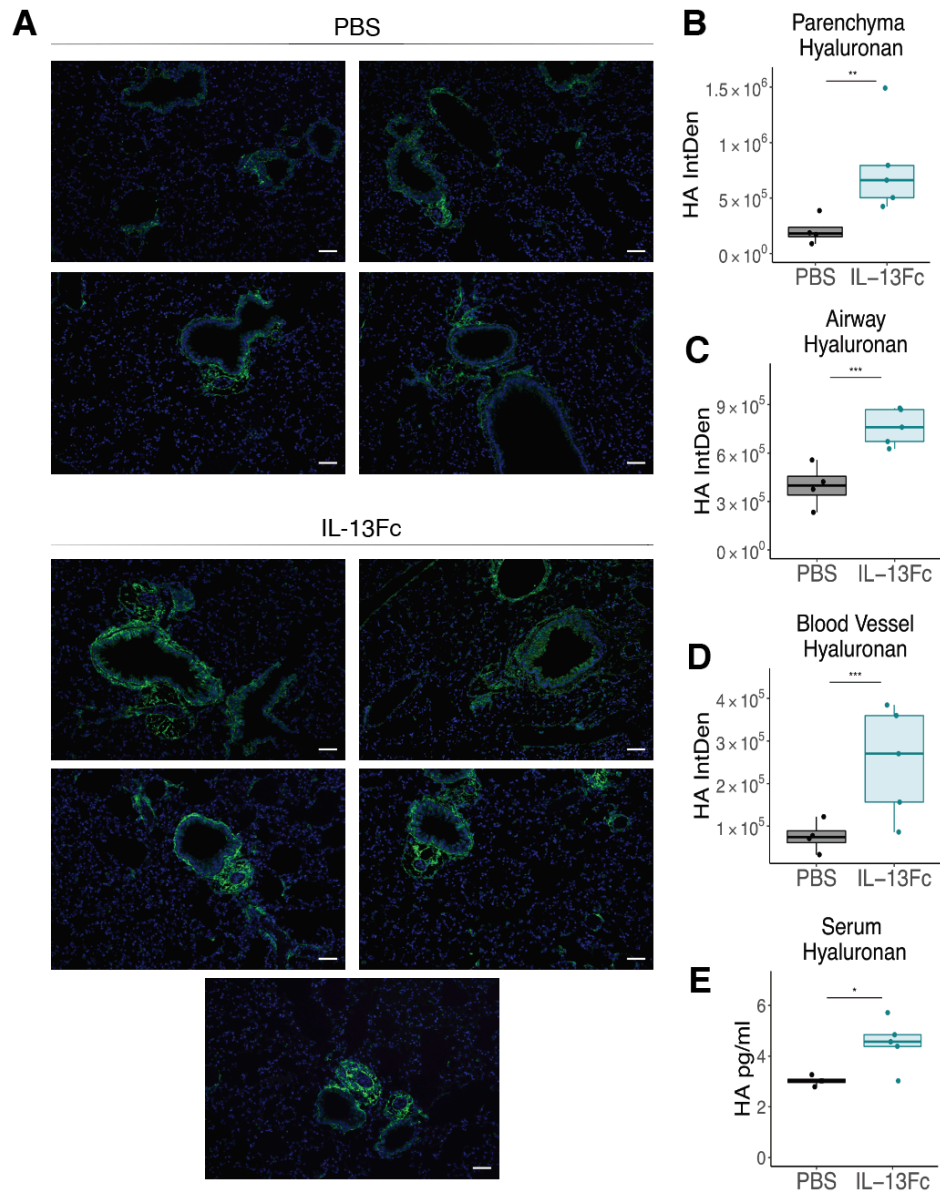


Figure 4.10. IL-13 administration promotes hyaluronan accumulation in mice. Uninfected mice were administered IL-13Fc on days 0 and 2 and lung tissue and serum was collected 24 hours later. Lung tissue was sectioned and stained for HAPB. A) Representative images from each mouse. Quantification of HAPB staining in the B) parenchyma, C) airway, and D) blood vessels for quantification of hyaluronan deposition in the tissue (mixed effect model). E) Hyaluronan was measured in the serum by ELISA. Scale bar = 70 μ m. * = P<0.05; ** = p<0.01; *** = p<0.001.

Chapter 5: Conclusions and Future Directions

The primary functions for type 2 inflammation are to maintain metabolic homeostasis, protect against infections with helminths or parasites, and to promote tissue repair and the resolution of inflammation²³⁰. However, this immune response can contribute to other contexts as well, including infections caused by viral and bacterial pathogens, or immunopathology associated with asthma or colitis. As such, it is important to recognize that the role for type 2 inflammation is dependent on a variety of factors including tissue site, homeostasis or diseased state, and type of infectious pathogen.

In this thesis, we investigated the contribution of type 2 inflammation to *C. difficile* infection and COVID-19, and found contrasting consequences within these diseases. Infection with *C. difficile* occurs within the colon and causes a hyperinflammatory immune response primarily mediated by neutrophils and type 3 inflammation. Here, we reported the IL-4, IL-5, and IL-13 all provided protection from severe outcomes, supporting previous work showing that type 2 immunity is protective during this disease. During SARS-CoV-2 infection, however, we discovered that IL-13 promoted more severe disease, in part by promoting CD44 expression and hyaluronan deposition in the lung. These opposing outcomes are likely the result of differences in tissue site and the primary immune response to the pathogen. During CDI, epithelial damage and high levels of inflammation are present, and type 2 immunity likely functions to reduce the production of pathogenic cytokines and to promote tissue healing. In the lungs during COVID-

19 the effects of IL-13 on type 1 inflammation may impede effective anti-viral immunity and decrease lung oxygen capacity, partially through the production of hyaluronan. While studies into whether IL-13 regulates hyaluronan in the intestines will need to be done (discussed below), increased deposition of hyaluronan in the colon may be less detrimental to tissue function. This site may be more tolerant due to increased turnover of the epithelium, or that the colon is not necessary for a function as critical as oxygen uptake. Overall, we report on the differing responses to type 2 inflammation during either CDI or COVID-19, supporting the recognition that this immune response has context dependent consequences.

5.1 Type 2 immunity is protective during *C. difficile* infection

Infection with *C. difficile* results in a strong pro-inflammatory host response that serves to control the infection and protect the host. However, in humans and murine models of disease, high levels of pro-inflammatory mediators such as IL-1 β , IL-8, and neutrophils are associated with worse outcomes, supporting the hypothesis that excessive inflammation can be detrimental to the host, independent of bacterial burden^{147,170,171}. Our lab has previously shown that the presence of type 2 immune responses, those most often associated with anti-helminth immunity or allergy or asthmatic responses, are beneficial to the host during *C. difficile* infection. The administration of either IL-25 or IL-33 resulted in decreased weight loss and clinical scores following

infection, as well as a decrease in inflammatory mediators, such as the ones described above^{90,91}. Treatment with either cytokine resulted in increased eosinophils within the colon, however only IL-25 administration was dependent on these cells to provide protection. In contrast, IL-33 was dependent on ILC2s, which are likely upstream of eosinophils.

While the importance of ILC2s downstream of IL-25 during CDI has not been fully explored, the necessity of eosinophils for protection is dependent on which alarmin was administered during infection. This may suggest that eosinophils and ILC2s have some degree of overlap in their protective functions. The observation that these cells express predominantly IL-4 or IL-13 during CDI, respectively, further supports the hypothesis that there is overlapping, yet distinct, contributions to the immune response. As previously discussed, IL-4 and IL-13 are closely related cytokines with many similar functions due to the shared receptor subunit, IL-4R α ²⁴. Whether either cytokine is sufficient to mediate a shared signaling response may explain the predominance of one or the other downstream of IL-25 or IL-33. Additionally, ILC2s produce IL-5, which is an important eosinophil chemoattractant^{18–20}. Whether IL-25 produces a higher proportion of IL-5+ ILC2s, compared to IL-13+ ILC2s, could partially explain the higher dependence on eosinophils in that model.

Eosinophils and ILC2s were observed to produce IL-4 and IL-13 during murine CDI, respectively, and as such, we wanted to further explore the roles these cytokines may be having during this disease. Neutralization of IL-4

simultaneously with IL-25 treatment during infection did not recapitulate the loss of eosinophils, but rather, impeded the recovery response to infection⁹⁰. While this suggested that IL-4 was not the main mechanism of acute protection from eosinophils, it implicated IL-4 in the recovery response from disease. Following this, we hypothesized that treatment would promote recovery. Additionally, we hypothesized that IL-13 may be contributing a similar role to the recovery response due to the similar functions these cytokines can play. Chapter 2 of this thesis discussed data showing that treatment with IL-4 during CDI did, in fact, promote recovery from disease. In Chapter 3, we investigated the role of IL-13, and observed a similar contribution as was seen with IL-4. We delved further, however, and saw that loss of IL-13 during CDI resulted in elevated inflammatory cells, suggesting that IL-13 was important for either decreasing cell recruitment or facilitating cell clearing during resolution. Notably, we also identified a dysfunctional monocyte/macrophage compartment, with IL-13 neutralization resulting in an accumulation of transitional monocytes starting on day three post-infection, which may negatively impact total macrophages by day four. We also observed macrophages, in particular CD206+ AAMs, to be associated with the resolution phase of disease, and in line with this, loss of IL-13 resulted in dramatic reduction in CD206+ macrophages by day three. Together, this supports that IL-13 is important for monocyte engraftment into tissue macrophages, but independently important for the polarization of AAMs, in line with previous literature^{28,29}, and that these cells contribute to disease resolution.

Lastly, in Chapter 3 we discussed that IL-13 has a decoy receptor, IL-13Ra2, which is known to negatively regulate IL-13 signaling, and in a model of DSS colitis, neutralization of this receptor increase recovery from inflammation and tissue damage¹⁰⁵. Concordantly, the neutralization of IL-13Ra2 during CDI provided protection from disease, likely by resulting in increased bioavailable IL-13 within the colon. Because this approach does not introduce high levels of exogenous cytokine, but rather allows endogenous IL-13 to signal more effectively to IL-13Ra1, it may be a more desirable method for therapeutic intervention.

In addition to IL-4 and IL-13, IL-5 is also an important type 2 cytokine which is produced by ILC2s, and particularly important in the recruitment of eosinophils¹⁶. Because eosinophils are important for protection from disease, we were interested in understanding if IL-5 was involved during CDI. Although ILC2s were not investigated downstream of IL-25 during CDI, given what is known about this cytokine in the intestines, it is likely that these cells are an important component of this response. In line with this, the administration of IL-5 during CDI promoted protection from disease. Additionally, there were lower levels of CD45+ hematopoietic cells and neutrophils, but an increased proportion of eosinophils. Notably, eosinophils were only required for IL-25-mediated protection, and not IL-33, yet IL-33 treatment did result in an increase in ILC2s which would have the capacity to produce IL-5. Whether IL-33 induced ILC2s preferentially express other cytokines, such as IL-13, may explain this difference

in downstream responses between IL-25 and IL-33, however, future studies would be needed.

Altogether, the work shown here highlights the expanding knowledge into how type 2 immunity provides protection from infection with *C. difficile*. We provide a stepping stone into future research that can address many of our unanswered questions, which will be further discussed below. 1) Are macrophages the driving cell, downstream of IL-4 or IL-13, in promoting recovery? 2) How is IL-13 having an impact on the monocyte compartment, and how may these cells be contributing to infection. 3) And lastly, given our observation in COVID-19, could IL-13 be having an impact on hyaluronan deposition in the gut, and might hyaluronan have any role during CDI?

5.2 Type 2 immunity is pathogenic during COVID-19 pneumonia.

Following the onset of the pandemic caused by SARS-CoV-2, we were interested in characterizing the host immune response in patients at the University of Virginia and Virginia Commonwealth University's Medical Centers. We found many of the previously reported cytokines and chemokines, such as IL-6, IL-8, IL-10, IP-10, and MCP1, to be elevated in patients with severe disease. Additionally, we observed that IL-13 was also elevated in these patients. Given the role of this cytokine in promoting pathogenic responses in the lung during asthma and other viral infections, as well as the observation of increased

IL-33 and ILC2s in other studies^{207,208}, we were particularly interested in understanding the contribution of IL-13 to COVID-19.

Using a murine model of COVID-19, we found that the neutralization of IL-13 during infection resulted in decreased disease severity and mortality, supporting our hypothesis that IL-13 was pathogenic. Our efforts to uncover downstream mechanisms through which IL-13 could be acting, however, did not show a strong indication that typical mediators downstream of IL-13 were major contributors. This led to our discovery that the gene for hyaluronan synthase 1, *Has1*, was the most highly downregulated gene in the lung following IL-13 neutralization during COVID-19 in mice. Additionally, treatment with IL-13 in mice resulted in increased hyaluronan deposition in the lung supporting the regulation of this ECM component by IL-13. While the presence of hyaluronan has been noted in patients with asthma^{141,143,144}, the mechanism through which it is promoted has never fully been understood. Of note, there have been a few studies suggesting that IL-13 or IL-4 can regulate hyaluronan and its receptor, CD44^{141,145,264}, however these were performed in cell lines. Our data further support that IL-13 promotes hyaluronan production, likely through *Has1* activity, as well as increases CD44 expression, which may serve to facilitate immune cell recruitment or hyaluronan turnover.

The observation for increased hyaluronan during COVID-19 was mirrored by previous reports which found hyaluronan to be elevated in patients^{140,211,212,254,255}. We hypothesized, then, that hyaluronan was contributing

to disease severity. Although in our model, treatment with hyaluronidase did not protect from disease, neutralization of CD44 did provide protection, suggesting the interaction of these two components plays a pathogenic role in COVID-19.

Our data show the contribution of IL-13 to the host immune response during COVID-19, highlighting it as a mediator of disease severity, in part, through hyaluronan and CD44. These findings increase our understanding of this disease, and shed light into potential therapeutic options. As such, we observed that patients who had previously been prescribed the monoclonal antibody against IL-4Ra, Dupilumab, had no adverse events following infection with SARS-CoV-2 compared to the untreated cohort, implicating that this may be a potential approach to prevent severe disease. Given these findings, we have initiated a clinical trial at the University of Virginia's Medical Center to test the efficacy of Dupilumab for this purpose (ClinicalTrials.gov Identifier: NCT04920916).

This work represents a point from which future studies can further increase the understanding of not only the contribution of IL-13 to COVID-19, but also the capacity for IL-13 to regulate hyaluronan and CD44, and the role of these factors in COVID-19 severity as well.

5.3 Future Directions

5.3.1 Alternatively-activated macrophages and recovery from *C. difficile* infection

Both IL-13 and IL-4 are known to promote the polarization of AAMs^{28,29,40}. These cells are typically considered anti-inflammatory and have functions important for tissue remodeling and repair following damage^{30,59,267,268}. Additionally, they produce IL-10, Arg1, Ym1 and express the surface markers CD206 and CD163^{30,269}. During murine CDI, we observed that CD206+ AAMs increased during the recovery phase of disease, along with an increase in tissue IL-10, suggesting these components may be involved in promoting recovery. Additionally, IL-13 was significantly correlated with IL-10 levels in cecal tissue, and treating bone marrow-derived macrophages (BMDMs) with recombinant IL-13 resulted in increased expression of IL-10 in AAMs (**Figure 5.1B and C**), consistent with previous reports. Furthermore, given the high levels of inflammation and damage resulting from this infection, the involvement of AAMs may be a crucial step in promoting resolution from this disease. Together, this suggests that AAMs, driven by IL-13, are a mechanism for reducing inflammation in the colon following *C. difficile* infection.

Considering this hypothesis, it will be important to test the contribution of AAMs to recovery from disease, as well as what function they may be providing to promote this response. Adoptive transfers of AAMs have been used previously during models of inflammation, including DSS colitis. Incubation of BMDMs with either IL-13 or IL-4 to polarize cells towards an AAM phenotype results in increased CD206+ cells which express Arg1 and IL-10 (**Figure 5.1A-C**), which could then be injected into recipient mice. During DSS and

Figure 5.1

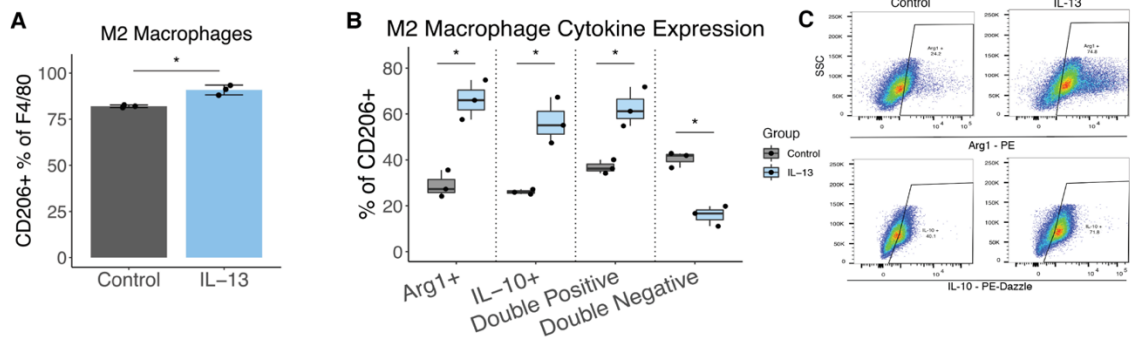


Figure 5.1. IL-13 increases AAM cytokine production. Bone marrow-derived macrophages (BMDMs) were cultured with 20ug/mL M-CSF for 7 days. On day 6, 20ug/mL of recombinant IL-13 was added and cells were allowed to incubate for 24hrs. AAMs were considered CD45⁺CD11B⁺F4/80⁺CD206⁺ cells. A) Percent CD206⁺ of F4/80⁺ BMDMs. B) Quantification of cytokine staining comparing control to IL-13-treated BMDMs. C) Intracellular staining for Arg1 and IL-10 is shown. * = $p < 0.05$. N = 3 wells/condition.

dinitrobenzene sulfonic acid (DNBS) models of colitis, researchers found that adoptive transfer of AAMs was important for resolving tissue damage and inflammation^{102,270,271}, highlighting that this method is feasible during enteric inflammation. Utilization of this approach during murine CDI may shed light on whether these cells are involved during type 2 mediated protective responses. Additionally, little is known about the mechanism of recovery from CDI, and therefore recognizing AAMs as a mediator of this response will increase our understanding on the disease process, as a whole.

5.3.2 Monocyte contributions to *C. difficile* immune response

Monocytes are critical immune cells as they can travel to sites of inflammation and develop into macrophages. The marker for monocytes, Ly6C is expressed highly on inflammatory monocytes as they circulate and enter tissue, where it will subsequently be downregulated as signals to differentiate into macrophages simultaneously promote the upregulation of markers such as MHCII, CX3CR1, and F4/80 or CD64 in the colon^{231,235}. This can be visually represented in a flow diagram, termed a Waterfall plot, which plots Ly6C with MHCII and indicates a cells position within this process²³¹. Additionally, in the colon, the surface expression level of CX3CR1 or CD64 can also provide an indication of the degree to which a monocyte has engrafted into a macrophage within the tissue. Utilization of these markers led us to observe that neutralization of IL-13 during *C. difficile* infection resulted in increased monocytes within the

colon, of which appeared to inappropriately accumulate as transitional, CD64-low, cells.

IL-13 can have some impact on the recruitment of monocytes to the tissue, wherein IL-13 can inhibit the expression of monocyte chemokines, such as CCL2/MCP-1^{92,272}. In support of this, treatment with IL-13 during CDI reduced cecal levels of CCL2 on day 3 post-infection (**Figure 5.2**). Notably, this appears to contrast our data suggesting that loss of CCR2-expressing cells negatively impacts disease. However, Ly6C-high, CCR2+ monocytes that give rise to AAMs also strongly rely on other chemokines such as CCL7²⁷³, suggesting that other mechanisms besides CCL2 could be promoting their recruitment during CDI.

Alternatively, or in concert with the above, loss of IL-13 may result in an inflammatory tissue environment that impedes the transition of monocytes into macrophages. The observation that inflammatory environments within the colon resulted in impaired monocyte engraftment has been observed in DSS colitis²³⁵, and these cells expressed increased levels of TNF α , IL-6, and TLR2 as well as other pro-inflammatory mediators. The factors that regulate this process of monocyte maturation are not well understood in the context of enteric inflammation, and the data shown here suggest that IL-13 plays a role in this process, either directly or indirectly.

Monocytes can be significant sources of iNOS, TNF α , and other inflammatory products, as well as give rise to classically- or alternatively-

Figure 5.2

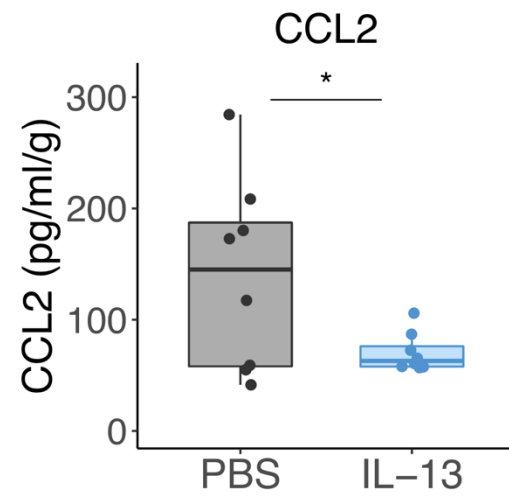


Figure 5.2. IL-13 treatment results in decreased CCL2 on day 3 in cecal lysates. Mice were i.p. injected with 100 μ L 5 μ g of recombinant IL-13 or PBS control on days 0, 1, and 2 post-infection with *C. difficile*. Cecal tissue was taken on day 3 post-infection and CCL2 levels were measured by ELISA and normalized to tissue weight. * = $p < 0.05$. N = 12.

activated macrophages, or dendritic cells. These cells can also express TLRs, which upon activation can increase production of IL-23 and IL-1 β ²⁷⁴, both cytokines known to be important drivers of severe CDI. Furthermore, following inflammatory insults mediated by neutrophil recruitment and activity, macrophages that express TNF α on their surface promote neutrophil apoptosis²⁷⁵. Subsequently, the macrophages will engulf apoptosed neutrophils by a process known as efferocytosis, and in concert with IL-4 and IL-13, are polarized into a tissue healing state²⁶⁷. In our model, we observed that macrophage populations were reduced following IL-13 neutralization, both CD206+ macrophages starting on day three and total macrophages by day four post-infection (**Figure 3.2 and 3.3**). This indicates that monocyte dysregulation may result in the loss of macrophages that could be important for clearing inflammatory cells and promoting resolution. In support of this hypothesis, we also observed greater numbers of immune cells, including neutrophils, within the colon on day four post-infection following IL-13 neutralization (**Figure 3.2**). Therefore, impaired monocyte maturation may promote a variety of detrimental responses, including exacerbated inflammation and impaired anti-inflammatory macrophage polarization, that could contribute to worsened disease and impair recovery.

One method for testing the contribution of monocytes to disease progression would be by adoptively transferring these cells during disease. However, given the predilection for these cells to engraft into macrophages,

timing of administration as well as creating an environment in which they preferentially remain as monocytes would be important considerations. Utilization of IL-13 neutralization to create this inflammatory state, then, may be one approach to facilitate impaired monocyte maturation, upon which an increase in monocytes through adoptive transfer may shed some insight into their contribution to disease. Alternatively, administration after inflammation has already begun, post-infection, may also increase the likelihood for dysregulated differentiation into macrophages. Lastly, to test whether inflammatory environments reduces macrophages capable of clearing dying cells, we can stain lamina propria cells, following IL-13 neutralization, with markers such as anxa5-pHrodo which can measure efferocytosis²⁷⁶. Understanding a potential contribution of monocytes and macrophages may provide further understanding into how a strong host immune response contributes negatively to CDI. Additionally, through addressing our hypothesis that monocytes contribute to impaired recovery may also highlight the role for IL-13 in promoting monocyte maturation into macrophages.

5.3.3 Is hyaluronan mediated by IL-13 in the colon and involved in the host response to CDI?

In our murine model of COVID-19 we identified a role for IL-13 in promoting hyaluronan deposition and expression of its receptor, CD44, in the lung. Therefore, we wanted to test whether there could be an association

Figure 5.3

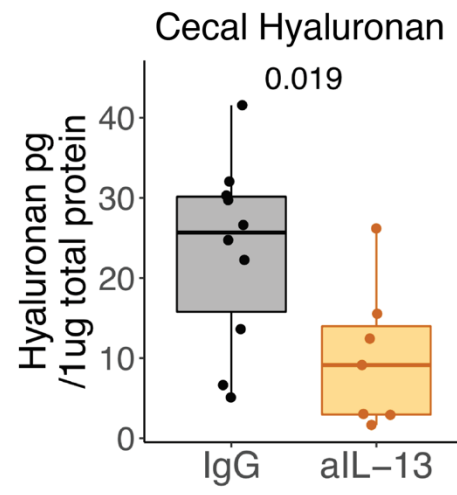


Figure 5.3. IL-13 neutralization results in decreased hyaluronan in cecal lysates. Mice were treated with 150 µg of anti-IL-13 on days 0 or 2, or IgG control. Mice were sacrificed on day 4 post-infection with *C. difficile*. Hyaluronan ELISA was performed on cecal lysates.

between IL-13 and hyaluronan during CDI. Hyaluronan was measured, by ELISA, in cecal lysates from day three post infection following neutralization of IL-13. We observed that IL-13 neutralization resulted in significantly lower levels of hyaluronan in the tissue (**Figure 5.3**), suggesting IL-13 may regulate hyaluronan deposition in the colon, similar to in the lung.

This observation further supports our hypothesis that IL-13 promotes hyaluronan deposition, and highlights that this is not specific to the lung tissue. In the intestines, hyaluronan plays an important role in maintaining tissue structure, facilitating water acquisition, and providing a matrix for cells to migrate across. Of note, in humans with IBD as well as in murine models of colitis, there have been increased levels of hyaluronan measured, although its distribution within the tissue was dysregulated^{138,277,278}. However, oral administration of HA 35 kDa resulted in protection from *Citrobacter rodentium* and *Salmonella* infection, partially through increased expression of tight-junction proteins zonula occludens-1 (ZO-1) and Claudin-2, respectively, as shown by IHC and Western blot analyses^{279,280}. Furthermore, hyaluronan administration was observed to increase the expression of the antimicrobial compound β -defensin in a TLR4-dependent manner^{279,281}. Additionally, intraperitoneal administration of hyaluronan 750kDa protected mice from DSS colitis-induced epithelial damage through TLR4, and resulted in increased expression of macrophage inflammatory protein 2 (MIP-2), cyclooxygenase (COX)-2 and TNF α ²⁸². Together, these studies suggest that tissue specific localization, size, and presence of

inflammatory modifications such as inter-alpha trypsin inhibitor ($\alpha 1$) may be important facilitators of a pathogenic role²⁸³.

Using immunofluorescence to stain for hyaluronan in the colonic tissue, similar to our COVID-19 studies, following infection with or without IL-13 neutralization would allow us to visualize the organization of hyaluronan during colitis, and may supply us with insights into its role during disease. To test the contribution of hyaluronan to CDI, we could orally administer fragments of either 750 or 35kDa, following the methods described from the above studies which found that fragments of these sizes contribute to beneficial responses in the colon. However, purification of hyaluronan fragments can be complicated and easily result in endotoxin contamination, and so proper precautions and controls for this would be necessary. Alternatively, administration of hyaluronidases that would break down hyaluronan, or use of 4-MU which prevents hyaluronan production²⁸⁴, may allow us to investigate how endogenous hyaluronan contributes to disease. The observation that neutralization of IL-13 is accompanied by decreased hyaluronan in the cecum leads us to hypothesize that hyaluronan is associated with protective responses, and may facilitate increased barrier function and prevent fluid loss. Additionally, using flow cytometry to observe which cells are expressing CD44, such as macrophage or monocytes, would be another tool to understanding the relationship of these components to CDI. Notably, one study found that CD44 clustering on monocytes was important for the ability to differentiate into macrophages²⁸⁵.

While this study was done using cell lines, and there is not a wide breadth of literature to support this finding, it could suggest that neutralization of IL-13 in our model results in decreased CD44, and subsequent accumulation of monocytes that cannot mature into macrophages in the tissue. Furthermore, it has been reported that *C. difficile* can produce hyaluronidases²⁸⁶. The consequences of this to the host are unknown, but are speculated to increase nutrient availability for the bacteria²⁸⁷. However, hyaluronan or CD44 may not contribute as significantly to *C. difficile* infection when compared to COVID-19, which may be due to differences in signaling downstream of these molecules, tissue site, type 1 or type 3-predominant immune response. Regardless, the potential contribution of hyaluronan and CD44 during CDI represents an exciting new area for future research.

5.3.4 Other downstream mediators of IL-13-induced pathology during COVID-19

In our model of COVID-19, neutralization of IL-13 resulted in the observation that *Has1* was the most highly downregulated gene. However, many other genes of interest were impacted by IL-13 signaling. Notably, *Arg1* (**Table 4.8**), which encodes for Arginase-1 (Arg1), was the second most downregulated gene. Arg1 is an enzyme that competes for Arginine with inducible nitric oxide synthase (iNOS) to produce ornithine and proline, while iNOS produces nitric oxide (NO) and citrulline²⁸⁸. In mice, Arg1 is often utilized as a marker for murine

AAMs^{30,289,290}, is also expressed by ILC2s²⁹¹, and has been shown to be important anti-inflammatory and have wound healing functions^{292–294}. Expression of Arg1 in macrophages is promoted by IL-13 and IL-4³⁰ (**Figure 5.1**), and downregulation of *Arg1* in our disease model indicated to us that neutralization of IL-13 in the lung was effective, and also implicated Arg1 or AAMs in the pathogenesis of COVID-19. One important note, however, is that while in mice, Arg1 production is downstream of IL-13 in AAMs, in humans, macrophages do not express Arg1 under the same regulations and much of the production of this enzyme is found within neutrophils^{290,295}. This may suggest two hypothesis: 1) Arg1 functions could be associated with disease severity, or 2) in mice, Arg1 may simply be a marker for the presence of AAMs, which may be playing a pathogenic role independently of Arg1. In support of both these considerations, Arg1 production and the presence of anti-inflammatory macrophages have been observed in patients with COVID-19. Arg1 protein was observed in the blood from patients with COVID-19^{296,297}, and utilization of Arg1 resulted in an ROC curve that had value in predicting positive COVID-19 cases. Arg1 is hypothesized to promote disease pathogenesis in part through suppressing T cell proliferation²⁹⁷, resulting in lymphopenia, or through depleting Arginine available for production into NO by iNOS to facilitate anti-viral responses²⁹⁶. Therefore, studies into the contribution for this enzyme to COVID-19 are warranted.

Conversely, dysregulated macrophages similar in phenotype to AAMs have been implicated in COVID-19 disease^{209,298,299}. Given the ability for these

cells to produce IL-10^{30,269}, along with other myeloid and lymphoid cells, they may represent a considerable source of this cytokine which is significantly associated with severe disease.

5.3.5 Hyaluronan and CD44 contributions to COVID-19

In this thesis, we report the finding that IL-13 regulates hyaluronan deposition and CD44 expression in the lungs of mice, and found evidence to suggest that they are involved in disease pathogenesis. Additionally, in our study and others, the observation that hyaluronan is increased in patients with COVID-19 supports the findings from our mouse model. As previously discussed, hyaluronan can be associated with lung pathology including the development of ARDS, which may be mediated by its ability to bind water thereby reducing lung function^{118,133}. Additionally, in combination with CD44, hyaluronan can provide tissue migratory surfaces and immune modulating signals to cells. The work presented here stops short of a full understanding of how IL-13 regulates these factors and how they are contributing to disease. Future work into these questions will be important in understanding the pathophysiology of COVID-19, as well as other pulmonary diseases.

Intranasal administration of hyaluronidase during COVID-19 in mice did not confer significant protection from disease. However, as noted in Chapter 4, this approach may not have been the most appropriate as the bovine hyaluronidase used here also reduces chondroitin sulfate²⁵⁷, which may have

unpredictable effects. Additionally, administration of hyaluronidase may not reach deep enough into the lung due to intranasal administration, thereby impeding its ability to break down hyaluronan that is found in the terminal bronchioles and alveoli. Therefore, other methods to reduce hyaluronan deposition would still be important to test whether accumulation of this polysaccharide contributes to disease. 4-MU is often utilized to reduce hyaluronan production in a variety of models, and is thought to prevent generation of polysaccharide formation by acting as a biological mimic of UDP²⁸⁴. It can be added to the diet or administered directly. This approach may be more appropriate in our model of COVID-19, as it is effective and may not be as strongly influenced by the timing of treatment, compared to the use of hyaluronidase. However, it is important to consider that 4-MU treatment may have some off-target effects or could inhibit other glycosaminoglycans³⁰⁰, although this has not been widely reported on³⁰¹.

If we were to observe an effect on disease severity following a reduction in hyaluronan, it would be important to understand how it and CD44 were contributing to pathology. Because the role of hyaluronan can be independent of CD44, we would expect unique, yet similar impacts to the tissue when comparing to CD44 neutralization. As previously discussed, hyaluronan can bind water and lead to decreased lung function, including the development of ARDS. These are commonly reported in severe COVID-19 outcomes, suggesting hyaluronan may contribute to these responses in patients. Conversely, CD44 is expressed in immune cells and may be indicative of increased cellular

inflammation¹¹⁹. Notably, however, neutralization of IL-13 did not result in overt changes to the cellular infiltration observed in the BALF by flow cytometry (**Figure 4.7**) Therefore, we would hypothesize that increased CD44 expression results in cells which may interact with the tissue more strongly, resulting in less extravasation into the airspace. Characterizing the lung tissue by flow cytometry with or without the neutralization of IL-13 may help address this question. Additionally, characterizing the tissue responses following neutralization of CD44 would further help us understand the contributions this receptor has to disease. Inflammatory cells such as T cells and macrophages are hypothesized to play a pathogenic role during COVID-19, and understanding whether CD44 influences their accumulation within the tissue, or inflammatory capabilities following activation, would be an important advancement into the host response to SARS-CoV-2 infection

In addition to understanding the pathogenic contributions of hyaluronan and CD44 to COVID-19, further exploring the relationship between IL-13 and these factors is an exciting new avenue to pursue following this work. As mentioned above, there are few studies identifying the capability for IL-13 to promote hyaluronan or CD44 production, and these mainly report findings from *in vitro* cell lines. Our work shows that *in vivo* IL-13 regulates expression of *Has1* and *Cd44* gene expression in the lung. Additionally, since both hyaluronan and CD44 have been implicated in asthma or other type 2-mediated responses, our work supports that IL-13 is capable of their promotion. IL-13 can involve both

STAT6 and STAT3 in mediating its downstream signaling response²⁴, and understanding whether either of these transcription factors is involved will further increase our understanding of this pathway. STAT3, which is involved in signaling by IL-6, IL-10, and IL-22³⁰², has previously shown promote hyaluronan responses, suggesting that this pathway may be involved downstream of IL-13. Conversely, there are some studies indicating that STAT6 could be involved in hyaluronan or CD44 production as well^{303,304}, however we could not identify a STAT6 motif in the promoter region of *Has1* or *Cd44*. Potential recognition that STAT6 is not involved in this pathway may further indicate that IL-4 does not have the same capacity to drive hyaluronan and/or CD44 production in the lung as IL-13, but studies of the role of IL-4 in this response are still needed.

5.3.6 Mechanisms driving IL-13 production in COVID-19

Lastly, the processes responsible for driving the induction of IL-13 during COVID-19 are still unknown. Originally, patients with asthma were expected to have increased susceptibility to severe COVID-19 due to the underlying tissue pathology. However, epidemiological studies have suggested that asthma is not a risk factor for severe disease^{190,305}. Further investigation by molecular studies showed that IL-13 could decrease expression of the ACE2 receptor^{306,307}, subsequently potentially decreasing the ability for SARS-CoV-2 to infect cells. Of note however, it was also observed that IL-13 and other type 2 cytokines resulted in the upregulated of the co-receptor for SARS-CoV-2,

TMPRSS2^{306,307}. Therefore, the presence of elevated IL-13 in patients likely represents cytokine that is induced following infection. Recognizing this, then, we hypothesize that IL-33 release from the epithelium results in increased ILC2s that express IL-13. As such, studies have identified the presence of IL-33 and ILC2s during COVID-19, as previously discussed ^{207,208}.

To test this in our mouse model of disease, we could administer soluble ST2 (sST2), which acts as a decoy receptor to neutralize IL-33 signaling. A decrease in clinical scores and mortality would support our hypothesis, following which we would characterize the ILC2 compartment as well as IL-13 production by these cells. In addition to this approach, we have recently adopted a murine model of disease using a mouse adapted strain of SARS-CoV-2, MA10²²², that causes disease in mice without the requirement of human ACE2 expression. Using this model, we can expand our studies into using other genetic mouse models, including ST2^{-/-} or RAG^{-/-} γ C^{-/-} mice, which lack ILCs, to be able to explore a contribution for ILC2s.

Identifying the source of IL-13 during COVID-19 would increase our understanding of how type 2 immunity is induced during viral pneumonia to promote severe disease. Additionally, it would help us address the question of why these patients have elevated IL-13 in the absence of previous type 2-mediated comorbidities.

5.4 Concluding remarks

Type 2 inflammation is an important branch of the host immunity for protecting against infections by helminths. However, increasingly, studies on this immune response have shed light on its involvement in many other infectious diseases, such as those mediated by viruses or bacteria. Recognizing and understanding the contribution of type 2 immunity can help us identify mechanisms to promote protection to the host through modulation of these responses, or serve as prognostic indicators for patient outcomes.

C. difficile is currently the leading cause of hospital-acquired gastrointestinal infections, and contributes a significant financial burden on the healthcare system each year in the United States. Strategies are being implemented to control the incidence of CDI in the population, such as increased sanitation policies and increased antibiotic stewardship, which have resulted in decreased incidence rates of health-care associated CDI³⁰⁸. However, it is still considered an Urgent Threat by the CDC³⁰⁹ as antibiotic resistance is increasing, albeit slowly^{310,311} and for patients who contract the disease, symptoms can be severe. Additionally, the use of antibiotics to treat infection may be promoting further dysbiosis in the colon that leaves patients susceptible to recurrent infections. Therefore, the identification and development of non-antibiotic therapeutics for the treatment of *C. difficile* infection may be an important step forward in combating this disease. Our data suggest that type 2 cytokines including IL-4,-5,-13,-25, or -33 all contribute to protection from disease, and could represent strategies for addressing these concerns.

For SARS-CoV-2 infections, as of the summer of 2021 the incidence of COVID-19 in the U.S., as well as around the world, has begun to decline while vaccination rates continue to increase^{312–314}. However, case rates are still high in many parts of the world, and infected individuals can still experience serious illness. Due to efforts to understand pathological drivers of disease, observations of elevated pro-inflammatory mediators such as IL-6, MCP-1, and others in patients with severe disease have indicated that the immune response is likely involved in promoting severe outcomes. The results from these studies has led to the use of protective steroidal drugs such as dexamethasone to reduce the inflammatory burden, however steroid-use can be associated with unwanted side-effects and protection is not complete²⁰⁶. Furthermore, there is concern that the virus, SARS-COV-2, will become endemic in many regions³¹⁵ as variants arise^{316–318} or potentially, immune responses wane³¹⁹, making it likely that vaccine boosters will be necessary in the near future. However, similar to influenza, the availability of a vaccine may not be sufficient to prevent cases of severe disease from occurring, particularly in those who do not receive it or following the appearance of immune-escaping variants. Tamiflu is an example of an FDA-approved medication for reduction of disease severity from influenza infection, and provides precedence for having multiple avenues for which to combat these infectious diseases. Therefore, continued efforts to characterize and understand the immune response to infection may provide further insight into more targeted and effective therapeutics.

We highlight here that IL-13 is a contributor to disease severity in COVID-19 patients, in part through increasing hyaluronan and CD44 in the lung. Using this knowledge, then, we propose that the FDA approved monoclonal antibody against IL-4Ra, Dupilumab, could be one strategy to reduce immunopathology in patients. Further studies into recognizing which patients this may provide the most significant benefit is warranted, as, given the highly heterogenous nature of this disease, it is unlikely that this approach will be beneficial for all patients.

In conclusion, type 2 immunity through cytokines such as IL-4, IL-5, and IL-13 can promote pathology in the lung, as evidenced in asthma and some viral infection, yet is required for host protection from helminth infections. In the intestines, aberrant type 2 inflammation is suspected to drive colitis, but our lab and others have shown that type 2 cytokines provide protection from bacterial infections and type 3-mediated pathology. Therefore, it is important to recognize that the role type 2 immunity plays is context dependent, and continued studies into the mechanisms resulting in these opposing outcomes will be informative to understanding this immune response. The work shown here highlights two examples, infection with *C. difficile* or SARS-CoV-2, for which type 2 responses play contrasting roles in promoting protection or pathology, respectively, and expands our knowledge on how this immune response regulates infectious diseases.

Chapter 6: Materials and Methods

6.1 Methods for *C. difficile* studies

Bacterial strains and culture:

To generate spore stocks, vegetative *C. difficile* strain R20291¹⁵⁷ [3] was plated on BHI agar from frozen stocks and incubated overnight at 37°C in an anaerobic chamber (Shel Labs). A single colony was then inoculated into 15 mL of Columbia broth overnight at 37°C anaerobically. Then 5 mL of turbid broth was moved into 45 mL of Clospore broth³²⁰ and incubated at 37°C for 5-7 days.

Cultures were spun down at 3200 rpm for 20 minutes at 4°C then resuspended in cold sterile water. This was repeated 3-5 times to lyse vegetative cells. The pellet was then resuspended in 1 mL sterile water and transferred to a 1.5 mL twist cap tube (Corning # 4309309). Spores were plated on BHIS +Taurocholate agar plates to determine concentration of stock. Spores were stored at 4°C. To make the inoculum, a 5×10^4 - 1×10^5 spores/mL dose was prepared in sterile water. Each mouse received 100 μ L (5×10^3 - 5×10^4 spores) by oral gavage. *C. difficile* burden was quantified from cecal contents following infection. Total cecal content was resuspended by weight in sterile, anaerobic PBS. Serial dilutions of cecal contents were plated on BHI agar supplemented with 1% taurocholate, 1 mg/mL D-cycloserine, and 0.032 mg/mL cefoxitin (Sigma) and incubated anaerobically at 37°C overnight before colonies were counted.

Mice:

Experiments were carried out using male, 8-12-week-old C57BL/6J mice ordered from Jackson Laboratory. All animals were housed under specific pathogen-free conditions at the University of Virginia's animal facility. Mice were infected following a previously published murine model of CDI^{91,157}. Six days prior to infection, mice were given a cocktail of antibiotics in their drinking water, consisting of 45 mg/L Vancomycin (Mylan), 35 mg/L Colistin (Sigma), 35 mg/mL Gentamicin (Sigma), and 215 mg/L Metronidazole (Hospira). Mice were then switched to normal drinking water for three days prior to infection. One day before infection, mice were given an IP injection (0.016mg/g) of Clindamycin (Hospira). On the day of infection, mice were orally gavaged with 5×10^3 - 5×10^4 spores of *C. difficile* strain R20291 in 100 μ L water. Mice were monitored twice daily over the course of infection and evaluated according to clinical scoring parameters. Scores were based on weight loss, coat condition, activity level, diarrhea, posture, and eye condition for a cumulative clinical score between 1 and 20; scores were not blinded. Weight loss and activity levels were scored between 0 and 4 with four being greater than or equal to 25% loss in weight. Coat condition, diarrhea, posture, and eye condition were scored between 0 and 3. Diarrhea scores were 1 for soft or yellow stool, 2 for wet tail, and 3 for liquid or no stool. Mice were euthanized if severe illness developed based on a clinical score ≥ 14 . For IL-5 treatment, mice were injected i.p. with 15 μ g of recombinant

murine IL-5 (Peprotech cat#215-15) in PBS (100 μ L dose) one day prior to infection. For IL-4 treatment, mice were i.p. injected with 5 μ g of recombinant murine IL-4 (Peprotech cat #214-14) in PBS (100 μ L dose) one day prior to infection. On the day of and one day post infection, mice were given additional treatments of 1 μ g of IL-4 in PBS. For IL-13 treatment, mice were i.p. injected with 5 μ g of recombinant murine IL-13 (Peprotech cat# 210-13) in PBS (100 μ L dose) on days -1 and 1 of infection. Control treatments for all groups were filter-sterilized PBS. For anti-IL-13 neutralization, mice were administered 150 μ g of anti-IL-13 (eBio1316H cat# 16-7135-85) or IgG (eBRG1 cat# 16430185) from Thermofisher. For anti-CCR2 cell depleting treatment, mice were administered 500 μ g of anti-CCR2 (MC-21; gifted from Dr. Matthias Mack) on either days two and four, or one and three. Anti-IL-13R α 2 treatment was administered using 250 μ g of anti-IL-13R α 2 (clone: 6D5) or IgG1 (HPRN) (gifted from Dr. Tom Wynn) on days two and four post-infection.

Flow cytometry:

Colons were dissected longitudinally and rinsed in HBSS (Thermofisher) supplemented with 25 mM HEPES and 5% FBS. Epithelial cells were separated from the lamina propria via a 40-min incubation with gentle agitation in dissociation buffer (HBSS with 15 mM HEPES (Thermofisher, 5 mM EDTA (Invitrogen), 10% FBS (Gibco), and 1 mM DTT (Bioworld)) at 37 °C. Next, the lamina propria tissue was manually diced using scissors and further digested in

RPML 1640 (Gibco) containing 0.17 mg/mL Liberase TL (Roche) and 30 μ g/mL DNase (Sigma). Samples were digested for 40 min at 37 °C with gentle shaking. Single-cell suspensions were generated by passaging samples through a 100 μ M cell strainer followed by a 40 μ M cell strainer (Fisher Scientific). For staining, single-cell suspensions were obtained and cells were stained with the following monoclonal antibodies: CD45 (APC-Cy7 #103116 1/200), CD11B (APC #101212, 1/200), Ly6G (PE-Cy7 #127618, 1/100) from Biolegend, Siglec-F (PE #552126, 1/100) from BD Biosciences, CD64 (BV711 clone: X54-5/7.1 #139311), CD206 (BV421 # 141717) from Biolegend, MHCII (PerCP-Cy7 clone: M5/114.15.2 #107626) from Biolegend, F4/80 (FITC clone: BM8 #123108) from Biolegend, IL-10 (PE-Dazzle #505033) from Biolegend, Arg1 (PE # 12-3697-82) from Thermofisher. For surface staining, 1×10^6 cells/sample were Fc-blocked with TruStain fcX (BioLegend, #101320, 1/200) for 10 minutes at room temperature followed by LIVE/DEAD Fixable Aqua (Life Technologies) for 30 min at 4 °C. Cells were washed twice in FACS buffer (PBS+ 2% FBS) and stained with fluorochrome conjugated antibodies for 30 min at 4 °C. Cells were washed twice before incubation for 20 minutes at 4 °C in BD Cytotfix (BD Cytotfix/Cytoperm Fixation/Permeabilization Solution Kit, #555028) and then were washed and resuspended in FACS buffer and incubated overnight at 4 °C. Flow cytometry was performed on an LSR Fortessa cytometer (BD Biosciences) and all data analysis performed via FlowJo.

ELISAs

R7D Mouse DuoSet Sandwich ELISA kits were used to measure levels of IL-13 (cat# DY413-05), IL-10 (cat# DY417-05), YM1 (CHI3L3) (cat# DY2446), IL-6 (cat# DY406-05), IL-13R α 2 (cat# DY539), and Hyaluronan (cat# DY3614-05) were detected in cecal tissue lysates according to manufacturer's instructions. Total cecal lysate was generated by removing the ceca and rinsing gently with 1x PBS. Tissue was bead beaten for 1 minute and resuspended in 400 μ L of Lysis Buffer I: 1x HALT Protease Inhibitor (Pierce), 5 mM HEPES. Following mechanical tissue disruption, 400 μ L of Lysis Buffer II was added: 1x HALT Protease Inhibitor (Pierce), 5 mM HEPES, 2% Triton X-100. Tissue samples were incubated on ice for 30 minutes after gently mixing. Lysed samples were pelleted to remove tissue debris in a 5-minute spin at 13,000 $\times g$ at 4°C. Supernatant was collected and total protein concentration was measured by BCA assay according to manufacturer's instructions (Pierce). Cytokine concentration was normalized to tissue weight.

Statistical Analyses

Survival differences between groups were tested using the log-rank test. Statistical differences in clinical scores and weight loss were evaluated using Student's t-test (two-tailed). Linear regressions were performed in R studio. A p-value below 0.05 was considered significant. All statistical tests were run using R Studio software (Version 1.2.1335).

6.2 Methods for COVID-19 studies

Patients:

Patients with a positive RT-qPCR test for COVID-19 at the Clinical Microbiology Laboratory at the University of Virginia Medical Center had any remnant EDTA-plasma samples within 48 hours of the time of diagnosis or hospitalization collected. EDTA-plasma from 178 patients diagnosed from March to September 2020 were analyzed in this study. Blood was centrifuged at 1300 x *g* for 10 minutes, then plasma was aliquoted and stored at -80°C until testing.

Demographics (age, gender, race), comorbidities, hospitalization status, lab results, and other clinical information were obtained from the electronic medical record (EMR) (Table 4.1). Severity of COVID-19 illness was assessed through review of the electronic medical record in two ways: first by inpatient admission vs outpatient care, and second by the use of supplemental oxygen (none vs any supplemental oxygen, and supplemental oxygen delineated as low flow nasal canula vs mechanical ventilation or high flow oxygen). In addition, supplemental oxygen was scored as occurring at the time of the blood draw or at a future time. Days from symptom onset was scored as per Lucas *et al* ¹⁹⁸ based on the patient's determination or by the earliest reported symptom from the patient as recorded in the EMR.

Cytokine concentrations in plasma were measured using the MILLIPLEX® MAP Human Cytokine/Chemokine/Growth Factor Panel A (48 Plex) (Millipore Sigma,

St. Louis) by the Flow Cytometry Facility of the University of Virginia. Cytokines detected were sCD40L, EGF, Eotaxin, FGF-2, Flt-3 ligand, Fractalkine, G-CSF, GM-CSF, GRO α , IFN α 2, IFN γ , IL-1 α , IL-1 β , IL-1ra, IL-2, IL-3, IL-4, IL-5, IL-6, IL-7, IL-8, IL-9, IL-10, IL-12 (p40), IL-12 (p70), IL-13, IL-15, IL-17A, IL-17E/IL-25, IL-17F, IL-18, IL-22, IL-27, IP-10, MCP-1, MCP-3, M-CSF, MDC (CCL22), MIG, MIP-1 α , MIP-1 β , PDGF-AA, PDGF-AB/BB, TGF α , TNF α , TNF β , and VEGF-A (Figure S1). (RANTES was excluded). Hyaluronan was measured using the Hyaluronan Duoset ELISA (R&D, cat# DY3614-05) with plasma diluted 1:50.

As a test of validation of the results from the University of Virginia Hospital, an additional 47 patients with symptomatic COVID-19 (all inpatients) from Virginia Commonwealth University Medical Center were analyzed. All procedures performed in this study were approved by the Virginia Commonwealth University Institutional Review Board and in accordance with the 1964 Helsinki Declaration and its later amendments or comparable ethical standards. Informed consent was obtained from all participants or by their legally authorized representatives if they were unable to give consent. Severe was defined as any patient requiring high flow nasal cannula (HFNC) oxygen delivery, intubation, or who's disease resulted in sepsis or death. IL-13 was measured in EDTA plasma from these patients using the Bio-Plex Pro Human Cytokine 27-plex Assay (R & D Systems, Minneapolis, MN) (Table S4).

Database and Inclusion Criteria for Dupilumab

Data were retrieved from the COVID-19 Research Network provided by TriNetX, comprising 400 million patients from 130 health care organizations in 30 countries (database access on 12/05/2020). COVID-19 patients were identified via the ICD-10 code U07.1 or the presence of a SARS-CoV-2-related RNA diagnosis within the last eleven months. Propensity scores matched cohorts 1:1 using a nearest neighbor greedy matching algorithm with a caliper of 0.25 times the standard deviation. Outcomes were defined as ventilation assist and death. Measures of association including risk differences with their respective 95% CI's were calculated. In addition, Kaplan-Meier curves were generated for each analysis.

A sub cohort with indications for Dupilumab use was generated using ICD-10 codes for asthma (J45), atopic dermatitis (L20.8), and pansinusitis (J01.40 and J32.4). Drug use was identified via RxNorm codes for Dupilumab (1876376) and the lab value for C-reactive protein (9063). Patients receiving Dupilumab are on average one year older.

N3C Dupilumab Analysis:

We utilized deidentified data in the National Cohort Collaborative Cohort (N3C) enclave, which currently contains 2 years of medical record data from 34 United States sites, to explore the association between Dupilumab use and COVID-19 outcomes. This enclave represents >2M persons (including ~300K COVID-19

cases) and medical facts from more than ~90M visits. Values less than 20 have been suppressed as per current N3C publication policy.

Cohort Definitions:

1. Dupilumab+: If Patient had Dupilumab within 61 days prior to their first COVID-19 diagnosis date
2. Controls+: Patients with no record of Dupilumab within 2 months prior to their first COVID-19 diagnosis date.

Outcome Definitions:

1. Hospitalized: Patients who became inpatient within 6 weeks post COVID-19 diagnosis date.
2. Death: If subjects death date is after their first COVID-19 diagnosis date.
3. With Ventilation: If patients were put on a ventilator within 6 weeks of any of their COVID-19 diagnosis dates (window is double sided: procedure could have been 6 weeks before or after any of their diagnosis dates).

The incidence of COVID positivity in people on dupilumab [cohort definition 1 above / (definition 1 + 2)], along with 95% confidence intervals, was calculated. Then, a case-control design was used. Dupilumab+ patients were matched to control+ patients in a 1:5 ratio, with exact matching on gender, race, ethnicity, N3C site, asthma and nearest matching on age. Conditional logistic regression was used to compare COVID-19 severity outcomes within this matched subset of

COVID+ patients. A sensitivity analyses was performed excluding asthma from the matching criteria.

Virus and Cell Lines:

SARS-Related Coronavirus 2 (SARS-CoV-2), isolate Hong Kong/VM20001061/2020 (NR-52282) was obtained from the Biodefense and Emerging Infections Research Resources Repository (BEI Resources), National Institute of Allergy and Infectious Diseases (NIAID), National Institutes of Health (NIH). Virus was propagated in Vero C1008, Clone E6 (ATCC CRL-1586) cells cultured in Dulbecco's Modified Eagle's Medium (DMEM, Gibco 11995040) supplemented with 10% fetal bovine serum (FBS) and grown at 37°C, 5% CO₂. Initial viral stocks were used to infect Vero E6 cells, generating passage 1 (P1) stocks. These P1 stocks were then used to infect additional Vero E6 cells, generating passage 2 (P2) stocks, which were used for all experiments.

Viral Propagation:

Vero E6 cells grown to 90% confluency in T75 tissue culture flasks (Thermo Scientific) were infected with SARS-CoV-2 at a multiplicity of infection of 0.025 in serum-free DMEM. Vero E6 cells were incubated with virus for two hours at 37°C, 5% CO₂, after which the virus was removed, media was replaced with DMEM supplemented with 10% FBS, and flasks were incubated at 37°C, 5% CO₂. After two days, infected flasks showed significant cytopathic effects, with

>50% of cells unattached. Cell supernatants were collected, filtered through a 0.22 μ m filter (Millipore, SLGP003RS), and centrifuged at 300 x g for ten minutes at 4°C. Cell supernatants were divided into cryogenic vials (Corning, 430487) as viral stocks and stored at -80°C until use.

Challenge:

8-16 week-old male Tg(K18-*hACE2*) 2PrImn (Jackson Laboratories)²⁴⁸ mice were challenged with 5000 plaque forming units (PFUs) of SARS-CoV-2 Hong Kong/VM20001061/2020 (BEI Resources) in 50 μ L by an intranasal route under 100 μ L ketamine/xylazine sedation. Mice were followed daily for clinical symptoms, which included weight loss (0-5), activity (0-3), fur appearance and posture (0-2), and eye closure (0-2). Mice were given 150 μ g of anti-IL-13 (clone eBio1316H; cat # 16-7135-85) or an isotype matched control IgG (clone eBRG1; # 16-4301-85) administered on day 0, 2, and 4 pi. For experiments utilizing hyaluronidase, 14 U in 70 μ L of ovine testicular hyaluronidase (Vitrax; 200 USP Units/mL) or saline control were administered intranasally following isoflurane anesthetization on day five pi. For anti-CD44 experiments, 100 μ g of anti-CD44 (BD Biosciences, clone IM7; cat # 553131) or IgG2 (BD Biosciences, clone A95-1; cat # 559478) were administered on day one pi, and then mice were given an additional 50 μ g on days 2, 3 and 4.

IL-13 delivery *in vivo*:

To extend the half-life of IL-13, fusion proteins of mouse IL-13 Fc portion of IgG1 were generated (custom order with Absolute Antibody)³²¹. Female C57BL/6 mice were anaesthetized with isoflurane inhalation and administered PBS or 10 μ g IL-13-Fc intranasally (in 40 μ L) on days 0 and 2. On day 3, serum and BALF were collected and stored (-80°C) until use for measurement of secreted HA levels. Lungs were inflated with 10% neutral buffered formalin and fixed to assess histological HA deposition.

Viral titers:

The left lobe of the lung was removed, placed in a disposable tissue grinder with 1 mL of serum-free DMEM on ice, and then ground. Lung homogenates were centrifuged at 300 xG for 10 minutes, and then the supernatants were collected and frozen at -80° C until use. Plaque assays were as described previously²⁴⁸. Briefly, Vero E6 cells seeded in 12-well tissue culture plates were infected with lung homogenates serially diluted in serum-free DMEM. Plates were then incubated at 37° C, 5% CO₂ for two hours to allow viral infection of the cells, before washing with sterile PBS (Gibco 10010-023) to remove virus and replacing with an overlay of DMEM, 2.5% FBS containing 1.2 % Avicel PH-101 (Sigma Aldrich). After incubation at 37°C, 5% CO₂ for two days the overlay was removed, wells were fixed with 10% formaldehyde and stained with 0.1% crystal violet to visualize plaques and calculate viral titers as PFU/ml.

Histology:

Tissues were fixed in formaldehyde, processed and embedded in paraffin. Slides were sectioned at 5 microns and stained with H&E or Periodic Acid-Schiff using standard protocols. Slides were scanned at 20X magnification. Histopathological scoring for lung tissue was done according to the guidelines of the American Thoracic Society³²².

For antibody and HA staining, lung sections were deparaffinized and heat-mediated antigen retrieval performed using Tris-EDTA buffer (10 mM Tris Base, 1 mM EDTA, 0.05 % Tween-20 pH 9.0; incubation 20 min 95°C). Non-specific protein was blocked (2% donkey serum, 1% BSA, 0.05% Tween-20) prior to blocking endogenous avidin and biotin (Thermofisher). Lung sections were incubated with primary antibodies or HA binding protein (Table S7) overnight at 4°C, washed in PBS containing 0.05% Tween-20 before incubation with secondary antibodies (Table S7) for 1 hr at room temperature followed by mounting with DAPI containing fluoromount (Southern biotech). Images were captured with an EVOS FL imaging system (Thermofisher). Analysis of images was performed using ImageJ software (version 2.09.0-rc69/1.52p) on sections where sample identification was blinded for the investigator. For calculation of antibody positive staining, background autofluorescence subtraction was performed to remove non-specific staining based on a secondary-only control stain. Analysis was limited to regions of interest (airway, vessels or parenchyma), and a threshold was then applied (by eye) to images in order to include positive

staining but to exclude areas of high autofluorescence (for example red blood cells). For measurements of airway positivity, stain intensity was normalized to the length of the basement membrane.

Mouse bronchioalveolar lavage

BAL fluid was collected from each animal through cannulation of the exposed trachea, and flushing twice with 0.7mL of PBS. BALF samples were centrifuged at 500xG for 5 minutes, and supernatant was immediately frozen for later cytokine analyses. For flow cytometry, pelleted cells were resuspended in FACS (PBS + 5% FBS) buffer for staining and with Zombie NIR (Biolegend, 423105, San Diego, CA), CD45, Alexa Fluor 532 (eBioscience, 58-0459-42, San Diego, CA), CD11c, PE-Cy7 (Biolegend, 117317, San Diego, CA), CD11b, BV480 (BD Biosciences, 566117, San Jose, CA), SIGLEC F, AF700 (eBioscience, 56-1702-80, San Diego, CA), Ly-6c, FITC (Biolegend, 128005, San Diego, CA), and Ly-6G, BV650 (Biolegend, 127641, San Diego, CA) and then fixed in IC-fixation buffer (eBioscience, 00-8222-49, San Diego, CA). Samples were run on a Cytex Aurora Borealis at the University of Virginia flow cytometry core. Neutrophils are Zombie NIR⁻, CD45⁺, CD11C⁻, CD11B⁺, and Ly-6G⁺; eosinophils are Zombie NIR⁻, CD45⁺, CD11C⁻, CD11B⁺, and Siglec-F⁺; inflammatory monocytes are Zombie NIR⁻, CD45⁺, CD11C⁻, CD11B⁺, Ly-6G⁻, and Ly-6C⁺. Cytokine analyses were performed via Luminex Mouse 32-plex (MCYTMAG-70K-PX32,

Millipore-sigma). Samples were run following manufacturers protocol after an 18-hour incubation before being run on Luminex® analyzer (MAGPIX®).

RNAseq

Snip from lower inferior lobe was taken and RNA was extracted from murine lung tissue preserved in trizol by bead beating (tissuelyserII, Qiagen), followed by a phenol-chloroform extraction and RNA Isolation Kit (Qiagen). RNA quality was assessed using Agilent Tape Station RNA kit (Agilent). Library preparation, sequencing, quality control, and read mapping was performed by the Genome Analysis and Technology Core, RRID:SCR_018883. Briefly, ribosomal RNA was depleted using the rRNA depletion kit (NEB E6310). Following rRNA depletion cDNA libraries were prepared using the NEB ultra-directional library preparation kit 2.0 (NEB E7760) and indexed using the NEBNext Multiplex Oligos for Illumina (NEB E7335, E7500). Library size and purity were verified using the Agilent Tape Station D5000 HS kit (Agilent). Library concentration was measured with a qubit DNA HS assay (Invitrogen). Libraries concentrations were normalized and 15 libraries were multiplexed per run. Diluted libraries were sequenced on the Illumina Nextseq 500 using a 150 high output kit (400 Million reads, 2x75bp paired end, 150 cycles).

RNAseq data analysis:

RNAseq reads were first processed using Cutadapt³²³ to trim the adapter sequences and then the quality of the reads was assessed by FastQC (<https://www.bioinformatics.babraham.ac.uk/projects/fastqc/>) and MultiQC³²⁵.

After these processes the reads were aligned to the mouse Ensembl GRCh38.76 primary assembly using STAR v2.5.3a³²⁶ in a two-passing mode to generate a gene matrix for differential gene expression. Differentially expressed genes were determined using the DESeq2 package³²⁷ in Rstudio (*RStudio Team (2020)*.

RStudio: Integrated Development for R. RStudio, PBC, Boston, MA

URL <http://www.rstudio.com/>.)

Enrichment analysis was applied to the total gene counts using the reactome GSA package³²⁸ in Rstudio. Enrichment analysis was applied to the total gene counts using the CAMERA algorithm³²⁹.

Statistical Methods:

For the clinical study, a total of 47 cytokines, chemokines and growth factors were measured in 178 COVID-19 positive patients with plasma samples. For cytokines of interest, levels at the time of COVID-19 diagnosis or admission were compared between patients with different severity of illness using a Mann-Whitney U test. The pheatmap function in the pheatmap library in R([R-project.org](https://www.r-project.org)) was used for hierarchical clustering. Cytokines were scaled by row (patients), and the clustering was calculated using the complete linkage method. Statistical analyses were performed using GraphPad Prism and R.

Since these cytokine measurements were highly correlated, principal component analysis (PCA) was performed to identify distinct features among correlated cytokines, and thus reduce the dimensionality. Due to their skewed distributions and variable scales, the cytokines were log-transformed first, and then standardized with mean of zero and standard deviation of one. The first five principal components (PCs) captured 62% of total variation in the cytokines. For each PC, those cytokines with loading score of 0.5 or above were retained, showing the strength of their influences within the component. Additionally, the network analysis using the qgraph package in R was performed to characterize the complex structural relationships among cytokine measurements and optimized with graphical LASSO. The nodes represented individual cytokines, and edges represented their correlations in that highly correlated cytokines were connected closer with thick edges

(<https://cran.rproject.org/web/packages/qgraph/qgraph.pdf>).

Survival Analysis was performed for patients from the time to ventilation since symptom onset. Those who were not ventilated were censored at 40 days.

Patients were classified into 4 quartiles based on the cumulative distribution of IL-13 levels, and the probabilities of ventilation were estimated by the Kaplan-Meier method. Since the two upper quartiles had statistically identical results in the preliminary analysis, they were combined in the final log-rank test and Cox regression done for their relative performance over the lower quartiles, and were

corrected for sex, age, and cumulative number of comorbidities (including: diabetes, cancer, stroke, and heart, liver, kidney, or lung diseases).

ROC curve was generated using pROC library in RStudio for IL-13 alone and in combination with IL-6, IL-8, and MIP-1b which were selected as within the top predictors for ventilation identified by conditional random forests analysis (data not shown).

For clinical scores, weight loss, and scored histological sections of mouse studies, a two-tailed Student's t test was used to determine statistical significance. For IHC sections with multiple quantified images per mouse or human tissue, response differences between groups (e.g., infected vs. uninfected, or IgG vs aIL-13) were evaluated in the mixed-effects model to account for within-individual correlation, and distributions were log transformed where appropriate. P value < 0.05 was considered significant.

Study Design:

Discarded human plasma samples from COVID-19 positive and negative patients at the University of Virginia Medical Center were collected for cytokine and growth factor analyses. The collection of biological specimens and de-identified patient information was approved by the University of Virginia Institutional Review Board (IRB-HSR #22231 and 200110). In mice, neutralizing antibodies or isotype controls were used to assess the role of IL-13 during COVID-19. All mouse work was approved by the University of Virginia Institutional Animal Care

and Use Committee, and all procedures were performed in the University certified animal Biosafety Level Three laboratory.

Chapter 7: References

References:

1. Allen, J. E. & Wynn, T. A. Evolution of Th2 Immunity: A Rapid Repair Response to Tissue Destructive Pathogens. *PLoS Pathog* **7**, e1002003 (2011).
2. Gause, W. C., Rothlin, C. & Loke, P. Heterogeneity in the initiation, development and function of type 2 immunity. *Nat Rev Immunol* **20**, 603–614 (2020).
3. Pulendran, B. & Artis, D. New Paradigms in Type 2 Immunity. *Science* **337**, 431–435 (2012).
4. Akdis, C. A. *et al.* Type 2 immunity in the skin and lungs. *Allergy* **75**, 1582–1605 (2020).
5. Spellberg, B. & Edwards, J. E. Type 1/Type 2 Immunity in Infectious Diseases. *Clinical Infectious Diseases* **32**, 76–102 (2001).
6. Tangye, S. G. *et al.* Deducator of cytokinesis 8-deficient CD4 + T cells are biased to a T H 2 effector fate at the expense of T H 1 and T H 17 cells. *Journal of Allergy and Clinical Immunology* **139**, 933–949 (2017).
7. Roan, F., Obata-Ninomiya, K. & Ziegler, S. F. Epithelial cell-derived cytokines: more than just signaling the alarm. *Journal of Clinical Investigation* **129**, 1441–1451 (2019).
8. Harris, N. L. & Loke, P. Recent Advances in Type-2-Cell-Mediated Immunity: Insights from Helminth Infection. *Immunity* **47**, 1024–1036 (2017).

9. Herbert, D., Douglas, B. & Zullo, K. Group 2 Innate Lymphoid Cells (ILC2): Type 2 Immunity and Helminth Immunity. *IJMS* **20**, 2276 (2019).
10. Spits, H. & Cupedo, T. Innate Lymphoid Cells: Emerging Insights in Development, Lineage Relationships, and Function. *Annu. Rev. Immunol.* **30**, 647–675 (2012).
11. Vivier, E. *et al.* Innate Lymphoid Cells: 10 Years On. *Cell* **174**, 1054–1066 (2018).
12. Bernink, J. H., Germar, K. & Spits, H. The role of ILC2 in pathology of type 2 inflammatory diseases. *Current Opinion in Immunology* **31**, 115–120 (2014).
13. Chang, Y.-J. *et al.* Innate lymphoid cells mediate influenza-induced airway hyper-reactivity independently of adaptive immunity. *Nat Immunol* **12**, 631–638 (2011).
14. Halim, T. Y. F., Krauß, R. H., Sun, A. C. & Takei, F. Lung Natural Helper Cells Are a Critical Source of Th2 Cell-Type Cytokines in Protease Allergen-Induced Airway Inflammation. *Immunity* **36**, 451–463 (2012).
15. Voehringer, D., Reese, T. A., Huang, X., Shinkai, K. & Locksley, R. M. Type 2 immunity is controlled by IL-4/IL-13 expression in hematopoietic non-eosinophil cells of the innate immune system. *Journal of Experimental Medicine* **203**, 1435–1446 (2006).
16. Kouro, T. & Takatsu, K. IL-5- and eosinophil-mediated inflammation: from discovery to therapy. *International Immunology* **21**, 1303–1309 (2009).

17. Mishra, A., Hogan, S. P., Brandt, E. B. & Rothenberg, M. E. IL-5 Promotes Eosinophil Trafficking to the Esophagus. *J Immunol* **168**, 2464–2469 (2002).
18. Fallon, P. G. *et al.* Identification of an interleukin (IL)-25–dependent cell population that provides IL-4, IL-5, and IL-13 at the onset of helminth expulsion. *Journal of Experimental Medicine* **203**, 1105–1116 (2006).
19. Ikutani, M. *et al.* Identification of Innate IL-5–Producing Cells and Their Role in Lung Eosinophil Regulation and Antitumor Immunity. *J.I.* **188**, 703–713 (2012).
20. Nussbaum, J. C. *et al.* Type 2 innate lymphoid cells control eosinophil homeostasis. *Nature* **502**, 245–248 (2013).
21. Johansson, K. B. C., Malmhäll, C., Ramos-Ramírez, P. & Rådinger, M. IL-33 elicits IL-5 dependent eosinophilia *in vivo*. *J. Immunol.* **198**, 194.8 (2017).
22. Schneider, C. *et al.* A Metabolite-Triggered Tuft Cell-ILC2 Circuit Drives Small Intestinal Remodeling. *Cell* **174**, 271-284.e14 (2018).
23. Busse, W. *et al.* Anti-IL-5 treatments in patients with severe asthma by blood eosinophil thresholds: Indirect treatment comparison. *Journal of Allergy and Clinical Immunology* **143**, 190-200.e20 (2019).
24. McCormick, S. M. & Heller, N. M. Commentary: IL-4 and IL-13 receptors and signaling. *Cytokine* **75**, 38–50 (2015).
25. Himmelrich, H. *et al.* In BALB/c Mice, IL-4 Production During the Initial Phase of Infection with *Leishmania major* Is Necessary and Sufficient to

- Instruct Th2 Cell Development Resulting in Progressive Disease. *J Immunol* **164**, 4819–4825 (2000).
26. Coffman, R. L. *et al.* B cell stimulatory factor-1 enhances the IgE response of lipopolysaccharide-activated B cells. *J. Immunol.* **136**, 4538 (1986).
 27. Wynn, T. A. IL-13 EFFECTOR FUNCTIONS. *Annu. Rev. Immunol.* **21**, 425–456 (2003).
 28. Doherty, T. M., Kastelein, R., Menon, S., Andrade, S. & Coffman, R. L. Modulation of murine macrophage function by IL-13. *J. Immunol.* **151**, 7151 (1993).
 29. Doyle, A. G. *et al.* Interleukin-13 alters the activation state of murine macrophages in vitro: Comparison with interleukin-4 and interferon- γ . *Eur. J. Immunol.* **24**, 1441–1445 (1994).
 30. Van Dyken, S. J. & Locksley, R. M. Interleukin-4- and Interleukin-13-Mediated Alternatively Activated Macrophages: Roles in Homeostasis and Disease. *Annu. Rev. Immunol.* **31**, 317–343 (2013).
 31. Bhattacharjee, A. *et al.* IL-4 and IL-13 employ discrete signaling pathways for target gene expression in alternatively activated monocytes/macrophages. *Free Radical Biology and Medicine* **54**, 1–16 (2013).
 32. Fichtner-Feigl, S., Strober, W., Kawakami, K., Puri, R. K. & Kitani, A. IL-13 signaling through the IL-13 α 2 receptor is involved in induction of TGF- β 1 production and fibrosis. *Nat Med* **12**, 99–106 (2006).

33. Tu, M. *et al.* IL-13 receptor $\alpha 2$ stimulates human glioma cell growth and metastasis through the Src/PI3K/Akt/mTOR signaling pathway. *Tumor Biol.* **37**, 14701–14709 (2016).
34. McKenzie, G. J., Bancroft, A., Grecis, R. K. & McKenzie, A. N. J. A distinct role for interleukin-13 in Th2-cell-mediated immune responses. *Current Biology* **8**, 339–342 (1998).
35. Gru nig, G. *et al.* Requirement for IL-13 Independently of IL-4 in Experimental Asthma. *Science* **282**, 2261–2263 (1998).
36. Wills-Karp, M. *et al.* Interleukin-13: Central Mediator of Allergic Asthma. *Science* **282**, 2258–2261 (1998).
37. Chiba, Y. *et al.* Interleukin-13 Augments Bronchial Smooth Muscle Contractility with an Up-Regulation of RhoA Protein. *Am J Respir Cell Mol Biol* **40**, 159–167 (2009).
38. Manson, M. L. *et al.* IL-13 and IL-4, but not IL-5 nor IL-17A, induce hyperresponsiveness in isolated human small airways. *Journal of Allergy and Clinical Immunology* **145**, 808-817.e2 (2020).
39. Saatian, B. *et al.* Interleukin-4 and interleukin-13 cause barrier dysfunction in human airway epithelial cells. *Tissue Barriers* **1**, e24333 (2013).
40. Stein, M., Keshav, S., Harris, N. & Gordon, S. Interleukin 4 potently enhances murine macrophage mannose receptor activity: a marker of alternative immunologic macrophage activation. *Journal of Experimental Medicine* **176**, 287–292 (1992).

41. Nomura, M. *et al.* Fatty acid oxidation in macrophage polarization. *Nat Immunol* **17**, 216–217 (2016).
42. Vats, D. *et al.* Oxidative metabolism and PGC-1 β attenuate macrophage-mediated inflammation. *Cell Metabolism* **4**, 13–24 (2006).
43. Gordon, S. Alternative activation of macrophages. *Nat Rev Immunol* **3**, 23–35 (2003).
44. Martinez, F. O., Helming, L. & Gordon, S. Alternative Activation of Macrophages: An Immunologic Functional Perspective. *Annu. Rev. Immunol.* **27**, 451–483 (2009).
45. Wollenberg, A. *et al.* Tralokinumab for moderate-to-severe atopic dermatitis: results from two 52-week, randomized, double-blind, multicentre, placebo-controlled phase III trials (ECZTRA 1 and ECZTRA 2)*. *Br J Dermatol* **184**, 437–449 (2021).
46. Guttman-Yassky, E. *et al.* Efficacy and Safety of Lebrikizumab, a High-Affinity Interleukin 13 Inhibitor, in Adults With Moderate to Severe Atopic Dermatitis: A Phase 2b Randomized Clinical Trial. *JAMA Dermatol* **156**, 411 (2020).
47. Beck, L. A. *et al.* Dupilumab Treatment in Adults with Moderate-to-Severe Atopic Dermatitis. *N Engl J Med* **371**, 130–139 (2014).
48. Wenzel, S. *et al.* Dupilumab in Persistent Asthma with Elevated Eosinophil Levels. *N Engl J Med* **368**, 2455–2466 (2013).

49. *Helminth Infections and their Impact on Global Public Health*. (Springer Vienna, 2014). doi:10.1007/978-3-7091-1782-8.
50. Pullan, R. L., Smith, J. L., Jasrasaria, R. & Brooker, S. J. Global numbers of infection and disease burden of soil transmitted helminth infections in 2010. *Parasit Vectors* **7**, 37 (2014).
51. Allen, J. E. & Sutherland, T. E. Host protective roles of type 2 immunity: Parasite killing and tissue repair, flip sides of the same coin. *Seminars in Immunology* **26**, 329–340 (2014).
52. Lynch, N. R. *et al.* Relationship between helminthic infection and IgE response in atopic and nonatopic children in a tropical environment☆☆☆★★★. *Journal of Allergy and Clinical Immunology* **101**, 217–221 (1998).
53. Kreider, T., Anthony, R. M., Urban, J. F. & Gause, W. C. Alternatively activated macrophages in helminth infections. *Current Opinion in Immunology* **19**, 448–453 (2007).
54. Camberis, M., Le Gros, G. & Urban, J. Animal Model of *Nippostrongylus brasiliensis* and *Heligmosomoides polygyrus*. in *Current Protocols in Immunology* (eds. Coligan, J. E., Bierer, B. E., Margulies, D. H., Shevach, E. M. & Strober, W.) im1912s55 (John Wiley & Sons, Inc., 2003). doi:10.1002/0471142735.im1912s55.

55. Urban, J. F. *et al.* IL-13, IL-4R α , and Stat6 Are Required for the Expulsion of the Gastrointestinal Nematode Parasite *Nippostrongylus brasiliensis*. *Immunity* **8**, 255–264 (1998).
56. Knott, M. L. *et al.* Impaired resistance in early secondary *Nippostrongylus brasiliensis* infections in mice with defective eosinophilopoiesis. *International Journal for Parasitology* **37**, 1367–1378 (2007).
57. Bouchery, T. *et al.* ILC2s and T cells cooperate to ensure maintenance of M2 macrophages for lung immunity against hookworms. *Nat Commun* **6**, 6970 (2015).
58. Oeser, K., Schwartz, C. & Voehringer, D. Conditional IL-4/IL-13-deficient mice reveal a critical role of innate immune cells for protective immunity against gastrointestinal helminths. *Mucosal Immunol* **8**, 672–682 (2015).
59. Krljanac, B. *et al.* RELM α -expressing macrophages protect against fatal lung damage and reduce parasite burden during helminth infection. *Sci. Immunol.* **4**, eaau3814 (2019).
60. Guenova, E. *et al.* IL-4 abrogates T_H 17 cell-mediated inflammation by selective silencing of IL-23 in antigen-presenting cells. *Proc Natl Acad Sci USA* **112**, 2163–2168 (2015).
61. Newcomb, D. C. *et al.* IL-13 Regulates Th17 Secretion of IL-17A in an IL-10–Dependent Manner. *J.I.* **188**, 1027–1035 (2012).
62. Keeler, S. P. *et al.* Influenza A Virus Infection Causes Chronic Lung Disease Linked to Sites of Active Viral RNA Remnants. *J.I.* **201**, 2354–2368 (2018).

63. Moran, T. M., Isobe, H., Fernandez-Sesma, A. & Schulman, J. L. Interleukin-4 causes delayed virus clearance in influenza virus-infected mice. *Journal of virology* **70**, 5230–5235 (1996).
64. Cox, M. A., Kahan, S. M. & Zajac, A. J. Anti-viral CD8 T cells and the cytokines that they love. *Virology* **435**, 157–169 (2013).
65. Hamerman, J. A., Ogasawara, K. & Lanier, L. L. NK cells in innate immunity. *Current Opinion in Immunology* **17**, 29–35 (2005).
66. Beigelman, A. & Bacharier, L. B. Early-life respiratory infections and asthma development: role in disease pathogenesis and potential targets for disease prevention. *Current Opinion in Allergy & Clinical Immunology* **16**, 172–178 (2016).
67. Feldman, A. S., He, Y., Moore, M. L., Hershenson, M. B. & Hartert, T. V. Toward Primary Prevention of Asthma. Reviewing the Evidence for Early-Life Respiratory Viral Infections as Modifiable Risk Factors to Prevent Childhood Asthma. *Am J Respir Crit Care Med* **191**, 34–44 (2015).
68. Sigurs, N., Bjarnason, R., Sigurbergsson, F. & Kjellman, B. Respiratory Syncytial Virus Bronchiolitis in Infancy Is an Important Risk Factor for Asthma and Allergy at Age 7. *Am J Respir Crit Care Med* **161**, 1501–1507 (2000).
69. Turianov, L., Lachov, V., Svetlkova, D., Kostrbov, A. & Betkov, T. Comparison of cytokine profiles induced by nonlethal and lethal doses of influenza A virus in mice. *Exp Ther Med* (2019) doi:10.3892/etm.2019.8096.

70. Sato, M., Hosoya, M. & Wright, P. F. Differences in serum cytokine levels between influenza virus A and B infections in children. *Cytokine* **47**, 65–68 (2009).
71. Mukherjee, S. & Lukacs, N. W. Association of IL-13 in respiratory syncytial virus-induced pulmonary disease: still a promising target. *Expert Review of Anti-infective Therapy* **8**, 617–621 (2010).
72. Rynda-Apple, A. *et al.* Regulation of IFN- γ by IL-13 dictates susceptibility to secondary postinfluenza MRSA pneumonia: Immunity to infection. *Eur. J. Immunol.* **44**, 3263–3272 (2014).
73. Kloefer, K. M. *et al.* Increased H1N1 Infection Rate in Children with Asthma. *Am J Respir Crit Care Med* **185**, 1275–1279 (2012).
74. Gerke, A. K. *et al.* Association of hospitalizations for asthma with seasonal and pandemic influenza: Flu predicts asthma hospitalizations. *Respirology* **19**, 116–121 (2014).
75. Jha, A. *et al.* Patterns of systemic and local inflammation in patients with asthma hospitalised with influenza. *Eur Respir J* **54**, 1900949 (2019).
76. Samarasinghe, A. E. *et al.* The immune profile associated with acute allergic asthma accelerates clearance of influenza virus. *Immunol Cell Biol* **92**, 449–459 (2014).
77. Wobus, C. E. The Dual Tropism of Noroviruses. *J Virol* **92**, (2018).
78. Wilen, C. B. *et al.* Tropism for tuft cells determines immune promotion of norovirus pathogenesis. *Science* **360**, 204–208 (2018).

79. Osborne, L. C. *et al.* Virus-helminth coinfection reveals a microbiota-independent mechanism of immunomodulation. *Science* **345**, 578–582 (2014).
80. Desai, P. *et al.* Enteric helminth coinfection enhances host susceptibility to neurotropic flaviviruses via a tuft cell-IL-4 receptor signaling axis. *Cell* **184**, 1214-1231.e16 (2021).
81. Delves, P. J., Seamus, J. M., Dennis, R. B. & Ivan, M. R. *Roitt's essential immunology*. (John Wiley & Sons, 2017).
82. Annunziato, F., Romagnani, C. & Romagnani, S. The 3 major types of innate and adaptive cell-mediated effector immunity. *Journal of Allergy and Clinical Immunology* **135**, 626–635 (2015).
83. Harrington, L. E. *et al.* Interleukin 17–producing CD4⁺ effector T cells develop via a lineage distinct from the T helper type 1 and 2 lineages. *Nat Immunol* **6**, 1123–1132 (2005).
84. Feng, Y., Zou, L., Si, R., Nagasaka, Y. & Chao, W. Bone marrow MyD88 signaling modulates neutrophil function and ischemic myocardial injury. *American Journal of Physiology-Cell Physiology* **299**, C760–C769 (2010).
85. Miller, L. S. *et al.* MyD88 Mediates Neutrophil Recruitment Initiated by IL-1R but Not TLR2 Activation in Immunity against *Staphylococcus aureus*. *Immunity* **24**, 79–91 (2006).

86. Jarchum, I., Liu, M., Shi, C., Equinda, M. & Pamer, E. G. Critical Role for MyD88-Mediated Neutrophil Recruitment during *Clostridium difficile* Colitis. *Infect. Immun.* **80**, 2989–2996 (2012).
87. Koedel, U. *et al.* MyD88 is required for mounting a robust host immune response to *Streptococcus pneumoniae* in the CNS. *Brain* **127**, 1437–1445 (2004).
88. Saleh, M. M. *et al.* Colitis-Induced Th17 Cells Increase the Risk for Severe Subsequent *Clostridium difficile* Infection. *Cell Host & Microbe* **25**, 756-765.e5 (2019).
89. Arnold, I. C. *et al.* Eosinophils suppress Th1 responses and restrict bacterially induced gastrointestinal inflammation. *Journal of Experimental Medicine* **215**, 2055–2072 (2018).
90. Buonomo, E. L. *et al.* Microbiota-Regulated IL-25 Increases Eosinophil Number to Provide Protection during *Clostridium difficile* Infection. *Cell Reports* **16**, 432–443 (2016).
91. Frisbee, A. L. *et al.* IL-33 drives group 2 innate lymphoid cell-mediated protection during *Clostridium difficile* infection. *Nat Commun* **10**, 2712 (2019).
92. Zhu, C. *et al.* Interleukin-13 inhibits cytokines synthesis by blocking nuclear factor- κ B and c-Jun N-terminal kinase in human mesangial cells. *Journal of Biomedical Research* **24**, 308–316 (2010).

93. Newcomb, D. C. *et al.* A Functional IL-13 Receptor Is Expressed on Polarized Murine CD4⁺ Th17 Cells and IL-13 Signaling Attenuates Th17 Cytokine Production. *J Immunol* **182**, 5317–5321 (2009).
94. Ortega-Gómez, A., Perretti, M. & Soehnlein, O. Resolution of inflammation: an integrated view. *EMBO Mol Med* **5**, 661–674 (2013).
95. Cox, J. H. *et al.* Opposing consequences of IL-23 signaling mediated by innate and adaptive cells in chemically induced colitis in mice. *Mucosal Immunol* **5**, 99–109 (2012).
96. Ito, R. *et al.* Involvement of IL-17A in the pathogenesis of DSS-induced colitis in mice. *Biochemical and Biophysical Research Communications* **377**, 12–16 (2008).
97. Lin, Y. *et al.* Chemerin aggravates DSS-induced colitis by suppressing M2 macrophage polarization. *Cell Mol Immunol* **11**, 355–366 (2014).
98. Liu, Q. *et al.* IL-33-Driven Innate Tissue-Protective Function of ST2⁺ T_{reg} Cells. *J. Immunol.* **196**, 51.7 (2016).
99. Monticelli, L. A. *et al.* IL-33 promotes an innate immune pathway of intestinal tissue protection dependent on amphiregulin–EGFR interactions. *Proc Natl Acad Sci USA* **112**, 10762–10767 (2015).
100. Seo, D. H. *et al.* Interleukin-33 regulates intestinal inflammation by modulating macrophages in inflammatory bowel disease. *Sci Rep* **7**, 851 (2017).

101. Ledesma-Soto, Y. *et al.* Extraintestinal Helminth Infection Limits Pathology and Proinflammatory Cytokine Expression during DSS-Induced Ulcerative Colitis: A Role for Alternatively Activated Macrophages and Prostaglandins. *BioMed Research International* **2015**, 1–17 (2015).
102. Weisser, S. B. *et al.* Arginase activity in alternatively activated macrophages protects PI3Kp110 δ deficient mice from dextran sodium sulfate induced intestinal inflammation: Innate Immunity. *Eur. J. Immunol.* **44**, 3353–3367 (2014).
103. Long, S. R., Liu, R. D., Kumar, D. V., Wang, Z. Q. & Su, C.-W. Immune Protection of a Helminth Protein in the DSS-Induced Colitis Model in Mice. *Front. Immunol.* **12**, 664998 (2021).
104. Verstockt, B. *et al.* Mucosal IL13RA2 expression predicts nonresponse to anti-TNF therapy in Crohn's disease. *Aliment Pharmacol Ther* **49**, 572–581 (2019).
105. Karmelet, E. P. *et al.* Anti-IL-13Ra2 therapy promotes recovery in a murine model of inflammatory bowel disease. *Mucosal Immunol* **12**, 1174–1186 (2019).
106. Fuss, I. J. *et al.* Disparate CD4+ lamina propria (LP) lymphokine secretion profiles in inflammatory bowel disease. Crohn's disease LP cells manifest increased secretion of IFN-gamma, whereas ulcerative colitis LP cells manifest increased secretion of IL-5. *J. Immunol.* **157**, 1261 (1996).

107. Fuss, I. J. *et al.* Nonclassical CD1d-restricted NK T cells that produce IL-13 characterize an atypical Th2 response in ulcerative colitis. *J. Clin. Invest.* **113**, 1490–1497 (2004).
108. Heller, F., Fuss, I. J., Nieuwenhuis, E. E., Blumberg, R. S. & Strober, W. Oxazolone Colitis, a Th2 Colitis Model Resembling Ulcerative Colitis, Is Mediated by IL-13-Producing NK-T Cells. *Immunity* **17**, 629–638 (2002).
109. Bettelli, E. *et al.* Reciprocal developmental pathways for the generation of pathogenic effector TH17 and regulatory T cells. *Nature* **441**, 235–238 (2006).
110. Bradding, P. *et al.* Immunolocalization of cytokines in the nasal mucosa of normal and perennial rhinitic subjects. The mast cell as a source of IL-4, IL-5, and IL-6 in human allergic mucosal inflammation. *J. Immunol.* **151**, 3853 (1993).
111. Fernando, M. R., Reyes, J. L., Iannuzzi, J., Leung, G. & McKay, D. M. The Pro-Inflammatory Cytokine, Interleukin-6, Enhances the Polarization of Alternatively Activated Macrophages. *PLoS ONE* **9**, e94188 (2014).
112. Mauer, J. *et al.* Signaling by IL-6 promotes alternative activation of macrophages to limit endotoxemia and obesity-associated resistance to insulin. *Nat Immunol* **15**, 423–430 (2014).
113. Allen, J. E., Sutherland, T. E. & Rückerl, D. IL-17 and neutrophils: unexpected players in the type 2 immune response. *Current Opinion in Immunology* **34**, 99–106 (2015).

114. de la Motte, C. A. & Kessler, S. P. The Role of Hyaluronan in Innate Defense Responses of the Intestine. *International Journal of Cell Biology* **2015**, 1–5 (2015).
115. Tammi, M. I., Day, A. J. & Turley, E. A. Hyaluronan and Homeostasis: A Balancing Act. *Journal of Biological Chemistry* **277**, 4581–4584 (2002).
116. Dong, Y. *et al.* The survival of fetal and bone marrow monocyte-derived alveolar macrophages is promoted by CD44 and its interaction with hyaluronan. *Mucosal Immunol* **11**, 601–614 (2018).
117. Jiang, D., Liang, J. & Noble, P. W. Hyaluronan as an Immune Regulator in Human Diseases. *Physiological Reviews* **91**, 221–264 (2011).
118. Lennon, F. E. & Singleton, P. A. Role of hyaluronan and hyaluronan-binding proteins in lung pathobiology. *American Journal of Physiology-Lung Cellular and Molecular Physiology* **301**, L137–L147 (2011).
119. Ponta, H., Sherman, L. & Herrlich, P. A. CD44: From adhesion molecules to signalling regulators. *Nat Rev Mol Cell Biol* **4**, 33–45 (2003).
120. Yamamoto, H. *et al.* A mammalian homolog of the zebrafish transmembrane protein 2 (TMEM2) is the long-sought-after cell-surface hyaluronidase. *Journal of Biological Chemistry* **292**, 7304–7313 (2017).
121. Petrey, A. C. & de la Motte, C. A. Hyaluronan, a Crucial Regulator of Inflammation. *Front. Immunol.* **5**, (2014).

122. Muto, J., Yamasaki, K., Taylor, K. R. & Gallo, R. L. Engagement of CD44 by hyaluronan suppresses TLR4 signaling and the septic response to LPS. *Molecular Immunology* **47**, 449–456 (2009).
123. Jiang, D., Liang, J. & Noble, P. W. Hyaluronan in Tissue Injury and Repair. *Annu. Rev. Cell Dev. Biol.* **23**, 435–461 (2007).
124. Dong, Y. *et al.* Endotoxin free hyaluronan and hyaluronan fragments do not stimulate TNF- α , interleukin-12 or upregulate co-stimulatory molecules in dendritic cells or macrophages. *Sci Rep* **6**, 36928 (2016).
125. Huang, Z. *et al.* Recombinant Human Hyaluronidase PH20 Does Not Stimulate an Acute Inflammatory Response and Inhibits Lipopolysaccharide-Induced Neutrophil Recruitment in the Air Pouch Model of Inflammation. *J.I.* **192**, 5285–5295 (2014).
126. Bell, T. J. *et al.* Defective lung function following influenza virus is due to prolonged, reversible hyaluronan synthesis. *Matrix Biology* **80**, 14–28 (2019).
127. Knudson, W., Chow, G. & Knudson, C. B. CD44-mediated uptake and degradation of hyaluronan. *Matrix Biology* **21**, 15–23 (2002).
128. Chen, C., Zhao, S., Karnad, A. & Freeman, J. W. The biology and role of CD44 in cancer progression: therapeutic implications. *J Hematol Oncol* **11**, 64 (2018).

129. Schommer, N. N., Muto, J., Nizet, V. & Gallo, R. L. Hyaluronan Breakdown Contributes to Immune Defense against Group A Streptococcus. *Journal of Biological Chemistry* **289**, 26914–26921 (2014).
130. Abe, T. *et al.* CD44 Participates in IP-10 Induction in Cells in Which Hepatitis C Virus RNA Is Replicating, through an Interaction with Toll-Like Receptor 2 and Hyaluronan. *Journal of Virology* **86**, 6159–6170 (2012).
131. Ghatak, S. *et al.* Overexpression of c-Met and CD44v6 Receptors Contributes to Autocrine TGF- β 1 Signaling in Interstitial Lung Disease. *Journal of Biological Chemistry* **289**, 7856–7872 (2014).
132. Li, Y. *et al.* Severe lung fibrosis requires an invasive fibroblast phenotype regulated by hyaluronan and CD44. *Journal of Experimental Medicine* **208**, 1459–1471 (2011).
133. A. Singleton, P. Acute Lung Injury Regulation by Hyaluronan. *J Aller Ther* **01**, (2012).
134. Hällgren, R., Samuelsson, T., Laurent, T. C. & Modig, J. Accumulation of Hyaluronan (Hyaluronic Acid) in the Lung in Adult Respiratory Distress Syndrome. *Am Rev Respir Dis* **139**, 682–687 (1989).
135. Galdi, F. *et al.* Inhaled high molecular weight hyaluronan ameliorates respiratory failure in acute COPD exacerbation: a pilot study. *Respir Res* **22**, 30 (2021).
136. Summah, H. & Qu, J.-M. Biomarkers: A Definite Plus in Pneumonia. *Mediators of Inflammation* **2009**, 1–9 (2009).

137. de la Motte, C. A. Hyaluronan in intestinal homeostasis and inflammation: implications for fibrosis. *American Journal of Physiology-Gastrointestinal and Liver Physiology* **301**, G945–G949 (2011).
138. Kessler, S. P., Obery, D. R. & de la Motte, C. Hyaluronan Synthase 3 Null Mice Exhibit Decreased Intestinal Inflammation and Tissue Damage in the DSS-Induced Colitis Model. *International Journal of Cell Biology* **2015**, 1–13 (2015).
139. Grandoch, M., Bollyky, P. L. & Fischer, J. W. Hyaluronan: A Master Switch Between Vascular Homeostasis and Inflammation. *Circ Res* **122**, 1341–1343 (2018).
140. Nagy, N. *et al.* Hyaluronan in immune dysregulation and autoimmune diseases. *Matrix Biology* **78–79**, 292–313 (2019).
141. Liang, J. *et al.* Role of hyaluronan and hyaluronan-binding proteins in human asthma. *Journal of Allergy and Clinical Immunology* **128**, 403-411.e3 (2011).
142. Vignola, A. M. *et al.* Airway Inflammation in Mild Intermittent and in Persistent Asthma. *Am J Respir Crit Care Med* **157**, 403–409 (1998).
143. Lauer, M. E. *et al.* Hyaluronan and Its Heavy Chain Modification in Asthma Severity and Experimental Asthma Exacerbation. *Journal of Biological Chemistry* **290**, 23124–23134 (2015).
144. Ayars, A. G. *et al.* Sputum Hyaluronan and Versican in Severe Eosinophilic Asthma. *Int Arch Allergy Immunol* **161**, 65–73 (2013).

145. Ohtani, T. *et al.* Increased Hyaluronan Production and Decreased E-Cadherin Expression by Cytokine-Stimulated Keratinocytes Lead to Spongiosis Formation. *Journal of Investigative Dermatology* **129**, 1412–1420 (2009).
146. Abou Chakra, C. N., Pepin, J., Sirard, S. & Valiquette, L. Risk Factors for Recurrence, Complications and Mortality in Clostridium difficile Infection: A Systematic Review. *PLoS ONE* **9**, e98400 (2014).
147. El Feghaly, R. E. *et al.* Markers of Intestinal Inflammation, Not Bacterial Burden, Correlate With Clinical Outcomes in Clostridium difficile Infection. *Clinical Infectious Diseases* **56**, 1713–1721 (2013).
148. Pothoulakis, C. Effects of Clostridium difficile Toxins on Epithelial Cell Barrier. *Annals of the New York Academy of Sciences* **915**, 347–356 (2006).
149. Cowardin, C. A. *et al.* Inflammasome Activation Contributes to Interleukin-23 Production in Response to Clostridium difficile. *mBio* **6**, (2015).
150. Barbut, F. *et al.* Prospective study of Clostridium difficile infections in Europe with phenotypic and genotypic characterisation of the isolates. *Clinical Microbiology and Infection* **13**, 1048–1057 (2007).
151. Bauer, M. P. *et al.* Clostridium difficile infection in Europe: a hospital-based survey. *The Lancet* **377**, 63–73 (2011).
152. Kuehne, S. A. *et al.* Importance of Toxin A, Toxin B, and CDT in Virulence of an Epidemic Clostridium difficile Strain. *The Journal of Infectious Diseases* **209**, 83–86 (2014).

153. Buckley, A. M., Spencer, J., Candlish, D., Irvine, J. J. & Douce, G. R. Infection of hamsters with the UK *Clostridium difficile* ribotype 027 outbreak strain R20291. *Journal of Medical Microbiology* **60**, 1174–1180 (2011).
154. Carter, G. P. *et al.* Defining the Roles of TcdA and TcdB in Localized Gastrointestinal Disease, Systemic Organ Damage, and the Host Response during *Clostridium difficile* Infections. *mBio* **6**, e00551-15 (2015).
155. Cohen, N. A. *et al.* *Clostridium difficile* fecal toxin level is associated with disease severity and prognosis. *United European Gastroenterol. j.* **6**, 773–780 (2018).
156. Gerding, D. N., Johnson, S., Rupnik, M. & Aktories, K. *Clostridium difficile* binary toxin CDT: Mechanism, epidemiology, and potential clinical importance. *Gut Microbes* **5**, 15–27 (2014).
157. Cowardin, C. A. *et al.* The binary toxin CDT enhances *Clostridium difficile* virulence by suppressing protective colonic eosinophilia. *Nat Microbiol* **1**, 16108 (2016).
158. Buonomo, E. L. & Petri, W. A. The microbiota and immune response during *Clostridium difficile* infection. *Anaerobe* **41**, 79–84 (2016).
159. Sorg, J. A. & Sonenshein, A. L. Inhibiting the Initiation of *Clostridium difficile* Spore Germination using Analogs of Chenodeoxycholic Acid, a Bile Acid. *J Bacteriol* **192**, 4983–4990 (2010).

160. Francis, M. B., Allen, C. A., Shrestha, R. & Sorg, J. A. Bile Acid Recognition by the *Clostridium difficile* Germinant Receptor, CspC, Is Important for Establishing Infection. *PLoS Pathog* **9**, e1003356 (2013).
161. Theriot, C. M., Bowman, A. A. & Young, V. B. Antibiotic-Induced Alterations of the Gut Microbiota Alter Secondary Bile Acid Production and Allow for *Clostridium difficile* Spore Germination and Outgrowth in the Large Intestine. *mSphere* **1**, (2016).
162. Péchiné, S. & Collignon, A. Immune responses induced by *Clostridium difficile*. *Anaerobe* **41**, 68–78 (2016).
163. Chaves-Olarte, E., Weidmann, M., Eichel-Streiber, C. & Thelestam, M. Toxins A and B from *Clostridium difficile* differ with respect to enzymatic potencies, cellular substrate specificities, and surface binding to cultured cells. *J. Clin. Invest.* **100**, 1734–1741 (1997).
164. Bobo, L. D. *et al.* MAPK-Activated Protein Kinase 2 Contributes to *Clostridium difficile*-Associated Inflammation. *Infect. Immun.* **81**, 713–722 (2013).
165. Xu, H. *et al.* Innate immune sensing of bacterial modifications of Rho GTPases by the Pyrin inflammasome. *Nature* **513**, 237–241 (2014).
166. Jafari, N. V. *et al.* *Clostridium difficile* Modulates Host Innate Immunity via Toxin-Independent and Dependent Mechanism(s). *PLoS ONE* **8**, e69846 (2013).

167. Ng, J. *et al.* Clostridium difficile Toxin–Induced Inflammation and Intestinal Injury Are Mediated by the Inflammasome. *Gastroenterology* **139**, 542–552.e3 (2010).
168. Schön, M. P. & Erpenbeck, L. The Interleukin-23/Interleukin-17 Axis Links Adaptive and Innate Immunity in Psoriasis. *Front. Immunol.* **9**, 1323 (2018).
169. Yang, X. O. *et al.* STAT3 Regulates Cytokine-mediated Generation of Inflammatory Helper T Cells. *Journal of Biological Chemistry* **282**, 9358–9363 (2007).
170. Abhyankar, M. M. *et al.* Immune Profiling To Predict Outcome of *Clostridioides difficile* Infection. *mBio* **11**, e00905-20, /mbio/11/3/mBio.00905-20.atom (2020).
171. Jose, S. & Madan, R. Neutrophil-mediated inflammation in the pathogenesis of Clostridium difficile infections. *Anaerobe* **41**, 85–90 (2016).
172. Solomon, K. *et al.* Mortality in patients with Clostridium difficile infection correlates with host pro-inflammatory and humoral immune responses. *Journal of Medical Microbiology* **62**, 1453–1460 (2013).
173. Luo, R., Greenberg, A. & Stone, C. D. Outcomes of *Clostridium difficile* Infection in Hospitalized Leukemia Patients: A Nationwide Analysis. *Infect. Control Hosp. Epidemiol.* **36**, 794–801 (2015).
174. Powell, N. *et al.* The Transcription Factor T-bet Regulates Intestinal Inflammation Mediated by Interleukin-7 Receptor+ Innate Lymphoid Cells. *Immunity* **37**, 674–684 (2012).

175. Abt, M. C. *et al.* Innate Immune Defenses Mediated by Two ILC Subsets Are Critical for Protection against Acute *Clostridium difficile* Infection. *Cell Host & Microbe* **18**, 27–37 (2015).
176. Huang, C. *et al.* Clinical features of patients infected with 2019 novel coronavirus in Wuhan, China. *The Lancet* **395**, 497–506 (2020).
177. Paules, C. I., Marston, H. D. & Fauci, A. S. Coronavirus Infections—More Than Just the Common Cold. *JAMA* **323**, 707 (2020).
178. Petrosillo, N., Viceconte, G., Ergonul, O., Ippolito, G. & Petersen, E. COVID-19, SARS and MERS: are they closely related? *Clinical Microbiology and Infection* **26**, 729–734 (2020).
179. Wan, Y., Shang, J., Graham, R., Baric, R. S. & Li, F. Receptor Recognition by the Novel Coronavirus from Wuhan: an Analysis Based on Decade-Long Structural Studies of SARS Coronavirus. *J Virol* **94**, (2020).
180. Raj, V. S. *et al.* Dipeptidyl peptidase 4 is a functional receptor for the emerging human coronavirus-EMC. *Nature* **495**, 251–254 (2013).
181. Hoffmann, M. *et al.* SARS-CoV-2 Cell Entry Depends on ACE2 and TMPRSS2 and Is Blocked by a Clinically Proven Protease Inhibitor. *Cell* **181**, 271-280.e8 (2020).
182. V'kovski, P., Kratzel, A., Steiner, S., Stalder, H. & Thiel, V. Coronavirus biology and replication: implications for SARS-CoV-2. *Nat Rev Microbiol* **19**, 155–170 (2021).

183. Petersen, E. *et al.* Comparing SARS-CoV-2 with SARS-CoV and influenza pandemics. *The Lancet Infectious Diseases* **20**, e238–e244 (2020).
184. Ioannidis, J. P. A. Infection fatality rate of COVID-19 inferred from seroprevalence data. *Bull. World Health Organ.* **99**, 19-33F (2021).
185. WHO. Consensus document on the epidemiology of severe acute respiratory syndrome (SARS). (2003).
186. Cevik, M., Kuppalli, K., Kindrachuk, J. & Peiris, M. Virology, transmission, and pathogenesis of SARS-CoV-2. *BMJ* m3862 (2020)
doi:10.1136/bmj.m3862.
187. Cevik, M. *et al.* SARS-CoV-2, SARS-CoV, and MERS-CoV viral load dynamics, duration of viral shedding, and infectiousness: a systematic review and meta-analysis. *The Lancet Microbe* **2**, e13–e22 (2021).
188. Wölfel, R. *et al.* Virological assessment of hospitalized patients with COVID-2019. *Nature* **581**, 465–469 (2020).
189. Zou, L. *et al.* SARS-CoV-2 Viral Load in Upper Respiratory Specimens of Infected Patients. *N Engl J Med* **382**, 1177–1179 (2020).
190. Williamson, E. J. *et al.* Factors associated with COVID-19-related death using OpenSAFELY. *Nature* **584**, 430–436 (2020).
191. Peckham, H. *et al.* Male sex identified by global COVID-19 meta-analysis as a risk factor for death and ICU admission. *Nat Commun* **11**, 6317 (2020).
192. Takahashi, T. *et al.* Sex differences in immune responses that underlie COVID-19 disease outcomes. *Nature* **588**, 315–320 (2020).

193. Beigel, J. H. *et al.* Remdesivir for the Treatment of Covid-19 — Final Report. *N Engl J Med* **383**, 1813–1826 (2020).
194. Rochwerg, B. *et al.* Remdesivir for severe covid-19: a clinical practice guideline. *BMJ* m2924 (2020) doi:10.1136/bmj.m2924.
195. Yin, X. *et al.* MDA5 Governs the Innate Immune Response to SARS-CoV-2 in Lung Epithelial Cells. *Cell Reports* **34**, 108628 (2021).
196. Ferreira, A. C. *et al.* SARS-CoV-2 engages inflammasome and pyroptosis in human primary monocytes. *Cell Death Discov.* **7**, 43 (2021).
197. Tay, M. Z., Poh, C. M., Rénia, L., MacAry, P. A. & Ng, L. F. P. The trinity of COVID-19: immunity, inflammation and intervention. *Nat Rev Immunol* **20**, 363–374 (2020).
198. Lucas, C. *et al.* *Longitudinal immunological analyses reveal inflammatory misfiring in severe COVID-19 patients.*
<http://medrxiv.org/lookup/doi/10.1101/2020.06.23.20138289> (2020)
doi:10.1101/2020.06.23.20138289.
199. Mangalmurti, N. & Hunter, C. A. Cytokine Storms: Understanding COVID-19. *Immunity* **53**, 19–25 (2020).
200. Yang, Y. *et al.* Plasma IP-10 and MCP-3 levels are highly associated with disease severity and predict the progression of COVID-19. *Journal of Allergy and Clinical Immunology* **146**, 119-127.e4 (2020).
201. FDA. Pfizer-BioNTech COVID-19 Vaccine.
202. FDA. Moderna COVID-19 Vaccine.

203. Dagan, N. *et al.* BNT162b2 mRNA Covid-19 Vaccine in a Nationwide Mass Vaccination Setting. *N Engl J Med* **384**, 1412–1423 (2021).
204. Baden, L. R. *et al.* Efficacy and Safety of the mRNA-1273 SARS-CoV-2 Vaccine. *N Engl J Med* **384**, 403–416 (2021).
205. Tahaghoghi-Hajghorbani, S. *et al.* The role of dysregulated immune responses in COVID-19 pathogenesis. *Virus Research* **290**, 198197 (2020).
206. The RECOVERY Collaborative Group. Dexamethasone in Hospitalized Patients with Covid-19 — Preliminary Report. *N Engl J Med* NEJMoa2021436 (2020) doi:10.1056/NEJMoa2021436.
207. Gomez-Cadena, A. *et al.* Severe COVID-19 patients exhibit an ILC2 NKG2D+ population in their impaired ILC compartment. *Cell Mol Immunol* **18**, 484–486 (2021).
208. Stanczak, M. A. *et al.* IL-33 expression in response to SARS-CoV-2 correlates with seropositivity in COVID-19 convalescent individuals. *Nat Commun* **12**, 2133 (2021).
209. He, J. *et al.* Single-cell analysis reveals bronchoalveolar epithelial dysfunction in COVID-19 patients. *Protein Cell* **11**, 680–687 (2020).
210. Vaz de Paula, C. B. *et al.* IL-4/IL-13 remodeling pathway of COVID-19 lung injury. *Sci Rep* **10**, 18689 (2020).
211. Ding, M., Zhang, Q., Li, Q., Wu, T. & Huang, Y. Correlation analysis of the severity and clinical prognosis of 32 cases of patients with COVID-19. *Respiratory Medicine* **167**, 105981 (2020).

212. Hellman, U. *et al.* Presence of hyaluronan in lung alveoli in severe Covid-19: An opening for new treatment options? *J. Biol. Chem.* **295**, 15418–15422 (2020).
213. Kaber, G. *et al.* *Hyaluronan is abundant in COVID-19 respiratory secretions.* <http://medrxiv.org/lookup/doi/10.1101/2020.09.11.20191692> (2020)
doi:10.1101/2020.09.11.20191692.
214. Modig, J. & Hällgren, R. Increased hyaluronic acid production in lung — a possible important factor in interstitial and alveolar edema during general anesthesia and in adult respiratory distress syndrome. *Resuscitation* **17**, 223–231 (1989).
215. McCray, P. B. *et al.* Lethal Infection of K18-hACE2 Mice Infected with Severe Acute Respiratory Syndrome Coronavirus. *JVI* **81**, 813–821 (2007).
216. Winkler, E. S. *et al.* Publisher Correction: SARS-CoV-2 infection of human ACE2-transgenic mice causes severe lung inflammation and impaired function. *Nat Immunol* **21**, 1470–1470 (2020).
217. Hassan, A. O. *et al.* A SARS-CoV-2 Infection Model in Mice Demonstrates Protection by Neutralizing Antibodies. *Cell* **182**, 744-753.e4 (2020).
218. Israelow, B. *et al.* Mouse model of SARS-CoV-2 reveals inflammatory role of type I interferon signaling. *Journal of Experimental Medicine* **217**, e20201241 (2020).
219. Bao, L. *et al.* The pathogenicity of SARS-CoV-2 in hACE2 transgenic mice. *Nature* **583**, 830–833 (2020).

220. Sun, S.-H. *et al.* A Mouse Model of SARS-CoV-2 Infection and Pathogenesis. *Cell Host & Microbe* **28**, 124-133.e4 (2020).
221. Jiang, R.-D. *et al.* Pathogenesis of SARS-CoV-2 in Transgenic Mice Expressing Human Angiotensin-Converting Enzyme 2. *Cell* **182**, 50-58.e8 (2020).
222. Leist, S. R. *et al.* A Mouse-Adapted SARS-CoV-2 Induces Acute Lung Injury and Mortality in Standard Laboratory Mice. *Cell* **183**, 1070-1085.e12 (2020).
223. Abt, M. C., McKenney, P. T. & Pamer, E. G. Clostridium difficile colitis: pathogenesis and host defence. *Nat Rev Microbiol* **14**, 609–620 (2016).
224. Díaz, A. & Allen, J. E. Mapping immune response profiles: The emerging scenario from helminth immunology. *Eur. J. Immunol.* **37**, 3319–3326 (2007).
225. Kulaylat, A. S. *et al.* Development and Validation of a Prediction Model for Mortality and Adverse Outcomes Among Patients With Peripheral Eosinopenia on Admission for *Clostridium difficile* Infection. *JAMA Surg* **153**, 1127 (2018).
226. von Moltke, J., Ji, M., Liang, H.-E. & Locksley, R. M. Tuft-cell-derived IL-25 regulates an intestinal ILC2–epithelial response circuit. *Nature* **529**, 221–225 (2016).
227. Gadani, S. P., Cronk, J. C., Norris, G. T. & Kipnis, J. IL-4 in the Brain: A Cytokine To Remember. *J.I.* **189**, 4213–4219 (2012).

228. Yamaguchi, Y. *et al.* Highly purified murine interleukin 5 (IL-5) stimulates eosinophil function and prolongs in vitro survival. IL-5 as an eosinophil chemotactic factor. *Journal of Experimental Medicine* **167**, 1737–1742 (1988).
229. Gea-Sorlí, S. & Closa, D. In vitro, but not in vivo, reversibility of peritoneal macrophages activation during experimental acute pancreatitis. *BMC Immunol* **10**, 42 (2009).
230. Gieseck, R. L., Wilson, M. S. & Wynn, T. A. Type 2 immunity in tissue repair and fibrosis. *Nat Rev Immunol* **18**, 62–76 (2018).
231. Tamoutounour, S. *et al.* CD64 distinguishes macrophages from dendritic cells in the gut and reveals the Th1-inducing role of mesenteric lymph node macrophages during colitis: HIGHLIGHTS. *Eur. J. Immunol.* **42**, 3150–3166 (2012).
232. Gundra, U. M. *et al.* Alternatively activated macrophages derived from monocytes and tissue macrophages are phenotypically and functionally distinct. *Blood* **123**, e110–e122 (2014).
233. Mack, M. *et al.* Expression and Characterization of the Chemokine Receptors CCR2 and CCR5 in Mice. *J Immunol* **166**, 4697–4704 (2001).
234. Badalyan, V. *et al.* TNF- α /IL-17 synergy inhibits IL-13 bioactivity via IL-13R α 2 induction. *Journal of Allergy and Clinical Immunology* **134**, 975-978.e5 (2014).

235. Bain, C. C. *et al.* Resident and pro-inflammatory macrophages in the colon represent alternative context-dependent fates of the same Ly6Chi monocyte precursors. *Mucosal Immunol* **6**, 498–510 (2013).
236. Cantuti-Castelvetri, L. *et al.* Neuropilin-1 facilitates SARS-CoV-2 cell entry and infectivity. *Science* **370**, 856–860 (2020).
237. Pedersen, S. F. & Ho, Y.-C. SARS-CoV-2: a storm is raging. *Journal of Clinical Investigation* **130**, 2202–2205 (2020).
238. Tisoncik, J. R. *et al.* Into the Eye of the Cytokine Storm. *Microbiology and Molecular Biology Reviews* **76**, 16–32 (2012).
239. Kalil, A. C. *et al.* Baricitinib plus Remdesivir for Hospitalized Adults with Covid-19. *N Engl J Med* NEJMoa2031994 (2020)
doi:10.1056/NEJMoa2031994.
240. Del Valle, D. M. *et al.* An inflammatory cytokine signature predicts COVID-19 severity and survival. *Nat Med* **26**, 1636–1643 (2020).
241. Liao, M. *et al.* Single-cell landscape of bronchoalveolar immune cells in patients with COVID-19. *Nat Med* **26**, 842–844 (2020).
242. Nienhold, R. *et al.* Two distinct immunopathological profiles in autopsy lungs of COVID-19. *Nat Commun* **11**, 5086 (2020).
243. Su, H. *et al.* Renal histopathological analysis of 26 postmortem findings of patients with COVID-19 in China. *Kidney International* **98**, 219–227 (2020).

244. Weiskopf, D. *et al.* Phenotype and kinetics of SARS-CoV-2-specific T cells in COVID-19 patients with acute respiratory distress syndrome. *Sci. Immunol.* **5**, eabd2071 (2020).
245. Chiaramonte, M. Studies of murine schistosomiasis reveal interleukin-13 blockade as a treatment for established and progressive liver fibrosis. *Hepatology* **34**, 273–282 (2001).
246. Marone, G. *et al.* The Intriguing Role of Interleukin 13 in the Pathophysiology of Asthma. *Front. Pharmacol.* **10**, 1387 (2019).
247. Petrey, A. C. *et al.* Cytokine release syndrome in COVID-19: Innate immune, vascular, and platelet pathogenic factors differ in severity of disease and sex. *J Leukoc Biol* (2020) doi:10.1002/JLB.3COVA0820-410RRR.
248. Moreau, G. B. *et al.* Evaluation of K18-hACE2 Mice as a Model of SARS-CoV-2 Infection. *The American Journal of Tropical Medicine and Hygiene* **103**, 1215–1219 (2020).
249. Rathnasinghe, R. *et al.* Comparison of transgenic and adenovirus hACE2 mouse models for SARS-CoV-2 infection. *Emerging Microbes & Infections* **9**, 2433–2445 (2020).
250. Le Floch, A. *et al.* Dual blockade of IL-4 and IL-13 with dupilumab, an IL-4R α antibody, is required to broadly inhibit type 2 inflammation. *Allergy* **75**, 1188–1204 (2020).

251. Liu, F. *et al.* Prognostic value of interleukin-6, C-reactive protein, and procalcitonin in patients with COVID-19. *Journal of Clinical Virology* **127**, 104370 (2020).
252. Borthwick, L. A. *et al.* Macrophages are critical to the maintenance of IL-13-dependent lung inflammation and fibrosis. *Mucosal Immunol* **9**, 38–55 (2016).
253. Lee, C. G. *et al.* Role of Chitin and Chitinase/Chitinase-Like Proteins in Inflammation, Tissue Remodeling, and Injury. *Annu. Rev. Physiol.* **73**, 479–501 (2011).
254. Ruppert, S. M., Hawn, T. R., Arrigoni, A., Wight, T. N. & Bollyky, P. L. Tissue integrity signals communicated by high-molecular weight hyaluronan and the resolution of inflammation. *Immunol Res* **58**, 186–192 (2014).
255. Rayahin, J. E., Buhrman, J. S., Zhang, Y., Koh, T. J. & Gemeinhart, R. A. High and Low Molecular Weight Hyaluronic Acid Differentially Influence Macrophage Activation. *ACS Biomater. Sci. Eng.* **1**, 481–493 (2015).
256. Lauer, M. E., Dweik, R. A., Garantziotis, S. & Aronica, M. A. The Rise and Fall of Hyaluronan in Respiratory Diseases. *International Journal of Cell Biology* **2015**, 1–15 (2015).
257. Honda, T., Kaneiwa, T., Mizumoto, S., Sugahara, K. & Yamada, S. Hyaluronidases Have Strong Hydrolytic Activity toward Chondroitin 4-Sulfate Comparable to that for Hyaluronan. *Biomolecules* **2**, 549–563 (2012).

258. Misra, S., Hascall, V. C., Markwald, R. R. & Ghatak, S. Interactions between Hyaluronan and Its Receptors (CD44, RHAMM) Regulate the Activities of Inflammation and Cancer. *Front. Immunol.* **6**, (2015).
259. Heldin, P., Kolliopoulos, C., Lin, C.-Y. & Heldin, C.-H. Involvement of hyaluronan and CD44 in cancer and viral infections. *Cellular Signalling* **65**, 109427 (2020).
260. Jia, G. *et al.* Periostin is a systemic biomarker of eosinophilic airway inflammation in asthmatic patients. *Journal of Allergy and Clinical Immunology* **130**, 647-654.e10 (2012).
261. Stritesky, G. L. *et al.* The Transcription Factor STAT3 Is Required for T Helper 2 Cell Development. *Immunity* **34**, 39–49 (2011).
262. Simeone-Penney, M. C. *et al.* Airway Epithelial STAT3 Is Required for Allergic Inflammation in a Murine Model of Asthma. *J Immunol* **178**, 6191–6199 (2007).
263. Cao, H. *et al.* IL-13/STAT6 signaling plays a critical role in the epithelial-mesenchymal transition of colorectal cancer cells. *Oncotarget* **7**, 61183–61198 (2016).
264. Trejdosiewicz, L. K. *et al.* INTERLEUKINS 4 AND 13 UPREGULATE EXPRESSION OF CD44 IN HUMAN COLONIC EPITHELIAL CELL LINES. *Cytokine* **10**, 756–765 (1998).
265. Rothenberg, M. E. CD44 — a sticky target for asthma. *J. Clin. Invest.* **111**, 1460–1462 (2003).

266. Schulte-Schrepping, J. *et al.* Severe COVID-19 Is Marked by a Dysregulated Myeloid Cell Compartment. *Cell* **182**, 1419-1440.e23 (2020).
267. Bosurgi, L. *et al.* Macrophage function in tissue repair and remodeling requires IL-4 or IL-13 with apoptotic cells. *Science* **356**, 1072–1076 (2017).
268. D'Alessio, F. R. *et al.* Enhanced resolution of experimental ARDS through IL-4-mediated lung macrophage reprogramming. *American Journal of Physiology-Lung Cellular and Molecular Physiology* **310**, L733–L746 (2016).
269. Mosser, D. M. The many faces of macrophage activation. *Journal of Leukocyte Biology* **73**, 209–212 (2003).
270. Hunter, M. M. *et al.* In Vitro-Derived Alternatively Activated Macrophages Reduce Colonic Inflammation in Mice. *Gastroenterology* **138**, 1395–1405 (2010).
271. Leung, G., Wang, A., Fernando, M., Phan, V. C. & McKay, D. M. Bone marrow-derived alternatively activated macrophages reduce colitis without promoting fibrosis: participation of IL-10. *American Journal of Physiology-Gastrointestinal and Liver Physiology* **304**, G781–G792 (2013).
272. Kucharzik, LÜgering, Pauels, Domschke, & Stoll. IL-4, IL-10 and IL-13 down-regulate monocyte-chemoattracting protein-1 (MCP-1) production in activated intestinal epithelial cells: Th2 cytokines and intestinal epithelial cells. *Clinical & Experimental Immunology* **111**, 152–157 (1998).

273. Jia, T. *et al.* Additive Roles for MCP-1 and MCP-3 in CCR2-Mediated Recruitment of Inflammatory Monocytes during *Listeria monocytogenes* Infection. *J Immunol* **180**, 6846–6853 (2008).
274. Arnold, I. C. *et al.* CD11c+ monocyte/macrophages promote chronic *Helicobacter hepaticus*-induced intestinal inflammation through the production of IL-23. *Mucosal Immunol* **9**, 352–363 (2016).
275. Allenbach, C. *et al.* Macrophages Induce Neutrophil Apoptosis through Membrane TNF, a Process Amplified by *Leishmania major*. *J Immunol* **176**, 6656–6664 (2006).
276. Stöhr, R., Deckers, N., Schurgers, L., Marx, N. & Reutelingsperger, C. P. AnnexinA5-pHrodo: a new molecular probe for measuring efferocytosis. *Sci Rep* **8**, 17731 (2018).
277. Bandyopadhyay, S. K. *et al.* Hyaluronan-Mediated Leukocyte Adhesion and Dextran Sulfate Sodium-Induced Colitis Are Attenuated in the Absence of Signal Transducer and Activator of Transcription 1. *The American Journal of Pathology* **173**, 1361–1368 (2008).
278. de la Motte, C. A., Hascall, V. C., Drazba, J., Bandyopadhyay, S. K. & Strong, S. A. Mononuclear Leukocytes Bind to Specific Hyaluronan Structures on Colon Mucosal Smooth Muscle Cells Treated with Polyinosinic Acid:Polycytidylic Acid. *The American Journal of Pathology* **163**, 121–133 (2003).

279. Kessler, S. P. *et al.* Multifunctional Role of 35 Kilodalton Hyaluronan in Promoting Defense of the Intestinal Epithelium. *J Histochem Cytochem.* **66**, 273–287 (2018).
280. Kim, Y. *et al.* Hyaluronan 35 kDa treatment protects mice from *Citrobacter rodentium* infection and induces epithelial tight junction protein ZO-1 in vivo. *Matrix Biology* **62**, 28–39 (2017).
281. Hill, D. R., Kessler, S. P., Rho, H. K., Cowman, M. K. & de la Motte, C. A. Specific-sized Hyaluronan Fragments Promote Expression of Human β -Defensin 2 in Intestinal Epithelium*. *Journal of Biological Chemistry* **287**, 30610–30624 (2012).
282. Zheng, L., Riehl, T. E. & Stenson, W. F. Regulation of Colonic Epithelial Repair in Mice by Toll-Like Receptors and Hyaluronic Acid. *Gastroenterology* **137**, 2041–2051 (2009).
283. Zhuo, L. *et al.* SHAP Potentiates the CD44-mediated Leukocyte Adhesion to the Hyaluronan Substratum. *Journal of Biological Chemistry* **281**, 20303–20314 (2006).
284. Kultti, A. *et al.* 4-Methylumbelliferone inhibits hyaluronan synthesis by depletion of cellular UDP-glucuronic acid and downregulation of hyaluronan synthase 2 and 3. *Experimental Cell Research* **315**, 1914–1923 (2009).
285. Zhang, G. *et al.* CD44 clustering is involved in monocyte differentiation. *Acta Biochimica et Biophysica Sinica* **46**, 540–547 (2014).

286. Hafiz, S. & Oakley, C. L. Clostridium difficile: isolation and characteristics (Plate VIII). *Journal of Medical Microbiology* **9**, 129–136 (1976).
287. Seddon, S. V., Hemingway, I. & Borriello, S. P. Hydrolytic enzyme production by Clostridium difficile and its relationship to toxin production and virulence in the hamster model. *Journal of Medical Microbiology* **31**, 169–174 (1990).
288. Rath, M., Muller, I., Kropf, P., Closs, E. I. & Munder, M. Metabolism via Arginase or Nitric Oxide Synthase: Two Competing Arginine Pathways in Macrophages. *Front. Immunol.* **5**, (2014).
289. Munder, M., Eichmann, K. & Modolell, M. Alternative Metabolic States in Murine Macrophages Reflected by the Nitric Oxide Synthase/Arginase Balance: Competitive Regulation by CD4⁺ T Cells Correlates with Th1/Th2 Phenotype. *J. Immunol.* **160**, 5347 (1998).
290. Raes, G., Van den Bergh, R., De Baetselier, P. & Ghassabeh, G. H. Arginase-1 and Ym1 Are Markers for Murine, but Not Human, Alternatively Activated Myeloid Cells. *J Immunol* **174**, 6561–6562 (2005).
291. Monticelli, L. A. *et al.* Arginase 1 is an innate lymphoid-cell-intrinsic metabolic checkpoint controlling type 2 inflammation. *Nat Immunol* **17**, 656–665 (2016).
292. Albina, J. E., Mills, C. D., Henry, W. L. & Caldwell, M. D. Temporal expression of different pathways of 1-arginine metabolism in healing wounds. *J. Immunol.* **144**, 3877 (1990).

293. Campbell, L., Saville, C. R., Murray, P. J., Cruickshank, S. M. & Hardman, M. J. Local Arginase 1 Activity Is Required for Cutaneous Wound Healing. *Journal of Investigative Dermatology* **133**, 2461–2470 (2013).
294. Herbert, D. R. *et al.* Arginase I Suppresses IL-12/IL-23p40–Driven Intestinal Inflammation during Acute Schistosomiasis. *J.I.* **184**, 6438–6446 (2010).
295. Munder, M. Arginase: an emerging key player in the mammalian immune system: Arginase in the immune system. *British Journal of Pharmacology* **158**, 638–651 (2009).
296. Derakhshani, A. *et al.* Arginase 1 (Arg1) as an Up-Regulated Gene in COVID-19 Patients: A Promising Marker in COVID-19 Immunopathy. *JCM* **10**, 1051 (2021).
297. Falck-Jones, S. *et al.* Functional monocytic myeloid-derived suppressor cells increase in blood but not airways and predict COVID-19 severity. *Journal of Clinical Investigation* **131**, e144734 (2021).
298. Boumaza, A. *et al.* Monocytes and macrophages, targets of SARS-CoV-2: the clue for Covid-19 immunoparalysis. *The Journal of Infectious Diseases* jjab044 (2021) doi:10.1093/infdis/jjab044.
299. Page, C. *et al.* Induction of Alternatively Activated Macrophages Enhances Pathogenesis during Severe Acute Respiratory Syndrome Coronavirus Infection. *Journal of Virology* **86**, 13334–13349 (2012).
300. Clarkin, C. E., Allen, S., Wheeler-Jones, C. P., Bastow, E. R. & Pitsillides, A. A. Reduced chondrogenic matrix accumulation by 4-methylumbelliferone

reveals the potential for selective targeting of UDP-glucose dehydrogenase.

Matrix Biology **30**, 163–168 (2011).

301. Nagy, N. *et al.* 4-Methylumbelliferone Treatment and Hyaluronan Inhibition as a Therapeutic Strategy in Inflammation, Autoimmunity, and Cancer.

Front. Immunol. **6**, (2015).

302. Nguyen, P. M., Putoczki, T. L. & Ernst, M. STAT3-Activating Cytokines: A Therapeutic Opportunity for Inflammatory Bowel Disease? *Journal of*

Interferon & Cytokine Research **35**, 340–350 (2015).

303. Fukushi, S., Yamasaki, K. & Aiba, S. Nuclear localization of activated STAT6 and STAT3 in epidermis of prurigo nodularis: STAT6 and STAT3 activation

in epidermis of prurigo nodularis. *British Journal of Dermatology* **165**, 990–996 (2011).

304. Mishra, J. P., Mishra, S. & Kumar, A. STAT6 is a novel regulator of CD44 expression in human B cells (97.4). *J. Immunol.* **178**, S189 (2007).

305. Chhapola Shukla, S. ACE2 expression in allergic airway disease may decrease the risk and severity of COVID-19. *Eur Arch Otorhinolaryngol*

(2020) doi:10.1007/s00405-020-06408-7.

306. Kimura, H. *et al.* Type 2 inflammation modulates ACE2 and TMPRSS2 in airway epithelial cells. *Journal of Allergy and Clinical Immunology* **146**, 80-

88.e8 (2020).

307. Sajuthi, S. P. *et al.* Type 2 and interferon inflammation regulate SARS-CoV-2 entry factor expression in the airway epithelium. *Nat Commun* **11**, 5139 (2020).
308. Guh, A. Y. *et al.* Trends in U.S. Burden of *Clostridioides difficile* Infection and Outcomes. *N Engl J Med* **382**, 1320–1330 (2020).
309. Centers for Disease Control and Prevention (U.S.). *Antibiotic resistance threats in the United States, 2019*. <https://stacks.cdc.gov/view/cdc/82532> (2019) doi:10.15620/cdc:82532.
310. Chow, V. C. Y. *et al.* Surveillance of antibiotic resistance among common *Clostridium difficile* ribotypes in Hong Kong. *Sci Rep* **7**, 17218 (2017).
311. Saha, S. *et al.* Increasing antibiotic resistance in *Clostridioides difficile*: A systematic review and meta-analysis. *Anaerobe* **58**, 35–46 (2019).
312. WHO. COVID-19 Weekly Epidemiological Update Edition 42. (2021).
313. Holder, J. Tracking Coronavirus Vaccinations Around the World. (2021).
314. Ledford, H. Six months of COVID vaccines: what 1.7 billion doses have taught scientists. *Nature* **594**, 164–167 (2021).
315. Torjesen, I. Covid-19 will become endemic but with decreased potency over time, scientists believe. *BMJ* n494 (2021) doi:10.1136/bmj.n494.
316. Abdool Karim, S. S. & de Oliveira, T. New SARS-CoV-2 Variants — Clinical, Public Health, and Vaccine Implications. *N Engl J Med* **384**, 1866–1868 (2021).

317. Hoffmann, M. *et al.* SARS-CoV-2 variants B.1.351 and P.1 escape from neutralizing antibodies. *Cell* **184**, 2384-2393.e12 (2021).
318. Walensky, R. P., Walke, H. T. & Fauci, A. S. SARS-CoV-2 Variants of Concern in the United States—Challenges and Opportunities. *JAMA* **325**, 1037 (2021).
319. Dan, J. M. *et al.* Immunological memory to SARS-CoV-2 assessed for up to 8 months after infection. *Science* **371**, eabf4063 (2021).
320. Leslie, J. L., Vendrov, K. C., Jenior, M. L. & Young, V. B. The Gut Microbiota Is Associated with Clearance of *Clostridium difficile* Infection Independent of Adaptive Immunity. *mSphere* **4**, e00698-18, /msphere/4/1/mSphere698-18.atom (2019).
321. Chenery, A. *et al.* *IL-13 deficiency exacerbates lung damage and impairs epithelial-derived type 2 molecules during nematode infection.*
<http://biorxiv.org/lookup/doi/10.1101/2020.10.14.337949> (2020)
doi:10.1101/2020.10.14.337949.
322. Matute-Bello, G. *et al.* An Official American Thoracic Society Workshop Report: Features and Measurements of Experimental Acute Lung Injury in Animals. *Am J Respir Cell Mol Biol* **44**, 725–738 (2011).
323. Martin, M. Cutadapt removes adapter sequences from high-throughput sequencing reads. *EMBnet j.* **17**, 10 (2011).

324. Babraham Bioinformatics - FastQC A Quality Control tool for High Throughput Sequence Data.
<https://www.bioinformatics.babraham.ac.uk/projects/fastqc/>.
325. Ewels, P., Magnusson, M., Lundin, S. & Källér, M. MultiQC: summarize analysis results for multiple tools and samples in a single report. *Bioinformatics* **32**, 3047–3048 (2016).
326. Dobin, A. & Gingeras, T. R. Mapping RNA-seq Reads with STAR. *Current Protocols in Bioinformatics* **51**, (2015).
327. Love, M. I., Huber, W. & Anders, S. Moderated estimation of fold change and dispersion for RNA-seq data with DESeq2. *Genome Biol* **15**, 550 (2014).
328. Griss, J. *et al.* ReactomeGSA - Efficient Multi-Omics Comparative Pathway Analysis. *Molecular & Cellular Proteomics* **19**, 2115–2125 (2020).
329. Wu, D. & Smyth, G. K. Camera: a competitive gene set test accounting for inter-gene correlation. *Nucleic Acids Research* **40**, e133–e133 (2012).